EVALUATION OF GLACIATION AND GLACIAL SHAPES USING GEOGRAPHIC INFORMATION SYSTEMS AND REMOTE SENSING (EASTERN BLACK SEA)

A THESIS SUBMITTED TO
THE GRADUATE SCHOOL OF NATURAL AND APPLIED SCIENCES
OF
MIDDLE EAST TECHNICAL UNIVERSITY

BY

REŞAT GEÇEN

IN PARTIAL FULFILLMENT OF THE REQUIREMENTS
FOR
THE DEGREE OF DOCTOR OF PHILOSOPHY
IN
GEODETICAL AND GEOGRAPHICAL INFORMATION TECHNOLOGIES

SEPTEMBER 2011

Approval of the thesis:

EVALUATION OF GLACIATION AND GLACIAL SHAPES USING GEOGRAPHIC INFORMATION SYSTEMS AND REMOTE SENSING (EASTERN BLACK SEA)

submitted by **REŞAT GEÇEN** in partial fulfillment of the requirements for the degree of Doctor of Philosophy **in Geodetic and Geographic Information Technologies, Middle East Technical University** by,

Prof. Dr. Canan ÖZGEN ______________________
Dean, Graduate School of **Natural and Applied Sciences**

Assoc. Prof. Dr. Ayşegül AKSOY ______________________
Head of Department, **Geodetic and Geog. Inf. Tech.**

Prof. Dr. Vedat TOPRAK ______________________
Supervisor, **Geological Engineering Dept., METU**

Prof. Dr. Saadettin TONBUL ______________________
Co-Supervisor, **Geography Dept., Fırat University**

Examining Committee Members:

Prof. Dr. Şebnem DÜZGÜN ______________________
Mining Engineering Dept., METU

Prof. Dr. Vedat TOPRAK ______________________
Geological Engineering Dept., METU

Prof. Dr. İhsan ÇİÇEK ______________________
Geography Dept., Ankara University

Assoc. Prof. Dr. İsmail YÜCEL ______________________
Civil Engineering Dept., METU

Dr. Koray K. YILMAZ ______________________
Geological Engineering Dept., METU

Date: 16. 09. 2011

I hereby declare that all information in this document has been obtained and presented in accordance with academic rules and ethical conduct. I also declare that, as required by these rules and conduct, I have fully cited and referenced all material and results that are not original to this work.

Name, Last Name: REŞAT GEÇEN

Signature:

ABSTRACT

EVALUATION OF GLACIATION AND GLACIAL SHAPES USING GEOGRAPHIC INFORMATION SYSTEMS AND REMOTE SENSING (EASTERN BLACK SEA)

Geçen, Reşat

Ph.D., Department of Geodetic and Geographic Information Technologies

Supervisor: Prof. Dr. Vedat Toprak

Co-Supervisor: Prof. Dr. Saadettin Tonbul

September 2011, 141 pages

This study investigates the actual glaciers and the major properties of glacial landscapes (valleys, cirques and lakes) located over the Eastern Black Sea mountain chain using Geographic Information Systems (GIS) and Remote Sensing (RS) technologies. A database is created for each glacial feature that includes fundamental properties of each landscape. Data layers used in the study include digital and analog topographic maps, satellite images, geological maps and drainage maps.

The studies carried out yielded identification of 93 glacial valleys (30 main, 63 tributary), 1222 cirques and 685 lakes. Several properties (length, size, aspect, elevation, slope, orientation, roundness, elongation) of each glacial landscape are investigated for the northern and southern parts separately. The frequency of each landscape is found to be more in the northern part of the area. Total area of the actual glacier is found as 0.43 to 0.53 km^2 by two methods of remote sensing applications.

Keywords: Glacier, Glacial shapes, Geographic Information Systems, Remote Sensing, Eastern Black Sea

ÖZ

COĞRAFİ BİLGİ SİSTEMLERİ VE UZAKTAN ALGILAMA TEKNİKLERİ KULLANILARAK BUZUL VE BUZUL ŞEKİLLERİNİN DEĞERLENDİRİLMESİ (DOĞU KARADENİZ)

Geçen, Reşat

Doktora, Jeodezi ve Coğrafi Bilgi Teknolojileri Bölümü
Tez Yöneticisi: Prof. Dr. Vedat Toprak
Ortak Tez Yöneticisi: Prof. Dr. Saadettin Tonbul

Eylül 2011, 141 sayfa

Bu çalışma, Doğu Karadeniz Dağlarında görülen aktif buzul ve buzul şekillerinin (vadiler, sirkler ve göller) temel özellikleri Coğrafi Bilgi Sistemleri (CBS) ve Uzaktan Algılama (UA) teknikleri kullanılarak incelenmektedir. Her bir buzul şekli için özelliklerini kapsayan veritabanı oluşturulmaktadır. Çalışmada kullanılan veri setleri; sayısal ve analog topografya haritaları, uydu görüntüleri, jeoloji haritaları, drenaj haritalarını içermektedir.

Çalışma alanında 93 buzul vadisi (30 ana vadi, 63 tali buzul vadisi), 1222 sirk ve 685 buzul gölü tespit edilmiştir. Buzul şekillerinin çeşitli özellikleri (uzunluk, büyüklük, bakı, yükselti, eğim, yönelim, uzanım) kuzey ve güney yamaçları için ayrı ayrı hesaplanmakta ve karşılaştırılmaktadır. Kuzey yamaçta yer alan buzul şekilleri nicelik olarak daha fazla ve nitelik olarak daha belirgindir. Uzaktan algılama uygulamalarıyla çalışma alanında yer alan aktif buzullar farklı iki metot kullanılarak, 0.43-0.53 km^2 olarak hesaplanmaktadır.

Anahtar kelimeler: Buzul, Buzul şekilleri, Coğrafi Bilgi Sistemleri, Uzaktan Algılama, Doğu Karadeniz

To My Family

ACKNOWLEDGEMENTS

At first, I would like to express my sincerest thanks and deepest respect to my supervisor **Prof. Dr. Vedat Toprak** for his fantastic guidance, continuous support and unlimited thrust at every stage of this study. He is not only a good advisor and a teacher but also a very good friend. He has always been very patient to me during the course of this study. Thank you so much...

I want to thank to my co-advisor **Prof. Dr. Saadettin Tonbul** for his helps, sharing his ideas and wonderful guiding during this study.

I would like to express my special thanks to my committee members **Prof. Dr. H. Şebnem Düzgün**, and **Prof Dr. İhsan Çiçek** for their contributions and continuous support throughout this study.

I would like to thank to **Dr. Esra Özdenerol** from University of Memphis, Tennessee, USA for her hospitality, support and valuable suggestions.

I gratefully acknowledge my **professors** in Geodetic and Geographical Information Technologies Department, METU, for giving me their valuable time and for sharing their valuable comments during this graduate program.

Moreover, I would like to express my special thanks to friends, **research assistants** in Geodetic and Geographical Information Technologies Department, for their helps, patiences, and lovely friendships.

I acknowledge OYP programme for employing me and providing me support during my studies.

Finally but the most, I send my very special thanks to my family. I would like to show them my sincere gratitude to my lovely daugther **Zeynep Nevra Geçen,** and my wife **Nur Geçen.**

TABLE OF CONTENTS

LIST OF TABLES

TABLES

LIST OF FIGURES

FIGURES

CHAPTER 1

INTRODUCTION

1.1. Motivation

Turkey has a complex topography that has different characteristics in different parts of the country. The altitude can vary from one region to another. Although the country is mostly surrounded by seas, in several regions the elevation is above 3000 m. The altitude, generally, increases from west to east. Due to climatic conditions existing in the region, some parts of Turkey have been influenced by glaciation in Pleistocene era. Although they retreat due to global warming, several actual glaciers exist over high mountains.

In general, very limited data are available on Turkish glaciers. The recent observations indicate a glacier recession at least since the beginning of the 20th century (Çiner, 2003). Present-day glaciers and glacier-related landforms occur in 3 major regions in Turkey: 1) The Taurus Mountains, 2) The Eastern Black Sea Mountains, and 3) Volcanoes and independent mountain chains scattered throughout the Anatolian plateau (Çiner, 2003).

The Taurus Mountain Range (Mediterranean coast and SE Turkey) covers two-third of the present day glaciers which are mostly concentrated in the SE part. Among these, Mount Cilo (4168 m) alone supports more than ten glaciers. Here the actual snowline changes between 3400-3600 m and the Last Glacial snowline is estimated to have been at around 2800 m. In the Central part, Aladağ (3756 m) and Bolkardağ (3524 m) constitute two of the most important mountains where modern glaciers, although very small, are present. Even though there are signs of past glacial activity (Last Glacial snowline is estimated to be around 2200 m), no glaciers are present in the Western Taurus Mountains today (Çiner, 2003).

Eastern Black Sea region (Pontic Mountain Range) has the highest peak 3942 m located on Mount Koçkar where five glaciers are developed. Several other mountains such as Verçenik (3710 m), Bulut (3562 m), Altıparmak (3353 m), Karagöl (3107 m) and Karadağ (3331 m) also support various glaciers. The modern snowline elevation is much lower on the north facing slopes (3100-3200 m) compared to that of south face (3550 m), because of the effect of more humid air masses. The Last Glacial snowline elevation was 2600 m on average (Çiner, 2003).

Volcanoes and independent mountains are scattered in the Anatolian plateau. In the interior of the country, volcanoes such as Mount Agri (Ararat) (5165 m), with an ice cap of 10 km^2; Mount Süphan (4058 m) and Mount Erciyes (3917 m) show signs of glacial activity and active glaciers. On the other hand, Mount Uludağ (2543 m), Mount Mercan (3368 m) and Mount Mescid (3239 m) in Central Anatolia also bear traces of past glacial activity (Çiner, 2003).

Glacial geomorphology is an important aspect of geomorphology that investigates the actual glaciers, the history of glaciation, and landscapes formed by glaciers. Recently, the study of glacial geomorphology becomes more attractive because of direct effect on life and human due to global warming theories. However, the studies carried out on glacial geomorphology have several difficulties mostly because the glaciers and glacial landscapes are located at high altitudes. Exploring, mapping and surveying through such regions is not easy. In some case, it is impossible to carry out field surveys depending on the morphology and climatic conditions of the area. On the other hand, recent developments in the field of glacial geomorphology have dramatically increased the need to acquire, maintain, manipulate, and analyze large amounts of landform, landscape and sediment data. At this point, remote sensing (RS) and geographic information systems (GIS) seems to complete these requirements and can contribute a lot to the study of glacial geomorphology.

Because of its location, Turkey has been influenced by glaciers in Pleistocene era, and many glacial landscapes have been formed throughout the country during this period. Many scientists have studied the glaciation in Turkey mostly based on field surveys without using GIS and RS technologies. Making the use of GIS and RS technology in this field is the main motivation and the encouragement in this study.

1.2. Purpose and Scope

Although there is little area of actual glaciers over Turkey, in Pleistocene era many regions had been occupied by glaciers. The movement of the glaciers modified the earth's surface which in turn developed a glacial landform characterized by various glacial features such as valleys, cirques and lakes. Eastern Black Sea Mountain Range is a typical region holding actual glaciers with many landscapes formed by glaciers in Pleistocene era. These properties have attracted many scientists to carry out studies in this part of the country. Together with improvements on GIS and RS technology, particularly in the last decade, there is great opportunity and advantage of applying RS and GIS technologies to glacial terrains to delineate and map certain features.

The aim of this study is to investigate the glaciated area in the Eastern Black Sea Mountain range using GIS and RS technologies in order to map and evaluate several features associated with glaciers. Expected outcome of the study is a glacial geomorphology map with basic glacial features and landforms.

The scope of the study is limited to the identification of three glacial landscapes, namely "glacial valleys", "cirques", and "glacial lakes". Available high-resolution digital topographic maps are the main input to distinguish the glacial features. For each feature a database will be created which will be integrated and queried with other features. Remote sensing studies are used to determine "the actual glaciers" existing in the area. The product of this study will be used to assess the accuracy of determination of glacial features as well as the monitoring the glacial activity in relation to global warming.

1.3. Study Area

The study area is located in the northeastern part of Turkey located between the provinces of Trabzon, Rize, Artvin and Bayburt (Figure 1.1). The mountainous area between these settlements known as the Eastern Black Sea Mountains is the main focus of this study.

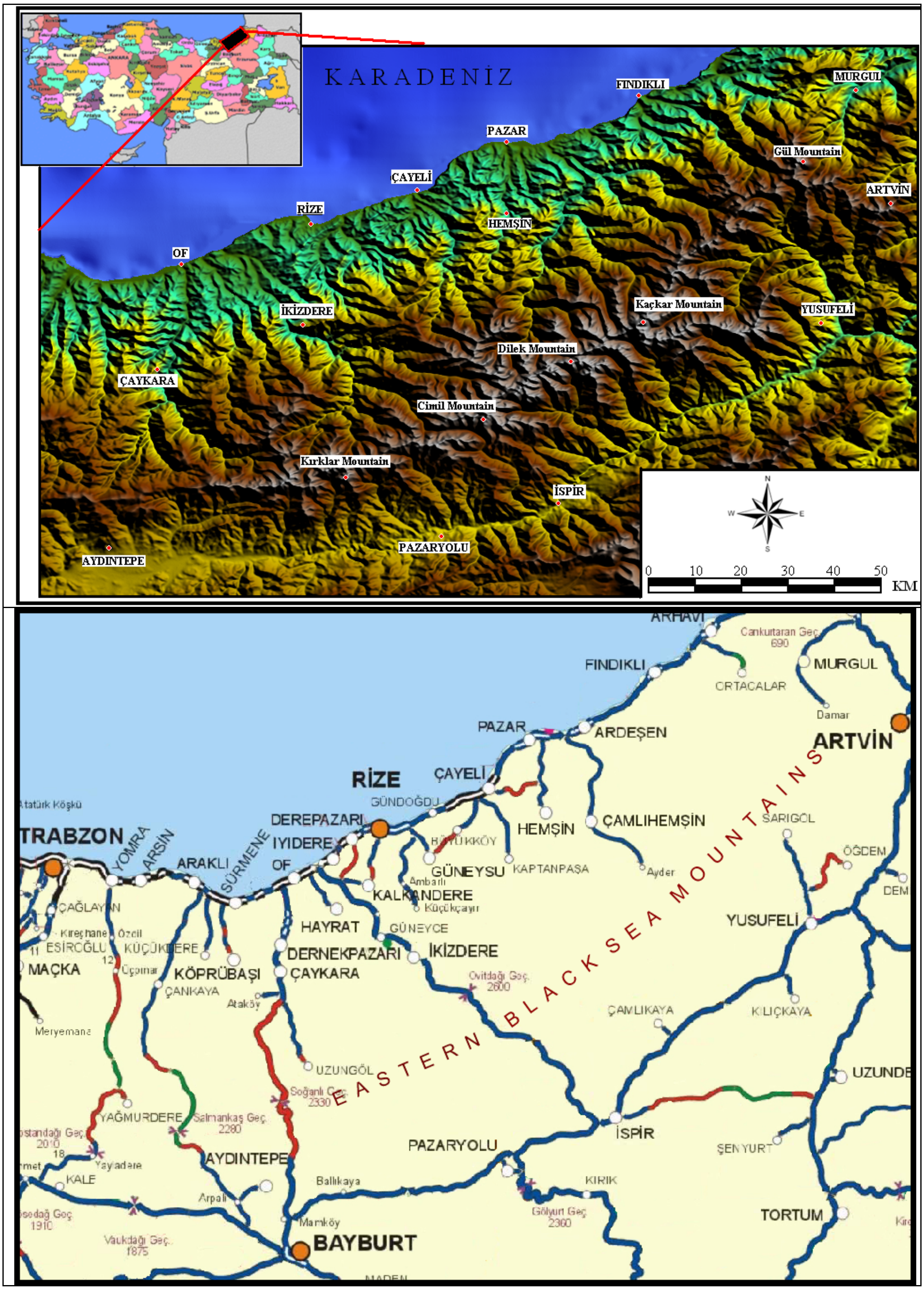

Figure 1.1: Location map of study area: a) Physical map (Generated from SRTM) (upper), b) Settlements and transportations map (lower).

The area covers approximately 6.000 km^2 of rough topography including the highest mountains of the region. The highest peak is the summit of Mount Kaçkar with an elevation of 3932 m elevation. Three highest peaks to the west of Kaçkar Mountain are Dilek, Cimil and Kırklar mountains with elevations of 3550, 3331 and 3354 m, respectively. To the west of Kaçkar Mountain the highest peak is the top of Gül Mountaion with an elevation of 3348 m.

The accessibility in the area is poor due to steepness and the climatic conditions. The whole region can be crossed only along two roads between İkizdere and İspir; and through Artvin. This harsh topography is reflected by the settlement pattern of the area. Most of large settlements are located at the lower slopes of the mountain chain on both sides (Figure 1.1). At higher elevations "yayla" (highland) type settlements exist which are settled for a short period and very common in the northeastern Anatolia.

Some climatic data are provided from Turkish State Meteorological Service to estimate the conditions in the region related to the glacial activity. Figure 1.2 shows amount of precipitation for major basins of Turkey for the 10 months (October to July) of the years 2010-2011. It is very clear in the diagram that the eastern Black Sea area receives the maximum precipitation compared to the other regions of the country.

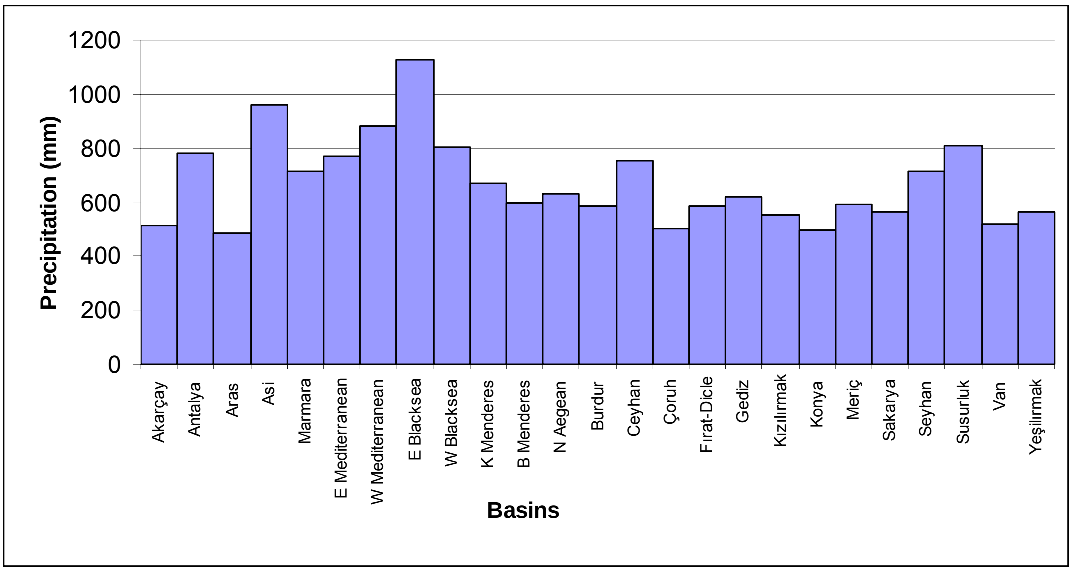

Figure 1.2: Amount of precipitation for the period between 2010 October and 2011 July (source: Turkish State Meteorological Service website).

Average monthly precipitation and temperature values for the provinces in the vicinity of the study area are illustrated in Tables 1.1 and 1.2, respectively. It should be kept in mind that the study area covers the higher parts of the region and therefore the values shown in the tables might change. For example, the temperature will be less than the given amount. Nevertheless, the numbers in general can give an idea on the climatic conditions. The period between September and January is the rainy season as indicated by the maximum precipitation values. The temperature, on the other hand is minimum between December and March. In July and August the temperature reaches the maximum values.

Table 1.1: Average monthly precipitation of the provinces in the vicinity of study area for the period 1975-2010 (source: Turkish State Meteorological Service website).

	January	**February**	**March**	**April**	**May**	**June**	**July**	**August**	**September**	**October**	**November**	**December**	**Total**
Rize	210.5	175.7	144.1	92.3	99.6	135.7	148.5	182.6	249.7	300.5	256.4	246.0	2241.6
Artvin	90.7	72.7	59.8	56.4	53.4	49.7	30.8	30.2	33.8	62.0	78.4	96.0	713.9
Trabzon	74.0	60.7	58.8	58.8	50.9	49.2	37.3	46.5	78.4	119.5	100.2	85.3	819.6
Bayburt	26.5	28.0	41.1	61.4	68.0	50.8	20.4	15.9	21.8	47.3	35.3	28.7	445.2
Erzurum	19.4	22.9	31.8	53.9	67.2	45.0	26.3	16.8	21.3	47.1	33.1	21.6	406.4
Average	84.2	72.0	67.1	64.6	67.8	66.1	52.7	58.4	81.0	115.3	100.7	95.5	925.4

Table 1.2: Average monthly temperature values of the provinces in the vicinity of study area for the period 1975-2010 (source: Turkish State Meteorological Service website).

	January	**February**	**March**	**April**	**May**	**June**	**July**	**August**	**September**	**October**	**November**	**December**	**Average**
Rize	6.4	6.5	8	11.8	16	20.4	23	23.2	20	16	11.5	8.2	14.3
Artvin	2.4	3.6	6.9	11.8	15.5	18.5	20.6	20.7	17.9	14	8.6	4	12.0
Trabzon	7.2	7.3	8.6	11.9	15.8	20.4	23.2	23.4	20.2	16.5	12.4	9.2	14.7
Bayburt	-6.7	-5.2	0.2	7	11.6	15.4	19.1	18.9	14.8	9.3	2.3	-3.6	6.9
Erzurum	-9.9	-8.2	-2.2	5.5	10.4	14.9	19.3	19.3	14.4	7.8	0.2	-6.5	5.4
Average	-0.1	0.8	4.3	9.6	13.9	17.9	21.0	21.1	17.5	12.7	7.0	2.3	10.7

1.4. Previous Works

Available literature related to the topic of this study is grouped into two categories as 1) RS and GIS applications in glacial studies, and 2) Studies carried out in the study area. The studies are summarized below in chronological order.

1.4.1. RS and GIS Applications in Glacial Studies

Glacial geomorphology is an attractive topic particularly among European and American scientists. There is a large literature on various aspects of glacial geomorphology that can be dated back to almost one century. However, considering the scope of this study, only the literature that comprises application of GIS and/or RS will be dealt here.

Kaufmann and Ploesch (2000) described the three-dimensional reconstruction of the glaciation of two neighboring cirques (Goessnitzkees and Hornkees located on Central Alps, Austria) from the Little Ice Age advance between 1850 and 1997, and the visualization of its spatio-temporal changes during this time period by means of standard methods of cartography and modern computer animation. They reconstructed 9 different glacial stages for 1850, 1873, 1929, 1954, 1969, 1974, 1983, 1992 and 1997 using GIS. The first three glacial stages are reconstructed using topographic contours, and the other six stages are derived using aerial photographs. They concluded that the glaciers lost 52 % (Goessnitzkees) and 61 % (Hornkees) of their respective area since 1850. The decrease in volume is 77.5 million m^3 and 38.2 million m^3, respectively.

Silverio and Jaquet (2005) investigated the changes of glaciers on Cordillera Blanca (Peru) between 1987 and 1996 using satellite imagery. By means of Normalized Difference Snow Index (NDSI) computations on TM images, they estimated the glaciated area in Cordillera Blanca for 1987 as 643 km^2 and for 1996 as 600 km^2. Compared to an estimate of 721 km^2 in 1970 which had been described by another scientist, they concluded that the glacial area has retreated in this massif by more than 15 % in 25 years.

Evans (2006) investigated 260 cirques in respect to their three dimensional shape in Wales. The size, shape, gradient, geological properties, and other effects such as length, width, and amplitude of cirques are computed and examined. The study leads to following conclusions:

- Maximum gradient, plan closure and number of cols increase with overall size.
- Headwall retreat, often by collapse following glacial erosion at the base, is faster than downward erosion.
- Welsh cirques form a scale-specific population and, as in other regions, size variables follow Gaussian distributions on a logarithmic scale.
- As in England, width commonly exceeds length. Vertical dimensions correlate with length more than with width.
- The form of the cirque varies with geology, but also with relief as both vary between mountain groups. The main contrast is between larger, better-developed cirques and higher relief on volcanic rocks in the northwest and smaller, less-developed cirques and lower relief on sedimentary rocks in the south.

Hendriks and Pellikka (2007) studied over Hintereisferner in the Austrian Alps in order to delineate the glaciers from Landsat images. They presented a semi-automatical model. The first step of the model creates a water mask as input the raw satellite image and an upper range of 20–30 % of digital number value counts in the histogram of the Normalized Difference Water Index. The second step, which creates the glacier mask, requires as input the raw satellite image and the water mask. It uses a threshold value for ETM+5 to mask clouds and assumes saturated pixels to be glacier if not identified as cloud. Finally the model automatically calculates a Normalized Difference Snow Index threshold value of 0.5–0.7 based on the variable range in Digital Number values for each image. Consequently they found out that in the period of 1985–1999, the area of Hintereisferner and its neighboring glaciers decreased from 159 km^2 to 138 km^2. During the period of 1991–1997 the decrease had been 6 km^2.

Amerson et al. (2008) investigated and compared the glaciated and fluvial valleys in central Idaho. They compared the relief and width properties of glaciated and fluvial valleys in order to discriminate the differences in otherwise similar geologic and geomorphic settings. They computed the local relief, width and cross-sectional area of valleys from USGS digital elevation model using GIS. They developed possible relationships for local valley relief, width, and cross-sectional area as a function of drainage area. They found out that the local valley relief in glaciated valleys relates to drainage area with an exponential relation similar to fluvial valleys. However, glaciated valleys are deeper for a given drainage area. Local valley width in glaciated valleys is greater than in fluvial valleys, but the exponent of the power-law relationship to drainage area is similar in both valley types. Local valley cross-sectional area in glaciated valleys increases with drainage area with a power-law exponent similar to fluvial valleys, however, glacial valleys have roughly 80 % greater cross-sectional area. Steep valley walls in glaciated basins increase the potential for bedrock landsliding relative to fluvial basins.

Chen et al. (2007) investigated the changes in glacial lakes and glaciers of post-1986 in the Poiqu River basin, Nyalam, Xizang (Tibet). The changes in the size and distribution of both glacial lakes and glaciers post-1986 are defined from Landsat images. They have used Landsat 5 MSS images taken in1985/1986 and Landsat 7 TM images taken in 2000/2001. They applied false color composite at certain wave bands to identify different features. Accordingly, the bands 4, 3, 2 for RGB show glacial lakes whereas the bands 7, 5, 2 for RGB show glaciers. They also determined the changes occurred in glacial activity in this period. The results indicate that area of glaciers decreased by 20 %, the number of glacial lakes increased by 11 %, and the total area of glacial lakes increased by 47 %. Three large glacial lakes (Galongco, Gangxico, and Cirenmaco) increased by 104, 118, and 156%, respectively. Between 1986 and 2001, the glaciers have decreased by 46.18 km^2 to 83.12 km^2, with an annual rate of change of 3.30 km^2/year.

Schneider et al. (2007) studied and presented a glacier inventory of the Gran Campo Nevado (GCN) made up by 27 drainage basins (in total 199,5 km^2) and other small cirque and valley glaciers of the southern part of Muñoz Gamero (PMG) (in total 53 km^2). The glacier inventory is based on a digital elevation model (DEM) and ortho-photos. They obtained a DEM of the area by combining contour lines from maps, relief information derived from Landsat TM satellite imagery from 1986 and 2002, and stereoscopic data from aerial photos. They also produced a digital ortho-photo map based on aerial photographs from 1998; and several ortho-photos based on aerial photographs from 1942 and 1984. They used a GIS service in order to outline the extent of present glaciation. Finally they found out that all major glaciers of the GCN show a significant retreat during the last 60 years. Some of the outlet glaciers had lost more than 20 % of their total area during this period. Average retreat in the length and area of glacier is 2.8 % and 2.4 %, respectively, per decade in the period from 1942 to 2002.

Frankl et al. (2010) presented an improved geomorphological methodology using remotely-sensed data, and Geographical Information System. The methodology is tested and the results are assessed during a short field survey. They carried out the study on eastern Pyrenees (France) consisting of the Quaternary glaciated part of the Coumelade valley which is located between 1450 and 2731 meter elevations. They used DEM for analyzing glacial landforms by extracting the slope gradient, valley profiles and the slope aspect. They gradually refined the results from interpretations of aerial photograph and the field investigation. They concluded that the glacial landforms are present above 1500 meter and include glacial and nivation cirques, cirque and latero–frontal moraines ($7.7 \times 106 m^3$) and micro-scale landforms such as chatter marks, crescent grooves and polished surfaces.

Bolch et al. (2010) developed a glacier inventory for the Canadian Cordillera south of 60°N, across the two western provinces of British Columbia and Alberta, containing ~30,000 km^2 of glaciated terrain. They proposed a semi-automated method extracting glacier extents from Landsat Thematic Mapper (TM) scenes for 2000 and 2005 using the band ratio of TM3 / TM5. They compared these results with glaciers for he mid-1980s from high-altitude aerial photography for British Columbia and from Landsat TM imagery for Alberta. They used a 25 m DEM in order to identify debris covered ice and to split the glaciers into their respective drainage basins. They concluded that the glaciers in British Columbia and Alberta respectively lost 10.8±3.8 % and 25.4%±4.1 % of their area over the period 1985–2005.

1.4.2. Studies carried out in the study area

Almost all studies carried out in the study area are concentrated on geomorphological aspects and/or the age of glaciation. These studies are briefly explained below.

Erinç (1952 b) studied the glacial evidences of climatic variations in Turkey. In order to reveal the climatic changes he investigated three best known glacial regions of Turkey: Erciyes glacier, glaciers of the Cilo region, and glaciers in the eastern Pontic Mountains. At Erciyes glacier he integrated his observations with previous researches and found out that the glacier has been shrunk from 700 m length to 550 m during 50 years period with an average of 3 m per year. For the glaciers of the Cilo region the author has estimated the change in two main glaciers in the region, namely, Suppa Durak and Mia Hvara using the pre-existing observations. Accordingly, the Suppa Durak glacier had receded from 2600 m to 3000 m; Mia Hvara glacier had receded from 2550 to 2750 m during 11 years period. He examined the glaciers in the eastern Pontic Mountains in order to reveal the climatic changes. This region is the study area for this thesis. Although he could not measure the exact changes he suggested the shrinkage of glaciers in the region based on the observations in the end and lateral moraines.

Çiner (2003) studied the recent glaciers and the late Quaternary glacial deposits of Turkey. He indicated that present day glaciers and Late Quaternary glacier related landforms and deposits in Turkey occur in three major regions: The Taurus Mountain Range, The Pontic Mountain Range and Volcanoes and independent mountains scattered in the Anatolian plateau. Two-third of the present day glaciers of Turkey are concentrated in the southeastern Taurus Mountain Range. Among these, Mount Cilo (4168 m) alone supports more than ten glaciers. Here the actual snowline changes between 3400-3600 m and the Last Glacial snowline is estimated to be at around 2800 m. In the Central part, Aladağ (3756 m) and Bolkardağ (3524 m) constitute two of the most important mountains where modern glaciers, although very small, are present. Even though there are signs of past glacial activity (Last Glacial snowline is estimated to be around 2200 m), no glaciers are present in the Western Taurus Mountains today. The highest peak of the Pontic Range (Eastern Black Sea coast) is Mount Kaçkar (3932 m) where five glaciers are developed.

Several other mountains such as Verçenik (3710 m), Bulut (3562 m), Altıparmak (3353 m), Karagöl (3107 m) and Karadağ (3331 m) also support various glaciers. The modern snowline elevation is much lower on the north facing slopes (3100-3200 m) compared to that of south face (3550 m), because of the effect of more humid air masses. The Last Glacial snowline elevation is 2600 m on average. Volcanoes and independent mountains are high regions scattered in the Anatolian plateau. In the interior of the country, volcanoes such as Mount Ararat (5165 m) with an ice cap of 10 km^2; Mount Süphan (4058 m) and Mount Erciyes (3917 m) show signs of glacial activity and active glaciers. On the other hand, Mount Uludağ (2543 m), Mount Mercan (3368 m) and Mount Mescid (3239 m) in Central Anatolia also bear traces of past glacial activity.

Akçar et al. (2007 a) studied paleoglacial records from Kavron glacial valley located in the Kaçkar Mountains. They defined this valley as U-shaped glacial valley consisting of a main and three tributary valleys. They mapped Quaternary units that outcrop in Kavron valley and processed 22 samples for surface exposure dating using ^{10}Be. Accordingly, the advance of the Kavron paleoglacier had begun at least 26.0 ± 1,2 kyr ago, with the Last Glacial Maximum (LGM) advance continuing until 18.3 ± 0,9 kyr. After this time the Kavron paleoglacier had receded, although the magnitude of this recession is still unknown. Subsequent to this retreat, the glacier most probably separated into three smaller glaciers that were restricted to the tributary valleys as in the case of Ifrit, Derebaşı and Mezovit paleoglaciers. The main valley was definitely ice-free by 15.5 ± 0.7 kyr ago, with the Mezovit paleoglacier completing its recession around 15.5 ± 0,6 kyr. A Late Glacial advance took place around 13.0 ± 0,8 to 11.5 ± 0,8 kyr, and Little Ice Age moraines appear to be absent. Their results from the Kavron Valley system seem to be consistent with the LGM paleoclimate record of Anatolia, which has been delineated by data gathered from lowlands and lakes, the deposition of red clay layers in the northwestern Black Sea.

Akçar et al. (2007 b) examined the field evidence of palaeoglacial records in the Verçenik valley in the Eastern Black Sea Mountains. In order to increase the knowledge on the amplitude and frequency of palaeoglacier advances in Anatolia they have collected 19 samples for surface exposure dating with cosmogenic ^{10}Be. They mapped glacial erosional features and determined the flow directions of the palaeoglaciers. They found out that Verçenik palaeoglacier had advanced before 26.1 k ±1.2 k yr. The Last Glacial Maximum (LGM) advance had continued until 18.8 k ± 1.0 k yr. The Verçenik palaeoglacier had collapsed during Termination I. After 17.7 k ± 0.8 kyr there was no more ice in the main valley. The Verçenik palaeoglacier most probably then had separated into five small glaciers that had been restricted to the tributary valleys. Among these, the Hemşin palaeoglacier had completed its recession around 15.7 k ± 0.8 k yr. On the basis of glacial erosion features, a Lateglacial glacier advance could be identified. Evidence of the Little Ice Age advance appears to be absent. The results from this valley system seem to be consistent with the first results from the adjacent Kavron valley and with the Anatolian LGM palaeoclimate, the sea surface temperature minima in the western Mediterranean, the deposition of red clay layers in the Black Sea.

Doğu et al. (1993) studied the glacial shapes on Kaçkar Mountains and generated a geomorphology map for this area (Figure 1.3). They have depicted glaciation on this area as four main glacial valleys groups named; Hastaf, Dübe, Ceymakcur , and Kavran Glacial Valleys and their tributary glacial valleys. They have computed properties for this valley as 5 kilometers length, 10 % average slope, and ending at elevation of 2270 meters. The second main glacial valley is Dübe with 5 kilometers length, 15 % average slope, and ending at 2200 meters elevation. The third one is Ceymakcur which starts at 3250 meters elevation, and reaches down to 2050 meters. This valley has 3 km length, and 16 % average slope. Kavran Glacial Valley has 7.5 kilometers length, 10 % average slope and lies between 2900 and 2020 meters elevations. They determined and evaluated several glacial lakes, cirques, and actual glaciers through this area. The elevations of snowline for these valleys systems in Pleistocene have been estimated as 2635, 2675, 2725, and 2835 meters, respectively, for four valleys mentioned above.

Doğu et al. (1994) studied the glacier shapes over Göller (Hunut) Mountain and mapped the area (Figure 1.4). In this area they have mainly defined three valley systems as Elevit, Trovit, Palovit glacial valleys and associated glacial landscapes within these valleys. The first valley system, Elevit Valley, is 12 km long with an average slope of 12 %. It starts from the cirque located at elevation of 3190 m and keeps U-shape consistently down to 1700 m elevation. The second system is Trovit

Valley that starts from cirques existing at 3329 meters elevation and connects to Elevit Valley at 1870 meters. Length and average slope for this valley are 10.5 km and 12 %, respectively. Palovit Valley is the other glacial system that has 11 km length with 10 % average slope. Starting from cirques located between 3000-3050 meters elevation, the valley changes into fluvial character at 2000 m elevation. They estimated the snowline during Pleistocene era for valley systems as 2525 m for Elevit Valley, and 2600 m for Palovit Valley. In addition, they have handled and evaluated periglacial landforms of this area.

Doğu et al. (1996) studied glacial landscapes on Üçdoruk (Verçenik) Mountain and prepared a geomorphology map of this region (Figure 1.5). In this context they have determined five glacial valleys. They investigated these valleys and other glacial shapes located in the valleys such as cirques, moraines, lakes etc. Accordingly, the main glacial valleys and their properties can be described as; 1) Tatos Valleys that has a length of 7.5 km starts at 2850 m elevations and ends at 2000 m elevations. Having an average slope of 10 % this valley contains several tributary valleys, cirques, and lakes. 2) Sarınçof Valley starts at 2800 m elevations with a length of 3.5 km and average slope of 28 % contains five lakes. The valley changes into fluvial valley at 2350 m elevation. 3) Verçenik Valley is the greatest valley in this area. It is 10 km long with an average slope of 10 % and contains many cirques, several actual glaciers located in cirques, moraine series and numerous glacial lakes. 4) Çermeç Valley has a length of 5 km with an average slope 15 %. 5) Cimil Valley is 4.5 km in length with an average slope of 10 %.

Doğu et al. (1997) studied the glacial landscapes on Bulut-Altıparmak Mountains and mapped the area (Figure 1.6). They determined six glacial valleys located to the north of area named as Palakcur, Avucur, Kaçkar, Bocunus, Topluca, and Ergusu which start from the cirques located between 2800 and 3000 m, and reach down to 1740-1920 meters. Mapping glacial landscapes they determined several properties of glacial valleys that can be summarized as follows: 1) Palakcur Glacial Valley starts at cirques situated on 2900 m and change into fluvial valley at 1900 m. The length and average slope of this valley are 4.5 km and 22 %, respectively. 2) Having 6.5 km length and 13.5 % average slope Avucur Glacial Valley starts from cirques located at face of Kemerlikaçkar summit (3125 m) and reaches down to 1920 m. They

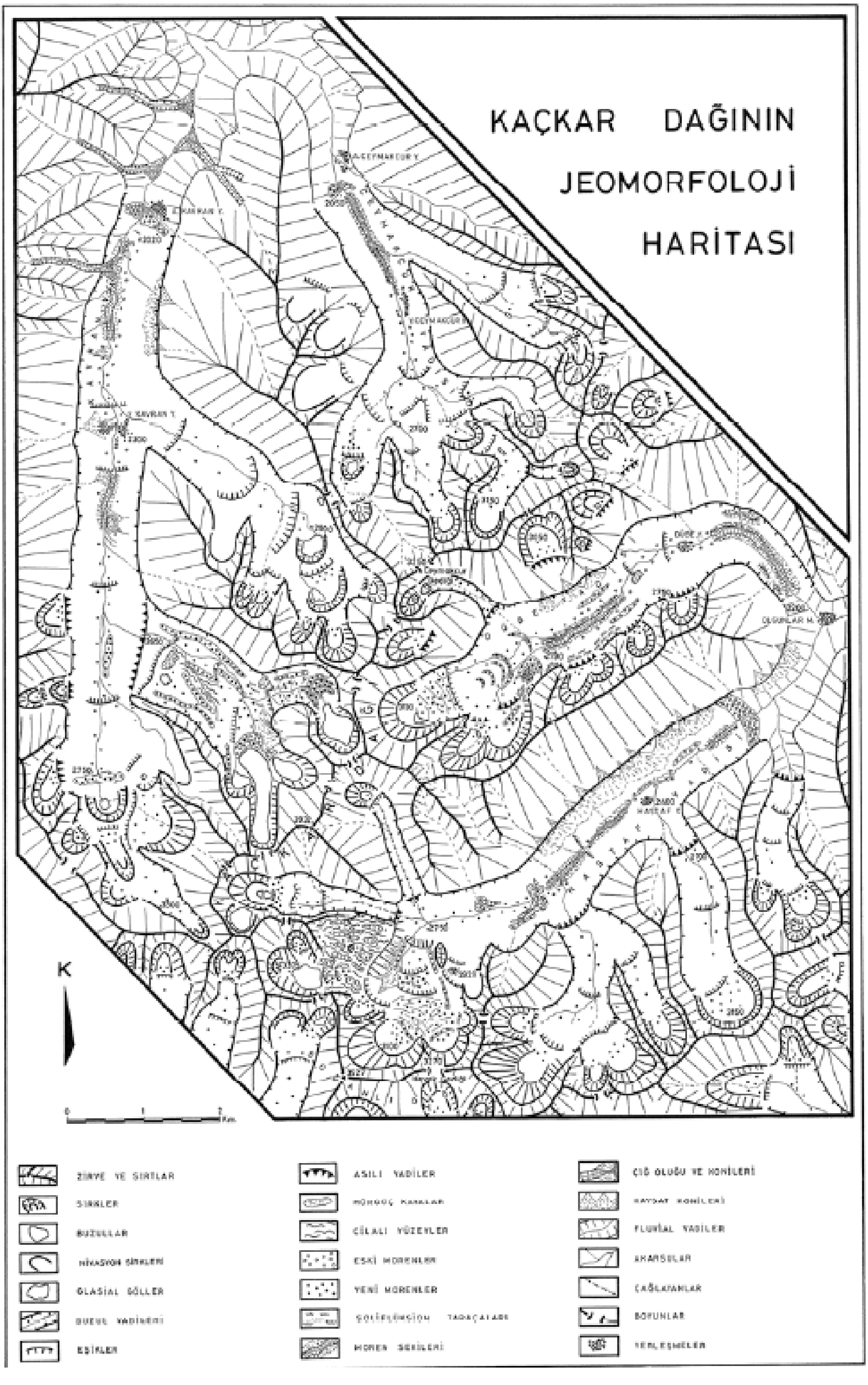

Figure 1.3: Geomorphology map of Kaçkar Mountains (by Doğu et al., 1993).

Figure 1.4: Geomorphology Map of Göller (Hunut) Mountain (by Doğu et al., 1994).

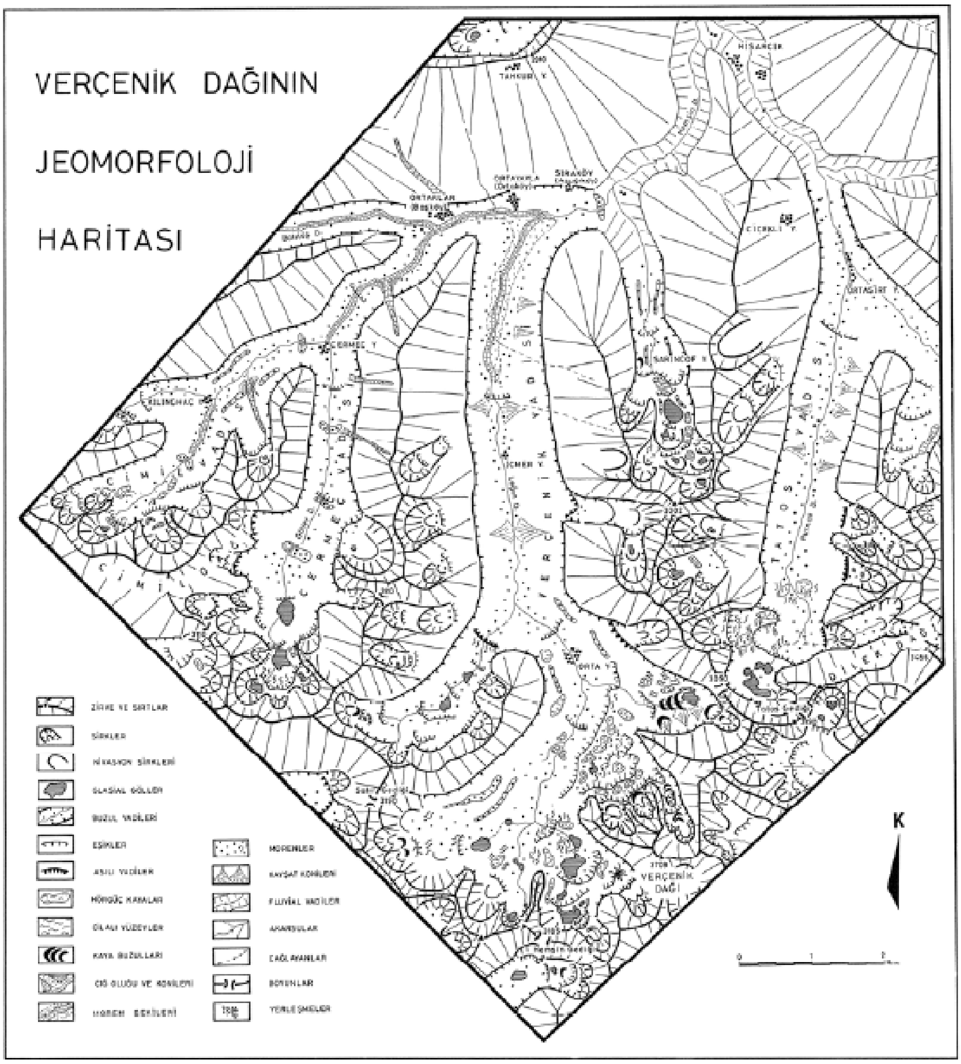

Figure 1.5: Geomorphology Map of Üçdoruk (Verçenik) Mountain (by Doğu et al., 1996).

identified an actual glacier with a width of 600 m and length of 500 m situated in a cirque existing in this valley. 3) Kaçkar Glacial Valley starts from cirques on 2900 m and change into fluvial valley at 1740 m. The valley is 8.5 km long. 4) Bocunus Glacial Valley is the shortest one in this area with 4 km length. It starts with cirques located between 2830 and 2480 m and ends by connecting to Topluca Glacial Valley. 5) Topluca Glacial Valley has a length of 6 km and an average slope of 17 %. Starting from cirques situated at 2800 m it reach down to 1800 m. 6) Ergusu Glacial Valley starts at a large cirque at 2850 m elevation after flowing down for 7 km it ends at 1800 m. They also mention some details of cirques, glacial lakes, and moraines within these glacial valleys. In addition, they have estimated the elevation of snowline in Pleistocene as 2550 m, 2645 m, 2470 m, 2385 m, and 2530 m for Palakcur, Avucur, Kaçkar, Topluca, and Ergusu glacial valleys, respectively.

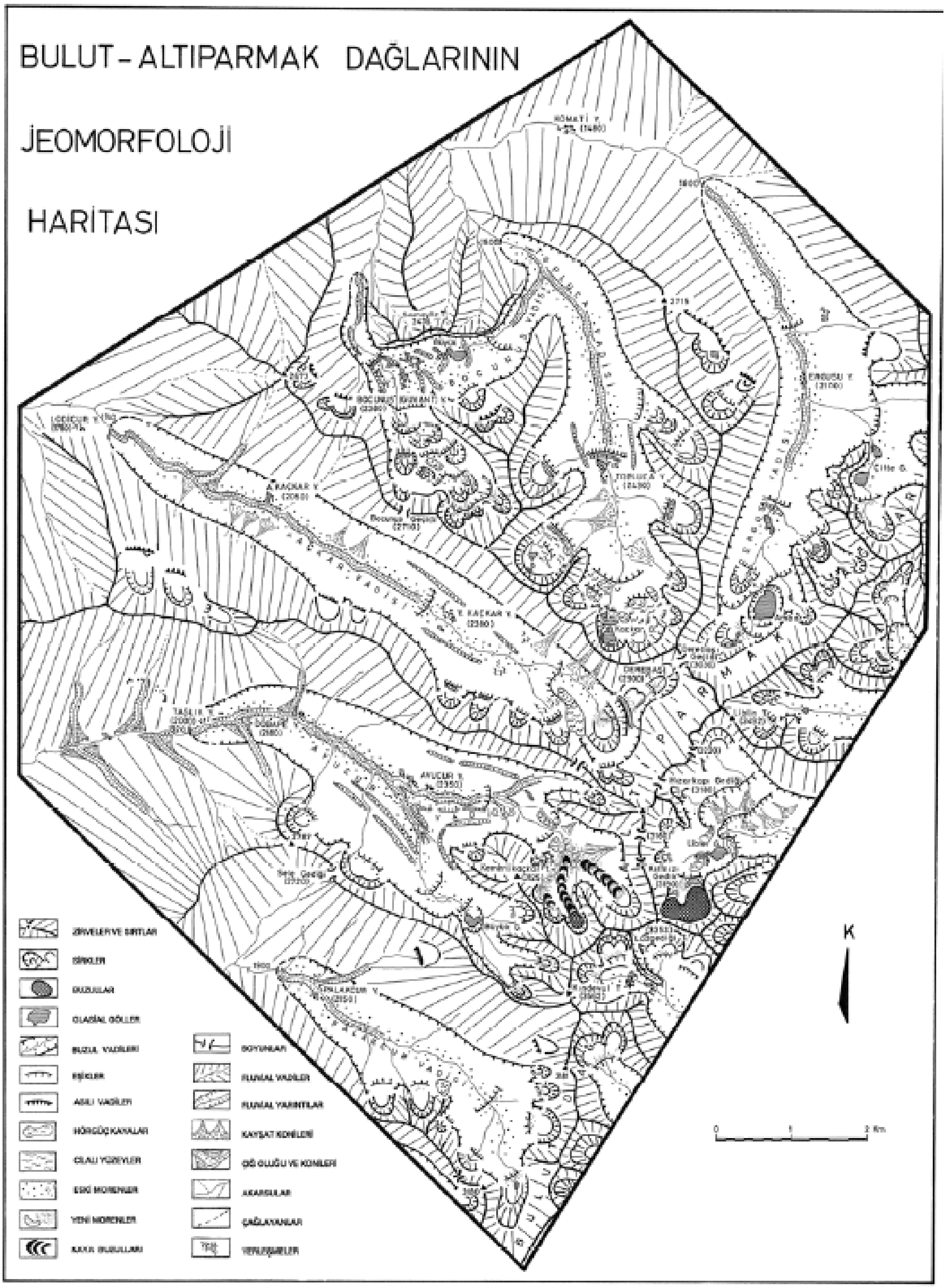

Figure 1.6: Geomorphology Map of Bulut-Altıparmak Mountain (by Doğu et al., 1997).

1.5. Thesis Organization

This thesis consists of nine chapters that can be summarized briefly as follow;

Chapter 1 includes the reasons and requirements for this study, the scope and purpose; it introduces the study area and its general characteristics, and the previous studies related to study area and subject.

Chapter 2 focuses on data and methodology. The raw datasets, their properties and sources, in addition the stages of method carried out during study are described in this chapter.

Chapter 3 describes general morphological features of the area. Geomorphologic properties of area, the boundary between glaciated and unglaciated areas (which will form the actual study boundary), the comparison between glaciated and unglaciated areas, and morphologic properties of glaciated area are the main focus of this chapter.

Chapter 4 deals with glacial valleys. In this chapter determination of glacial valleys, database creation, properties computation, and their analyses will be carried out.

Chapter 5 focuses on glacial cirques. Identification of them, computation of their properties, database creation, and analyses of cirques are handled in this chapter.

Chapter 6 focuses on glacial lakes. Identification of the lakes, computation of their properties, database creation, and their analyses are mentioned in this chapter.

Chapter 7 deals with the glaciers. This chapter is the part of the thesis where RS applications will be performed. Detection, properties, and distribution of glaciers are examined in this chapter.

Chapter 8 includes the results and discussions. The outputs determined in previous chapters are evaluated individually, and the relationships between these glacial shapes are analyzed and interpreted.

Chapter 9 consists of the results and recommendations.

CHAPTER 2

DATA AND METHODOLOGY

2.1. Data Used in the Study

This chapter describes the raw data used in this study including their types and formats, their extensions, and their sources. Some of them are used as primary data, whereas the others are used as ancillary data. Since the study is carried out via GIS and RS technologies, the input data should be in a suitable format. In this context five datasets are identified and obtained which include 1) Digital Topographic maps with scale of 1/25.000, 2) Analogue Topographic maps with scale of 1/25.000, 3) Digital hydrologic maps with scale of 1/25.000, 4) Geologic map with scale of 1/500.000, and 5) Satellite images. Necessary information and characteristic features of these data are described below.

2.1.1. Digital Topographic Maps

As the main input data of this study, the digital topographic maps of the area are taken from General Command of Mapping of Turkey (Harita Genel Komutanlığı, HGK) as 80 sheets with scale of 1/25.000. Each sheet contains contour lines with 10 m interval, points of summits with elevation values, shore lines of Black Sea, and lakes located in this area. The index of these 80 sheets is given in Figure 2.1. This raw dataset is in Arc Coverage format, with Universal Transverse Mercator (UTM) coordinate systems (Zone 37), and World Geodetic Systems 1984 (WGS 84) datum.

In the first step, these 80 sheets were merged into one single layer in order to use in GIS (Figure 2.2). Then the lines and points within this layer were separated into two different layers. These layers are later converted into several different formats for analyses and processing such as rvc (TNTmips), tab (MapInfo), shp (ArcGIS) etc.

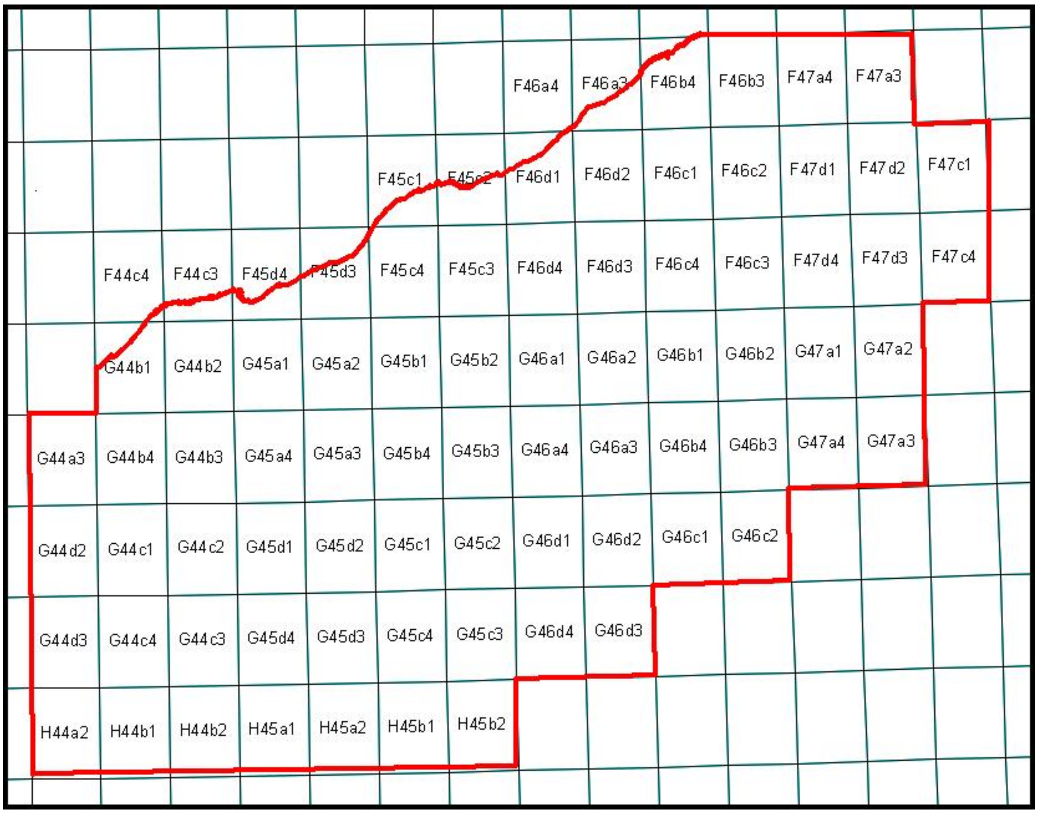

Figure 2.1: Index of 1/25.000 scale digital topographic maps used in the study.

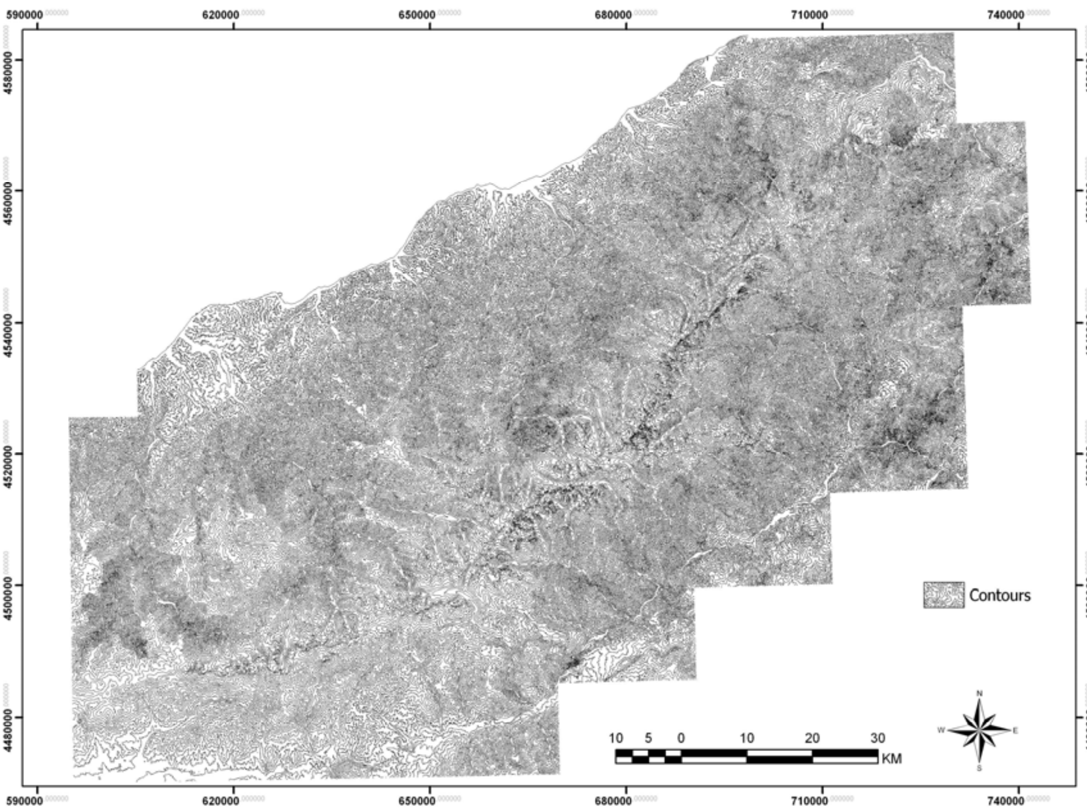

Figure 2.2: Digital Topographic Map containing contours with interval of 100 meters.

2.1.2. Analogue Topographic Maps

Analogue Topographic Maps with scale of 1/25000 are also obtained from HGK (Figure 2.3) as 80 sheets. These sheets, are scanned, georeferenced, and mosaiced. The resultant map contains contour lines, summit point elevations, locations of settlement, hydrologic elements (such as lakes, temporary and permanent rivers, water resources etc) and roads. This map is used as ancillary data for verification and complementing the missing data.

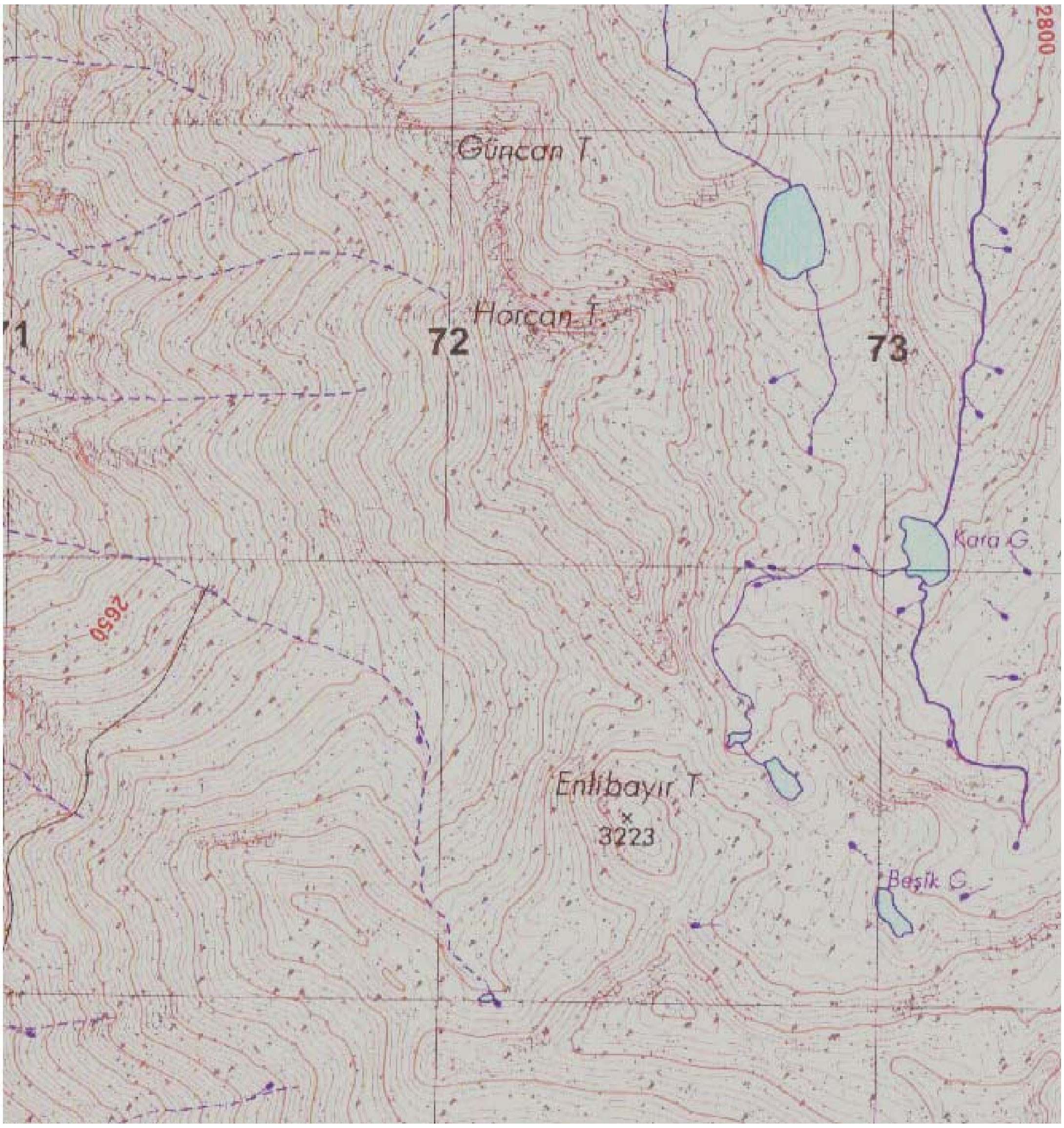

Figure 2.3: Example of Analogue map with scale of 1/25.000. (This part extracted from G46a4 sheet).

2.1.3. Digital Hydrologic Maps

This data is also taken from HGK as 80 sheets at 1/25000 scale. They have the same format and coordinate system. The main reason for acquiring this data is the presence of glacial lakes in the region. Since there is not any complete inventory of the lakes in the area, the identification of the lakes might be problematic. In order not to miss any lake that may exist in the region, it is believed that this data should be used because it will contribute to a more accurate determination of the glacial lakes. A lake could be missed easily in digital and/or analog topographic map.

A single layer of hydrologic map is generated by merging all the sheets (Figure 2.4). This layer contains rivers represented by polygons and lines, the lakes by polygons, and water resources (mostly springs) as points. The required objects from this layer are extracted and saved as separate GIS files to be used in the later sections of the study.

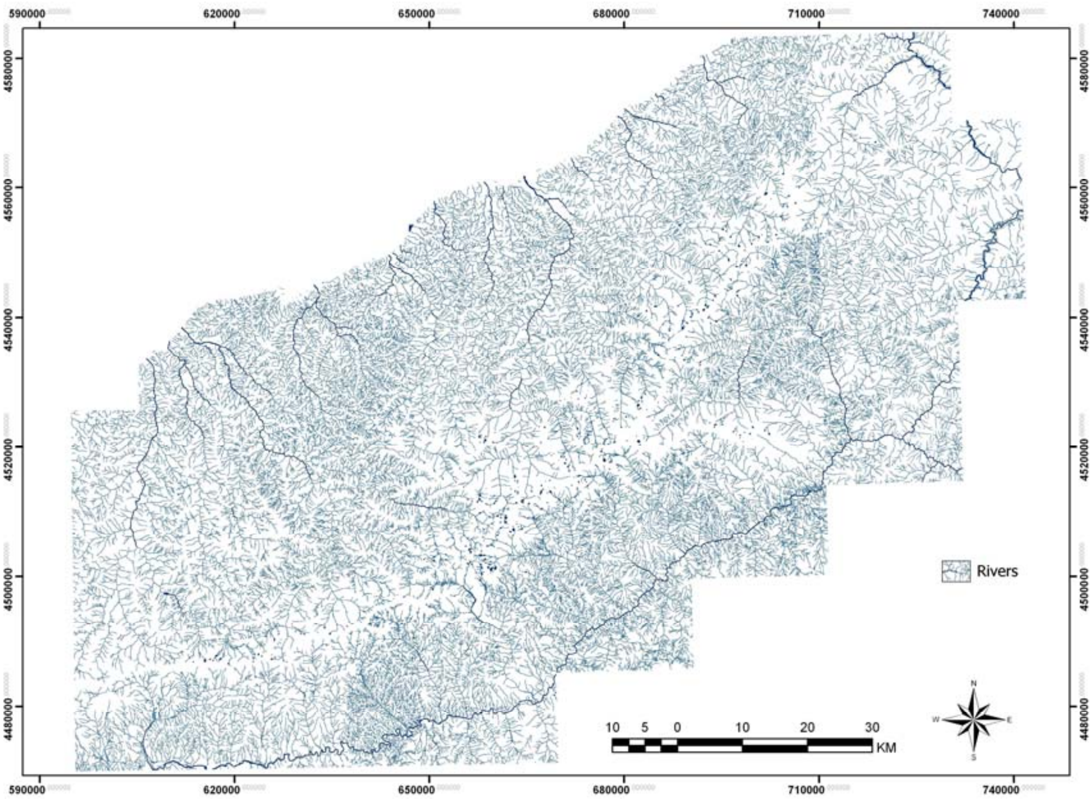

Figure 2.4: Digital Hydrology Map of the area with scale of 1/25000.

2.1.4. Geology Map

Geology map of study area is taken from General Directorate of Mineral Research and Exploration of Turkey (Maden Tetkik Arama Genel Müdürlüğü, MTA) with scale 1/500000 in raster format (Figure 2.5). First of all, the map is georeferenced in common coordinate systems (UTM WGS84 Zone 37). Then based on this raster map, a new digital layer is generated and the lithologic units of the area are digitized.

Finally, the digital geologic map is reclassified which is a simplification and generalization of the initial map. Considering the purpose of the study, total number of lithologic units is reduced to six. The new geological map is shown in Figure 2.6. Comparison of original and new maps is illustrated in Table 2.1.

It should be noted that the geology map is based only on the lithologies and other geological features such as faults are missed.

Table 2.3: Class labels of original and after generalization of geologic map.

Original Units Labels	New Classes Labels
Diorite, Quartz diorite, Tonalite (Paleocene-Eocene)	Intrusive Rocks
Granitoid (Paleocene-Eocene)	
Tonalite (Permo-Triassic)	
Granitoid (Carboniferious) (Upper Paleozoic)	
Clastic and Carbonate Rocks (Upper Cretaceous-Paleocene)	Clastic and Carbonate Rocks
Clastic and Carbonate Rocks (Upper Jurassic)	
Clastic and Carbonate Rocks (Upper Jurassic, Lower Cretaceous)	
Clastic and Carbonate Rocks (Senonian)	
Clastic Rocks (Lower-Middle Eocene)	Clastic Sedimentary Rocks
Evaporite Sedimentary Rocks (Lower-Middle Miocene)	
Clastic Rocks (Sarmation) (Middle-Upper Miocene)	
Pelagic Limestone (Cretaceous)	Limestone
Neritic Limestone (Upper Jurasic – Lower Cretaceous)	
Neritic Limestone (Upper Cretaceous - Paleocene)	
Dacid, Rhyolite, Rhyodacite (Upper Cretaceous)	Volcanic Rocks
Undifferentiated Volcanic Rocks (Eocene)	
Volcanic and Sedimentary Rocks (Middle-Upper Eocene)	Volcano-sedimentary Rocks
Volcanic and Sedimentary Rocks (Upper Cretaceous)	
Volcanic and Sedimentary Rocks (Lower-Middle Jurasic)	

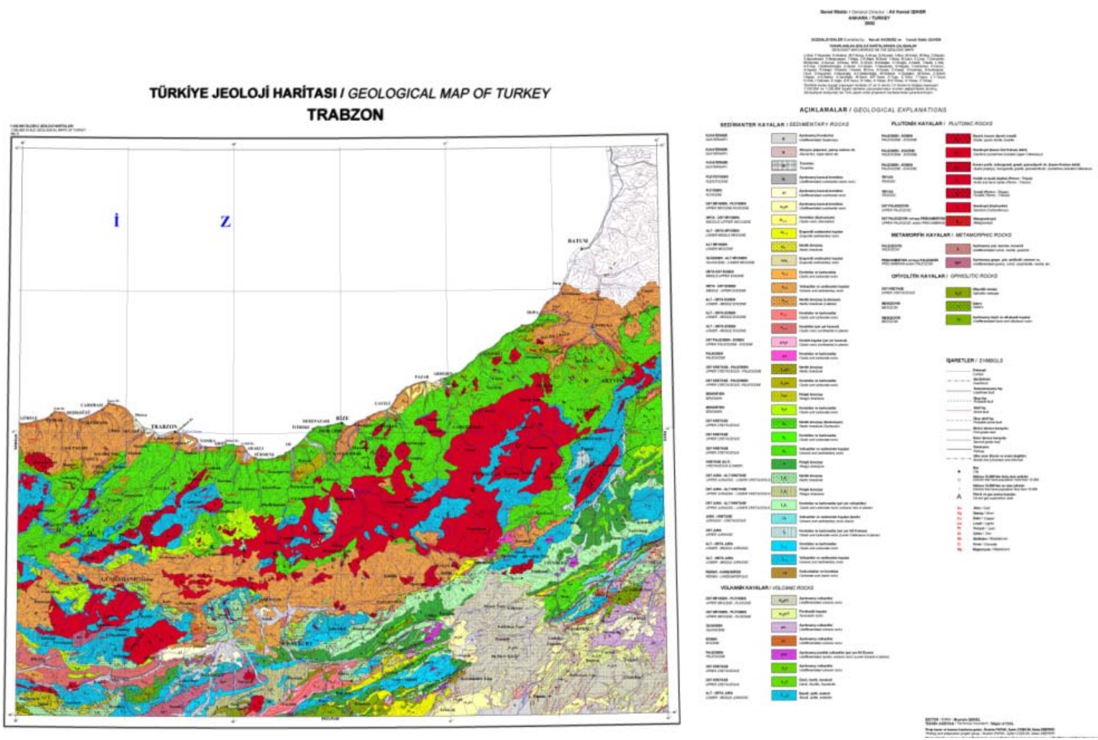

Figure 2.5: Geology map of area with scale of 1:500000.

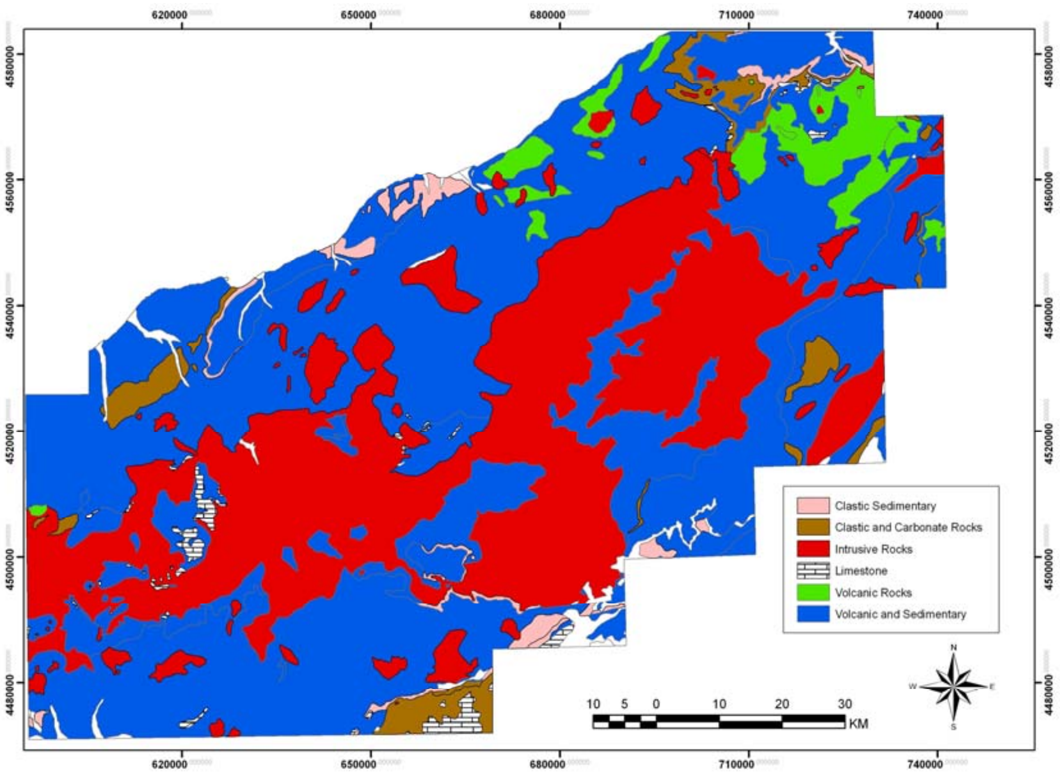

Figure 2.6: Digital Geology Map of study area that has been generalized to six lithologic units.

2.1.5. Satellite Images

One of the stages in this study is to detect the extent of actual glaciers existing in the area. Landsat 7 ETM+ (Enhanced Thematic Mapper) images are selected for this reason. Landsat images have been provided from USGS (United States Geological Survey) website as two frames; 172_31 and 172_32 (Figure 2.7). The date of image acquiring is 08.09.2007. Landsat 7 ETM+ produces images via seven bands at different range of electromagnetic spectrum. All bands have 30 meters spatial resolution except for thermal band which is 60 meters. Coordinate system of the images is UTM WGS84 Zone 37 being consistent with other data.

After obtaining the images, geometric and atmospheric corrections are performed. Then, histogram matching analyses is applied and two frames were mosaiced. In addition "histogram equalization" process which is the one of spectral enhancement technique is applied to each band in order to increase the interpretability of images. Consequently the satellite image became ready for processing and detecting actual glaciers in study area (Figure 2.8).

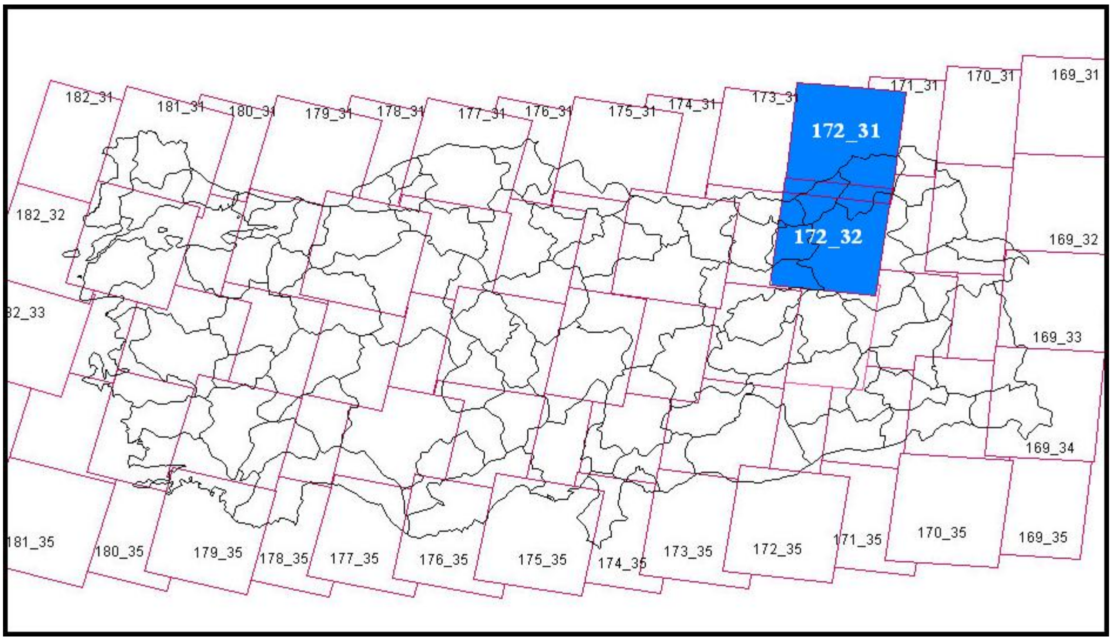

Figure 2.7: Index of Landsat 7 ETM for Turkey, and two frames used in the study.

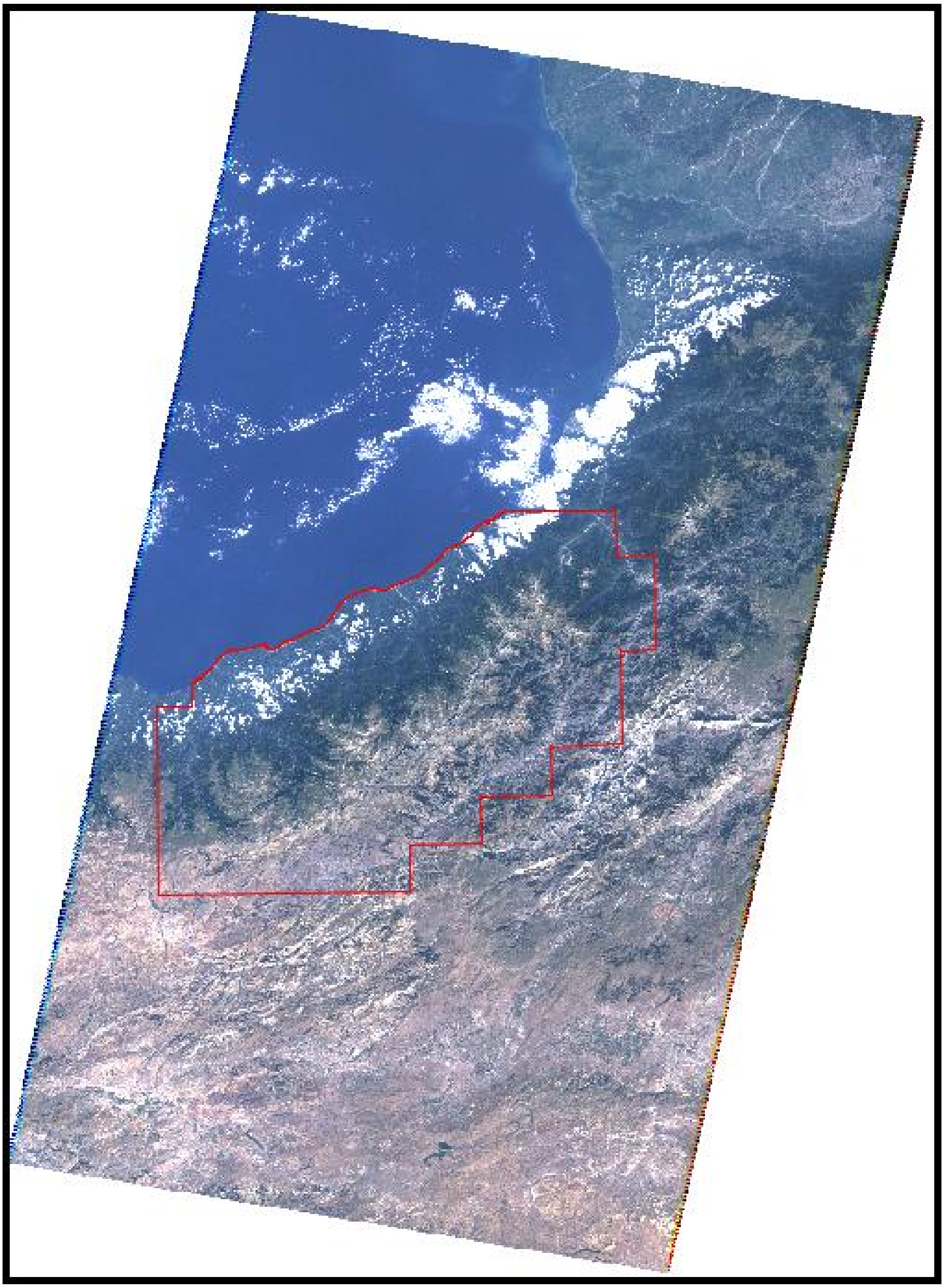

Figure 2.8: Landsat 7 ETM images displayed as colored images (1,2,3; RGB). (Overlaid with interested area).

2.2. Methodology

The methodology of study consists of three main stages: 1) Data input and pre-processing, 2) Data management and processing, and 3) Integration and evaluation. A simple flow-chart showing these stages are shown in Figure 2.9.

Data input and pre-processing: This stage includes data input that are provided from related institutions, and preprocessing of these raw data. Five data sets used in the study are digital topographic maps, analogue topographic maps, digital hydrographic maps, analogue geologic maps, and satellite images. Preprocessing of these input data vary depending on the properties of individual data. Digital maps (topographic and hydrographic) are merged and converted into applicable formats. Analogue maps (topographic and geologic) are scanned, georeferenced and mosaiced in raster format. They are digitized and converted into vector format followed by reclassification in accordance with the purpose of the study. Satellite images (two frames) are mosaiced after histogram matching.

Data management and processing: The second part of methodology consists of management, processing and analyses. After preprocessing of datasets, all layers are processed and analyzed individually.

For the digital topographic map a DEM and its derivatives (aspect and slope maps) are generated. For this, the contours lines are converted into point data. Applying Triangulation Irregular Network (TIN) model a surface model of study area is obtained. Finally this surface model is interpolated into raster format with pixel size of ten meters. Aspect and slope maps are derived from DEM, 360° for aspect and 90° for slope. At this point a general geomorphologic characterization of area is investigated. In order to examine the area from summit to sea level, the north side is extracted and the main rivers layer of this part is generated. Hypsometry analyses are carried out and longitudinal profiles of northern part are investigated. Depending on results and taking into account the previous studies, the 1500 meters elevation contour is accepted as the boundary between glaciated and unglaciated area. Thus this elevation is taken as the boundary of the study area and after this point this area is investigated in detail.

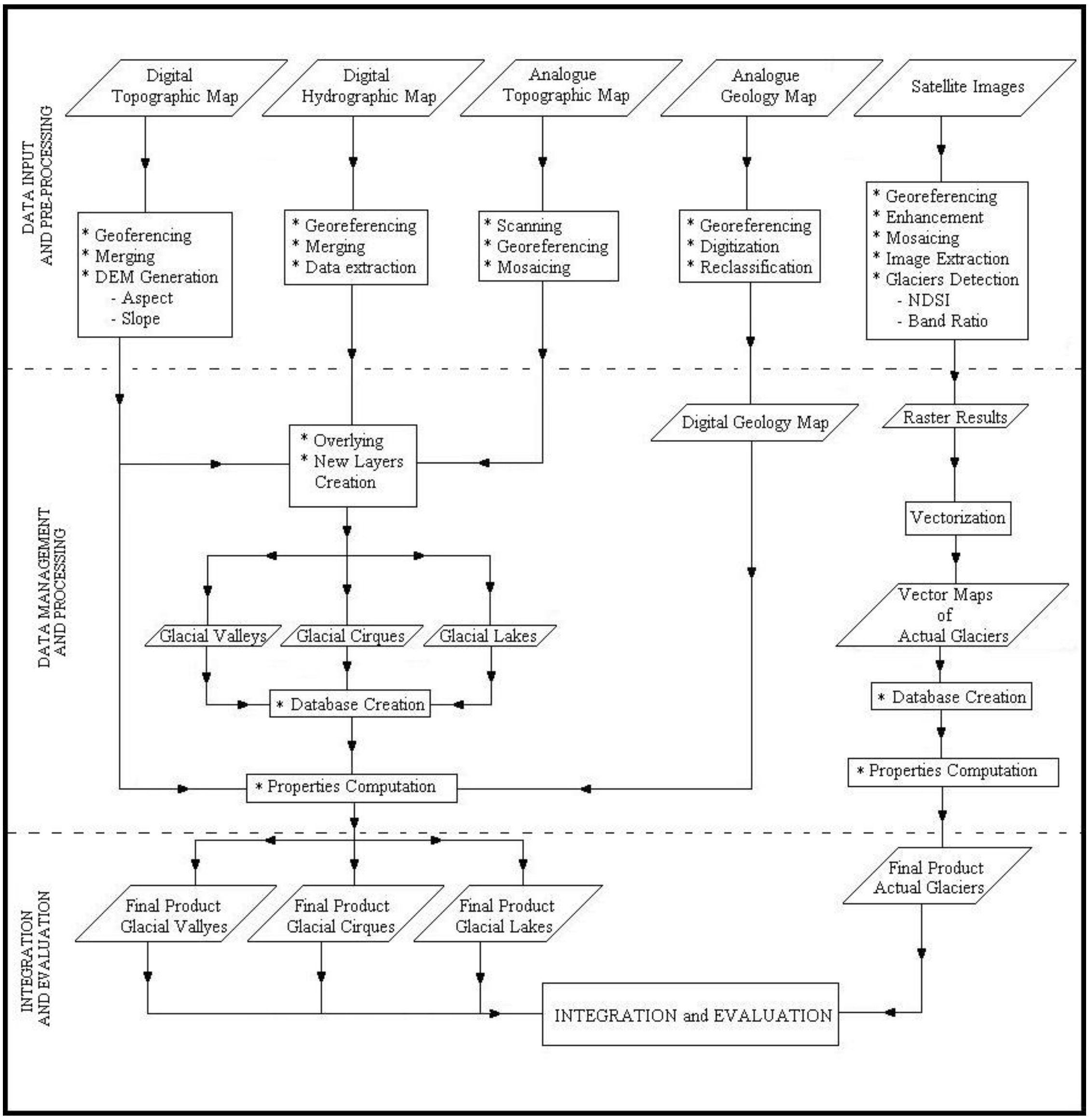

Figure 2.9: Flow-chart of methodology.

The areas over 1500 m are compared with the lower 1500 m with respect to elevation, aspect, and slope in order to interpret the differences between glaciated area and unglaciated areas. The study area above 1500 m is analyzed in two parts as northern and southern separated by the drainage divide.

The main part of this section is the creation of databases for glacial valleys, glacial cirques and glacial lakes. The databases are created by overlying the contour map, DEM, digital hydrographic map and mosaiced analogue topographic map. These glacial shapes are manually digitized on related layer. For each layer several parameters which represent these features are determined. Consequently the final products of glacial valleys, glacial cirques, and glacial lakes are prepared.

Parallel to GIS applications, in order to detect the actual glaciers, satellite images are processed via two methods; Normalized Difference Snow Index (NDSI), and Band Ratio. Accordingly, the glaciers existing in study area are detected in raster format. In order to use these data in GIS efficiently they are vectorized; spatial properties of glaciers are computed and saved into its database. Thus the final product of actual glaciers is prepared.

All these processes and analysis are organized in the following five chapters. Geomorphologic characterization of the area is explained in the next chapter followed by four chapters each focusing in one type of glacial features, namely, glacial valleys, glacial cirques, glacial lakes and actual glaciers.

Integration and evaluation: In the last stage of methodology, individual products generated are evaluated. In addition by integrating all final products the relationships between glacial shapes are determined and interpreted.

CHAPTER 3

GEOMORPHOLOGICAL CHARACTERIZATION OF THE AREA

3.1. Accuracy of DEM

DEM is the three dimensional model of a region that represents the surface. Several methods for creating DEM can be found in the literature. In this study the DEM was generated from digital topographic map containing lines and points of elevations. After merging the 80 topographic sheets at 1/25000 scale that contain lines and points, the nodes of lines are converted into points producing a point data. This point map is converted into three dimensional surface model using Triangulation Irregular Network (TIN); and finally TIN model is converted into raster format as DEM with 10 m pixel size (Figure 3.1).

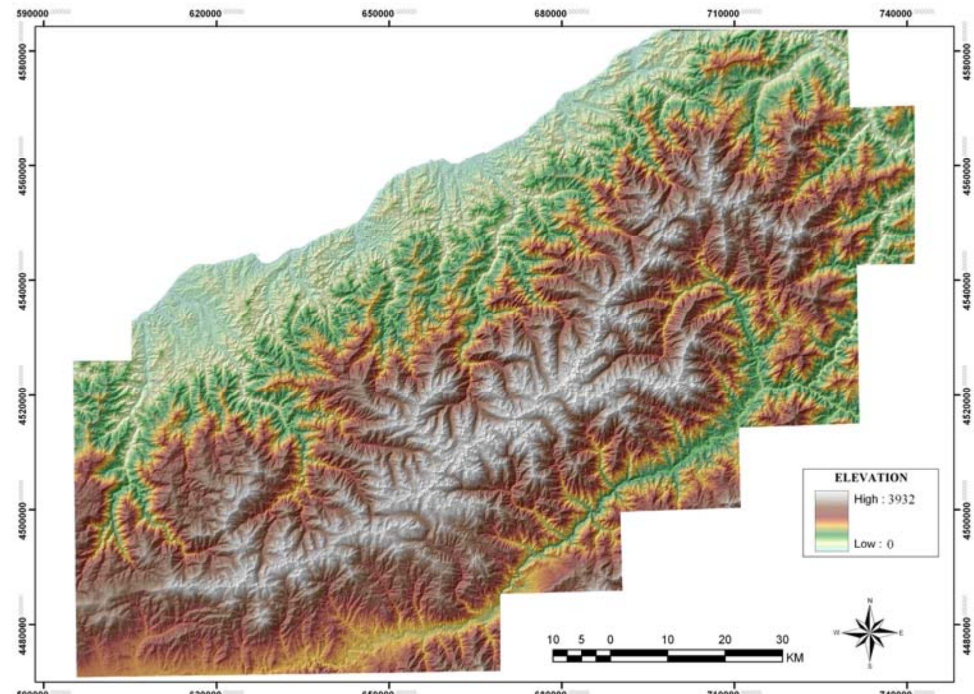

Figure 3.1: Digital Elevation Model of the region.

After the DEM is generated, its accuracy is computed. The Root Mean Squared Error (RMSE) which is the commonly used for accuracy assessment, was selected and used. The equation is illustrated below.

$$\text{RMSE} = \sqrt{\sum_{S=1}^{n} \frac{\left(Z_S - \hat{Z}_S\right)^2}{n}} \, ,$$

where the value Z_S is called observation at location s, $\hat{Z}_S$ is called prediction value and n is the number of observation.

In order to compute the accuracy, 40 points are generated randomly through study area. The true values of these points are obtained from topographic map and compared with values obtained from the DEM (Table 3.1). Accordingly, the DEM has a vertical accuracy of 2.06 m.

Table 3.1: The true and computed values of random points for accuracy assessment.

Point ID	Original Value (Z_S)	DEM Value ($\hat{Z}_S$)		Point ID	Original Value (Z_S)	DEM Value ($\hat{Z}_S$)
1	1010	1009		21	2530	2530
2	2190	2185		22	2790	2791
3	1360	1360		23	2800	2798
4	320	322		24	2000	2001
5	2440	2437		25	750	745
6	2650	2646		26	2050	2050
7	2270	2270		27	2520	2522
8	2230	2230		28	1400	1400
9	2500	2500		29	2040	2039
10	1530	1528		30	1170	1172
11	1780	1778		31	2960	2964
12	1660	1660		32	1490	1489
13	930	929		33	2760	2761
14	390	390		34	1140	1143
15	270	270		35	3380	3381
16	830	827		36	2180	2180
17	1250	1247		37	3020	3020
18	1710	1707		38	800	799
19	2160	2160		39	2440	2441
20	2020	2023		40	1650	1650

3.2. Determination of Study Area (glaciated vs unglaciated areas)

Since the main focus of this study is the area glaciated in the region, a boundary should be drawn to include this area. This boundary will then constitute the actual study area. To determine the boundary, a certain elevation should be selected so that the region above this elevation will be considered as glaciated area. In order to determine the most suitable elevation, two tools are used in this study. These are the hypsometry curve and longitudinal profiles of the main rivers.

3.2.1. Hypsometry curve

Hypsometry analysis shows the distribution of area according to elevation. Generally it is expected the area distributes linearly between minimum and maximum elevation, however this linearity could not be seen everywhere because of erosion and deformation of surface.

Hypsometry of northern part of the area shows that the elevation distributes irregularly with two peaks at 100-300 m and 2250-2750 m (Figure 3.2). The first peak points out the deposition zones and the other indicates erosion by glaciers. The hypsometry line gradually decreases from first peak up to 1700 m where it starts to increase up to second peak. This rising shows the effect of glaciers that flattened this area by their movements. Depending on this observation it can be claimed that glaciation acted down to 1700 m at minimum.

3.2.2. Longitudinal Profiles of Rivers

Longitudinal profiles of rivers are another indicator for finding lower boundary of glaciated area. These profiles show a clear change at end points of glaciation. The valley glaciers scrape their floor and flatten the valley bases. In addition, at the end points valley glaciers accumulate the materials that they had broken off from surface when moving. After this point valleys change into fluvial valleys. Therefore longitudinal profiles of rivers show lower slope when flowing in glacial valleys, especially at end point profiles become flat.

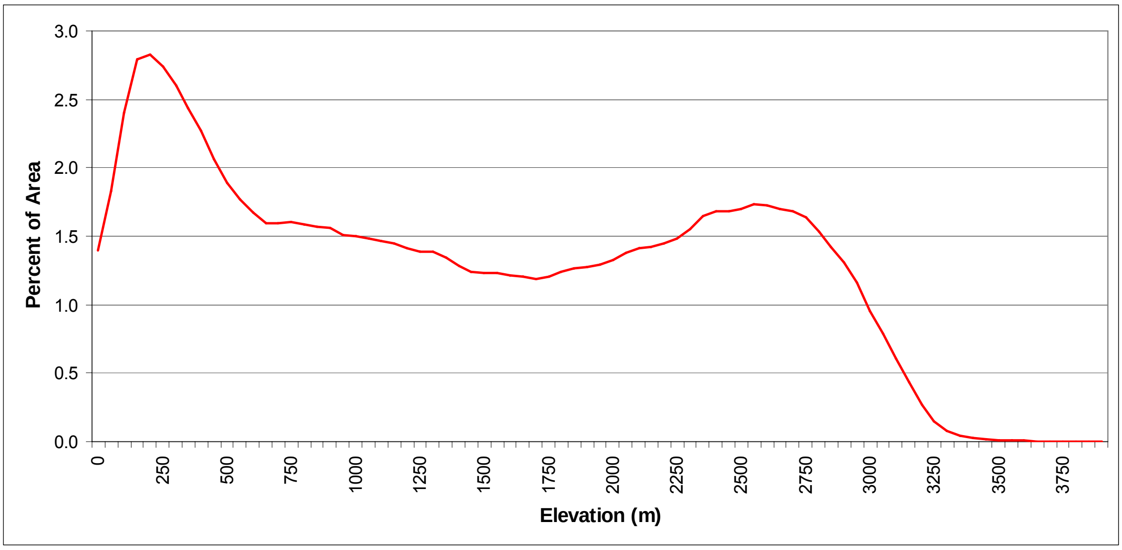

Figure 3.2: Hypsometry of northern side.

For the determination of the boundary between glacial and fluvial valley, the profiles of major rivers starting from the summit flowing down to Black Sea are examined. Accordingly, there are seven rivers to be investigated. These are Kabisre, Abunoga, Fırtına, Sabuncular, Iyidere, Baltacı, and Solaklı (Figure 3.3).

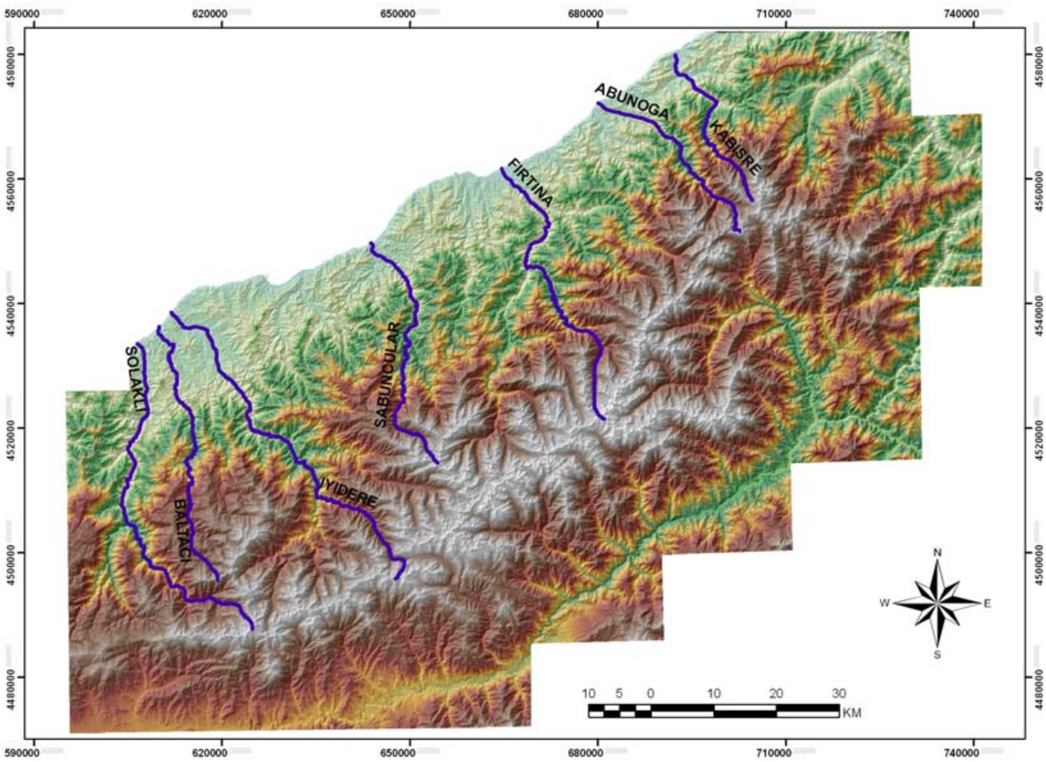

Figure 3.3: Main Rivers flowing through the northern part of the area.

Longitudinal profiles of seven streams are shown in Figure 3.4. An overall observation about these profiles suggests that they have a shape with two concave and one convex part. The first concave part represents the glacial valley while the second concave part indicates the fluvial valley. The convex part of profiles show the boundary between these two different valley types on the same river. The profiles suggest that the convex parts of profiles locate between 1500 and 2500 m. This means the valley glaciers flow down and end at elevation between 1500 and 2500 meters, and from this point the valleys change into fluvial valleys (Figure 3.4).

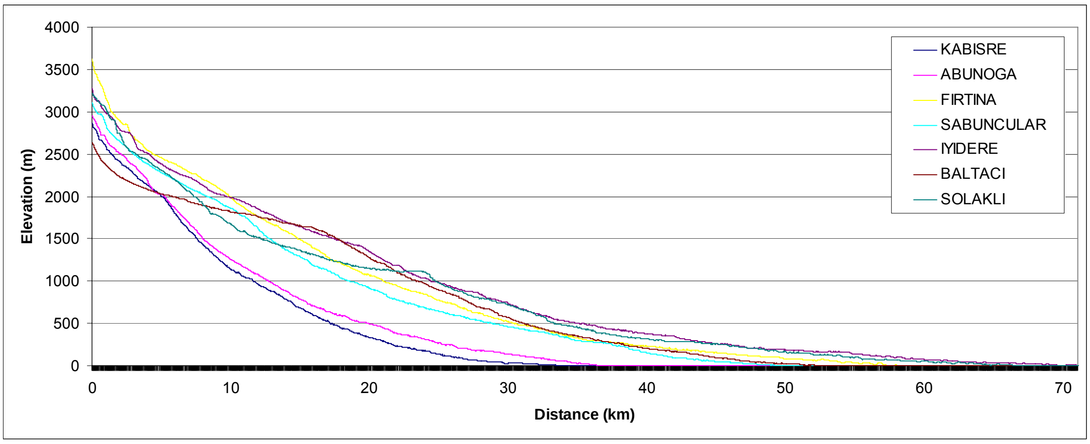

Figure 3.4: Overlapping longitudinal profiles of rivers on the northern side.

The profiles of the rivers are given separately in Figure 3.5. Kabisre River starts from about 2800 m, flowing for 32 km is connected to Black Sea. Its profile indicates that glacial valley changes into fluvial valley at about 2500 meters elevation. Abunoga river having 36 km length starts from about 3000 m and changes into fluvial valley about at 2400 m elevation. The next river, Fırtına River, on the other hand, has different profile characteristics because of having a large basin and starting from higher elevations. The total length of this river is 58 km. The profile of this river shows three concave parts and two convex parts. The summit points of convex parts have elevations of about 1500 m and 2300 m. The convex part of profiles shows the end point of glaciers. Therefore it can be claimed that the valley glaciers are developed in this valley at two different time periods. The first valley glacier had moved down to 1500 m during glaciation era; and it had melt and retreated during interglacial era. Then in next glacial era, valley glacier is developed for the second time, and moved down to 2300 m.

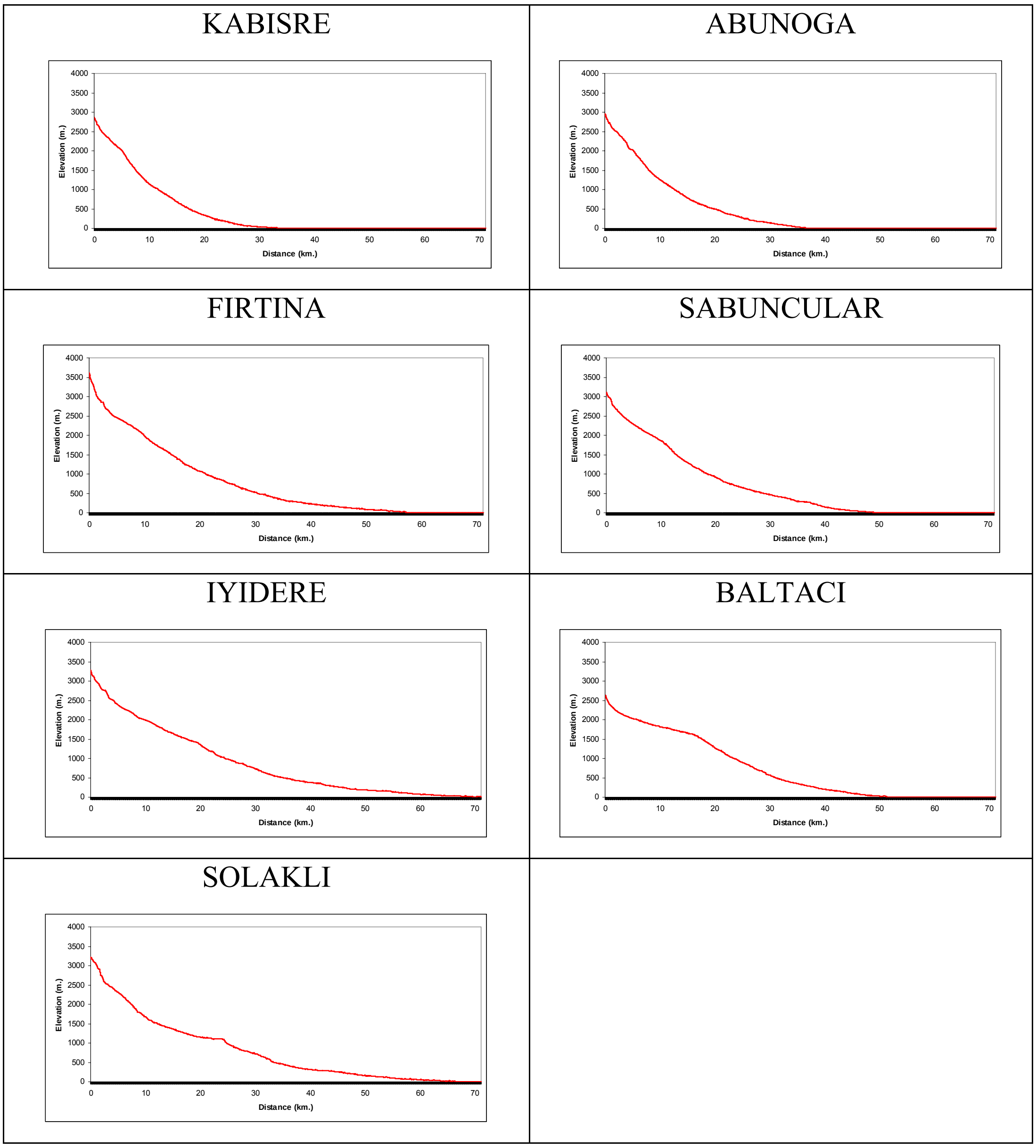

Figure 3.5: Longitudinal profiles of rivers on the northern side of the area.

The Sabuncular river starts around 3000 m with a length of 48 km. The glacier had ended at 1800 m. The elevations for end points of glaciation for other rivers (Iyidere River, Baltacı River, and Solaklı) are 1600, 1750, and 2100 meters respectively (Figure 3.5).

Based on these observations, the 1500 m elevation line is accepted as boundary between glaciated and unglaciated area. Therefore this elevation line has constituted the actual boundary for study area (Figure 3.6). The glacial features in the next four chapters will be investigated in this area.

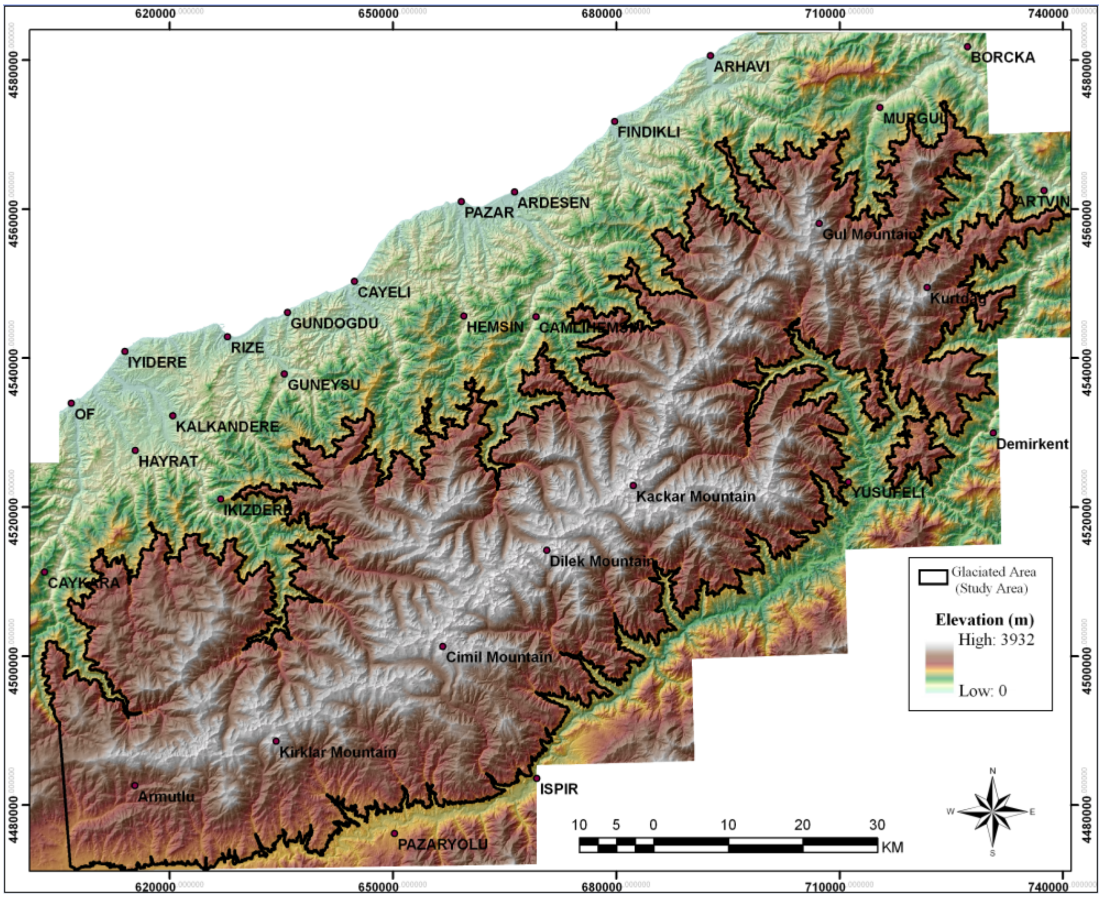

Figure 3.6: Boundary of the study area which is affected by glaciations.

3.3. Comparison of Glaciated and Unglaciated Area

In order to determine the effects of glaciation, the glaciated and unglaciated regions of the area are compared. This operation is carried out only on the northern part of the area because the southern boundary almost coincides with the Çoruh River. The northern part, on the other hand, include the region from the summit (drainage divide) to the sea level.

Northern part of the area is divided into two regions based on the 1500 m elevation line. Glaciated and unglaciated areas are located to the south and north of this line, respectively (Figure 3.7).

Slope and aspect values of these two regions are computed separately and compared in order to find out how glaciations influenced or changed the area with respect to these two properties.

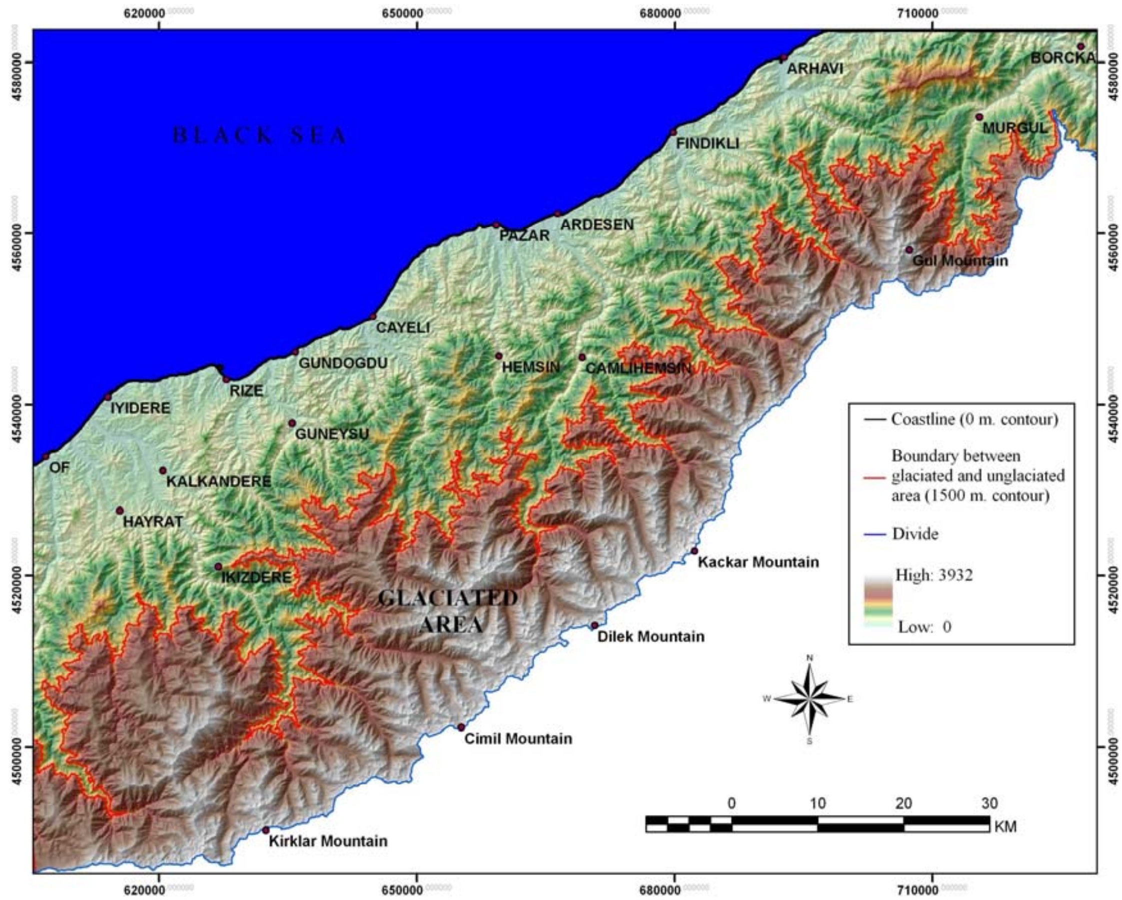

Figure 3.7: Distribution of glaciated and unglaciated area.

Glaciers scrape and erode the surface when moving. At the point where they melt, they accumulate the materials they carry. So, both erosion and accumulation can change the slope condition. The slope values of glaciated area (above 1500 m) and unglaciated area (below 1500 m) are calculated separately. The frequencies of individual slope intervals are converted to percentages in order to standardize both. Then the two values of the same interval are subtracted from each other to find the difference. The result of this operation is given in Figure 3.8 which obtained by subtracting percentage of unglaciated interval from glaciated intervals. Accordingly, the positive value in this resultant histogram indicates the dominance of "glaciation area" and the negative value shows the domination of "unglaciated area" at that part of slope.

The pattern of the histogram in the figure suggests that the slope forms four distinct intervals of positive and negative values. In the negative intervals the unglaciated values dominate whereas in the positive intervals the glaciated ones. Accordingly, the first interval (0-12 degrees) should correspond to low elevations in the region mostly in the coastal areas. The second interval (12-30 degrees) represents the floors of glacial valleys and cirques. The third interval (33-45 degrees) corresponds to low slope areas of glaciated areas such as the hill tops and gentle slopes of the cirques. The last interval (greater than 46 degrees) might represent the steep slopes of valleys and cirques, and ridges between cirques named known as arets. It should be, however, noted that the frequency of this interval is minimum among the others suggesting that spatial extend of this interval is limited in the area.

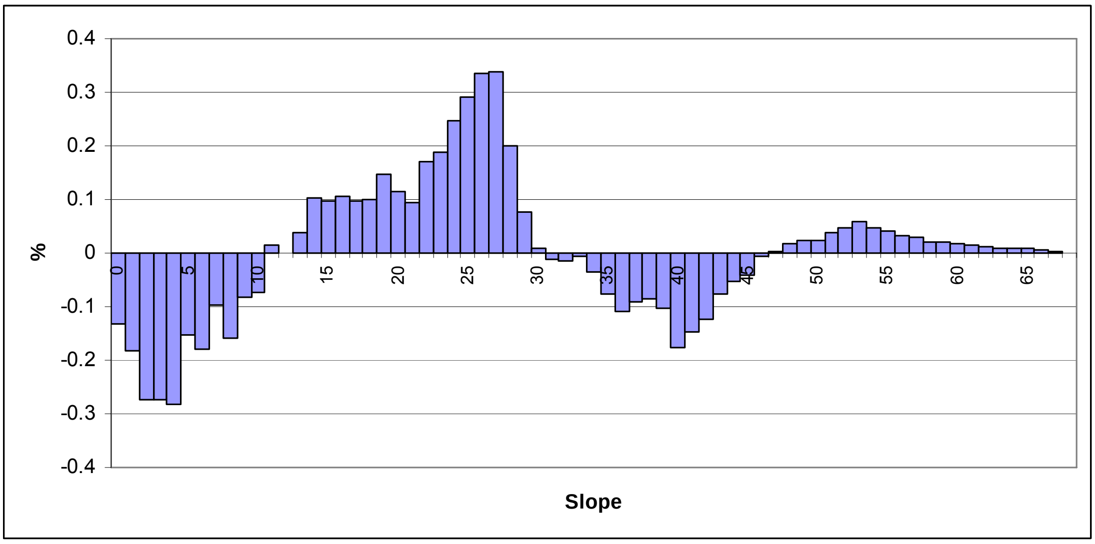

Figure 3.8: Slope differences between glaciated and unglaciated areas.

Similar to the slope the aspect values of glaciated and unglaciated areas are also investigated on histogram prepared at 10-degrees interval (Figure 3.9). Two most distinctive intervals are the negative interval between 90 and 200 degrees; and a positive interval between 210 and 300 degrees. The first interval represents the unglaciated areas that correspond to the area between 0 and 1500 m. The maximum concentration in this interval is between 140 and 160 degrees (SSE direction). The second interval with positive values, on the other hand, belongs to the elevations greater than 1500 m. Therefore, the aspect of glaciated areas points the direction of NWW.

Other regions in the histogram do not represent a consistent pattern suggesting that the aspects values in these regions belong to both glaciated and unglaciated regions.

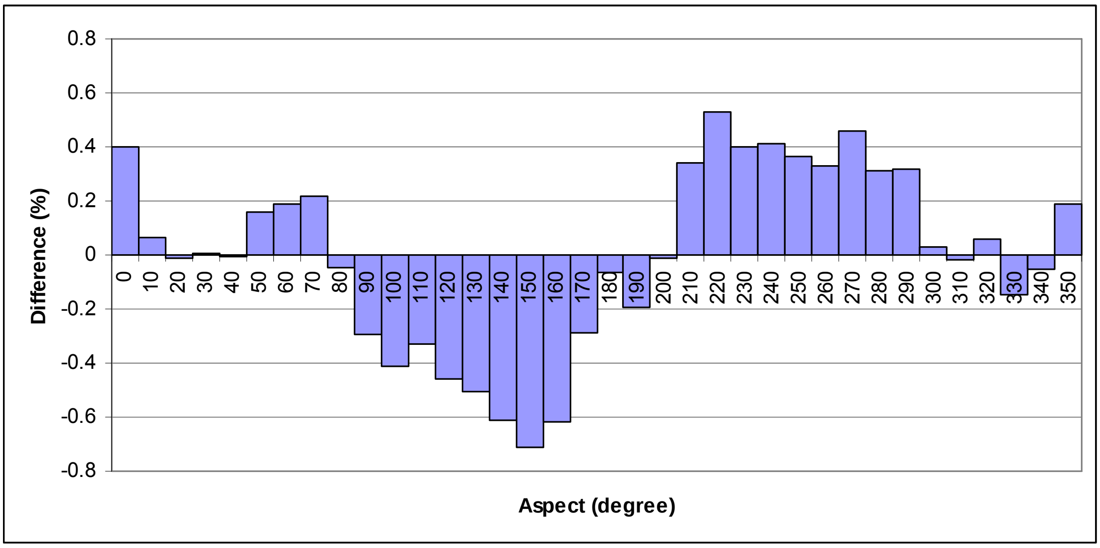

Figure 3.9: Aspect differences between glaciated and unglaciated areas.

3.4. Topographic Properties of the Study Area (Glaciated Area)

As indicated in the previous sections, the study area is considered to cover the region above 1500 m. Aerial extent of this area as shown in Figure 3.10 forms a belt in NE-SW direction. The drainage divide in the area passes almost in the middle of this belt dividing the area into two parts. These parts will be referred to as "northern side" and "southern side" from this point on. The whole study area covers approximately 5375 km^2. South side has approximately 2879 km^2 area, and North side has approximately 2496 km^2 area.

Main statistics of topographic properties for the study area are illustrated in Table 3.2. Minimum, maximum, mean, mode, median, and standard deviation values of elevation and slope for the whole area, for the northern part and for the southern part are illustrated separately. Because the statistic values are not applicable to aspect value, this property is not included in the computations.

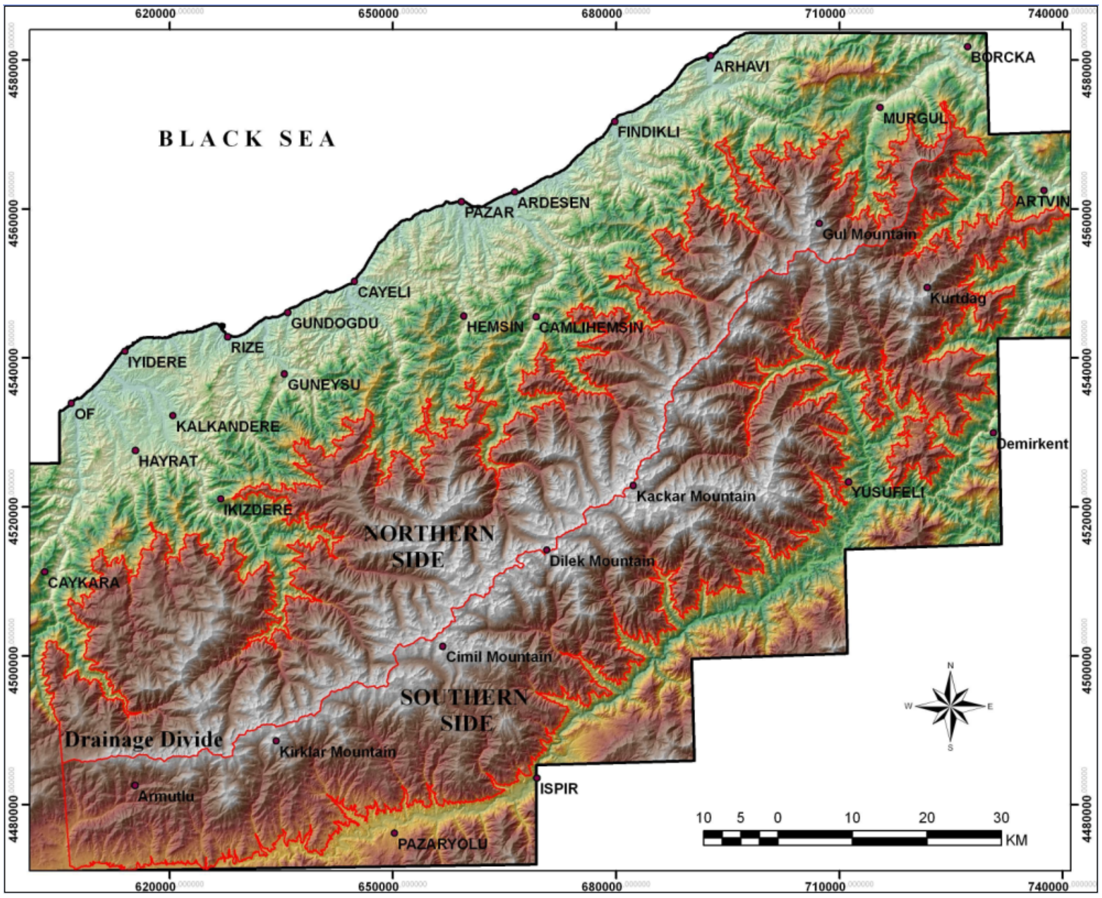

Figure 3.10: North and south side of study area.

Table 3.2: Main statistics of topographic properties of the study area.

		Min	Max	Mean	Mode	Median	StdDev
Elevation	Whole Area	1500.0	3932.0	2280.0	1652.0	2257.0	475.5
	North Side	1500.0	3932.0	2317.7	2397.0	2335.0	460.3
	South Side	1500.0	3932.0	2247.6	1652.0	2195.0	486.1
Slope	Whole Area	0.0	77.0	27.7	27.0	28.0	10.1
	North Side	0.0	77.0	27.8	27.0	28.0	10.1
	South Side	0.0	76.0	27.7	27.0	28.0	10.0

Elevation starts from 1500 m and rises to 3932 m at the summit. Mean elevations are 2317.7 m and 2247.6 m for the north and south, respectively. The variation is obtained by subtracting south side elevation values from north side values. The result is shown in Figure 3.11 at 50 m interval. The difference between north and south ranges from -1 to 1 indicating that the elevation for both sections is almost similar. However, there is a clear pattern in the diagram suggesting that in two intervals (1500 to 2150 m and 3050 to summit) southern part is dominating whereas between 2200 and 3000 m the northern part does. The positive zone suggests the glacial activity (such as truncation) and therefore contains the glacial features namely, the cirques and the glacial valleys.

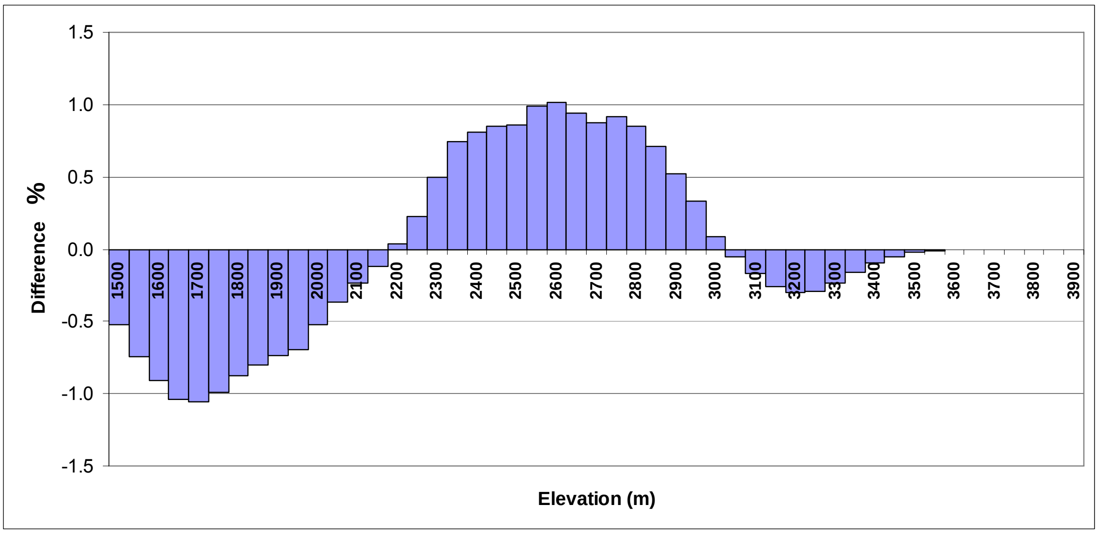

Figure 3.11: Difference of elevation between north and south side.

The statistics of slope indicate that the north and south sides of the study area have close slope values (Table 3.2) Mean slope values are around 28° for both parts. The difference slope values (north minus south), however, suggest that the area is not perfectly symmetric (Figure 3.12). At lower slope values (0 to 33 degrees) the southern and at the larger slope values (35 to 77 degrees) the northern parts are dominating with 0.08 percentages. Therefore, the northern part of the area is slightly steeper than the southern part.

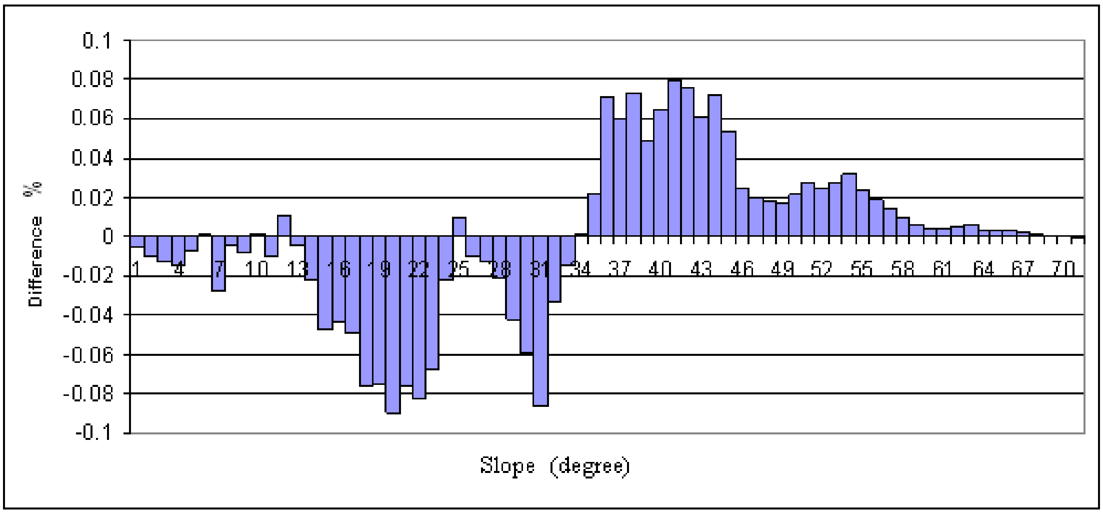

Figure 3.12: Difference of slope distribution between north and south side.

The aspect values of the study area is investigated by histograms at 10-degree interval prepared for the northern and southern parts separately (Figure 3.13 A and B, respectively). The maximum concentrations for both sections are observed at NW and SE, respectively. These values are consistent with the general trend of the mountain chain that extends in NE-SW direction.

One important observation is the presence of aspect values in almost all directions. This is best illustrated by the percentages of the minimum and maximum values which are about 1.5 % and 4.5 % for both parts. Accordingly, both parts of the area are not represented by smooth surfaces, but rather are frequently dissected in almost all directions.

The two histograms are subtracted from each other and is given in Figure 3.13-C. The general pattern of the difference well depicts the aspect property of northern and southern parts. Both positive and negative regions are represented by normal distribution with a maximum positive value between 310-340° for the north; and between 150-170° for the south.

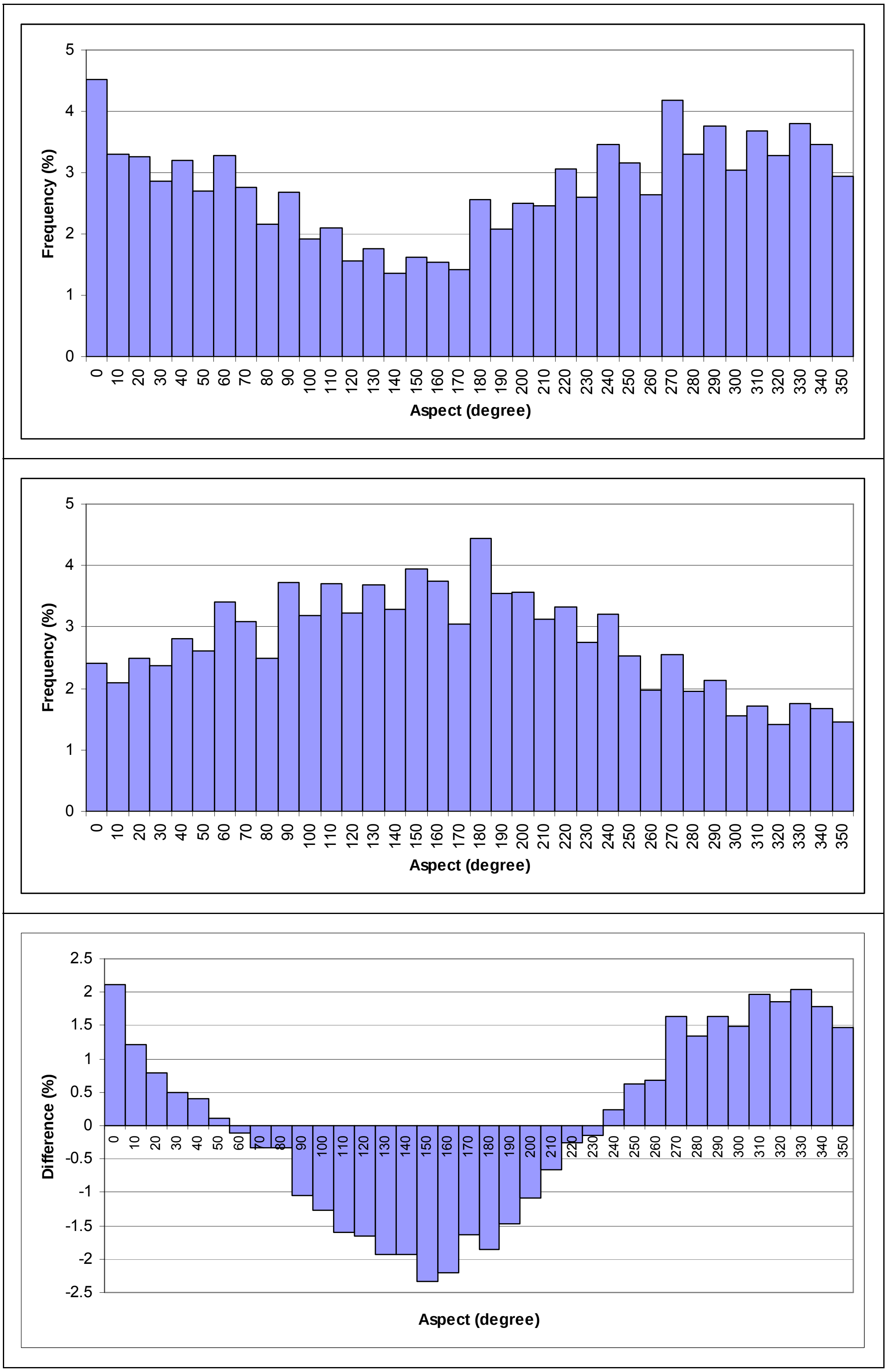

Figure 3.13: The aspect values of A) northern part of the area (upper), B) southern part of the area (middle) and, C) the difference between north and south (lower).

3.5. Hypsometry Analyses of Study Area

Hypsometry analyses are conducted for the whole study area, the northern side, and the southern side separately. The result is shown in Figure 3.14 for 50 m intervals for the whole area. The effect of glaciation is very obvious in this graph as indicated by its pattern. Under normal conditions the hypsometry line should be linear so that as the elevation increases the area should decrease linearly.

Hypsometric curve prepared for the area does not display a linear pattern and is composed four distinct shapes. The first section of the line is between 1500 and 2750 m characterized by a relatively gently slope. The second part is between 2750 and 2950 m with a steep slope. The third part is between 2950 and 3300 m having the steepest slope of the whole area. The last section is between 3300 and 3900 with a gentle slope. According to graph, the first three sections show the maximum deviation from the ideal trend, therefore an intense flattening and truncation is observed in this part. The first region most probably correspond to glacial valleys are surrounding regions. The second and the third region should represent the basal parts and the slopes of the cirques, respectively. The last region, on the other hand, indicates the summits of the area.

Hypsometric curves of northern and southern sections are computed separately to see a probable difference between two parts of the area (Figure 3.15)

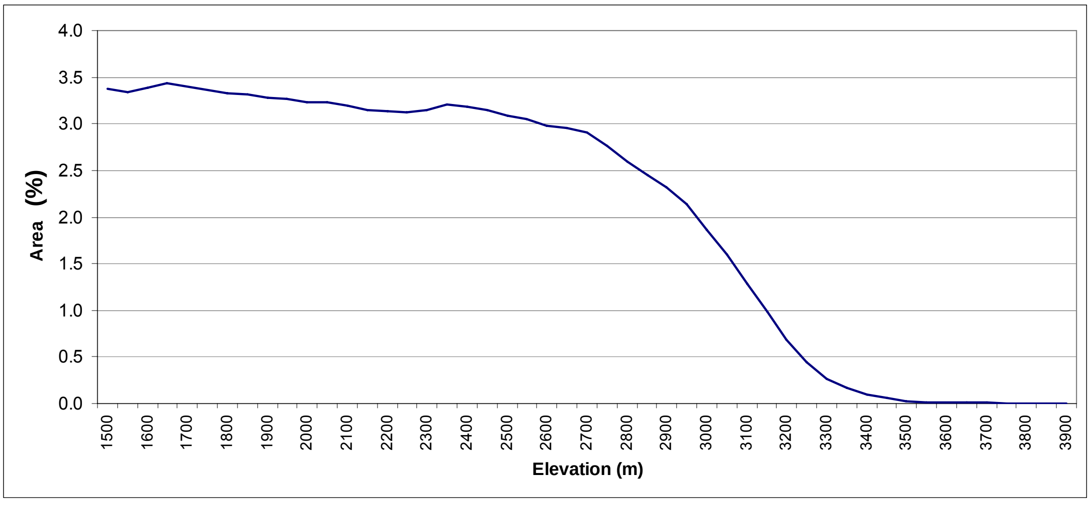

Figure 3.14: Hypsometry line of study area.

The hypsometric curve of the northern part is composed of five sections. Between 1500 and 2200 m, the area is represented by a gentle slope followed by a sudden change between 2200 and 2400 m. After this point the slope is decreasing rapidly as indicated by two sections from 2400 to 2800 and from 2800 to 3250 the latter one being steeper than the former one. The last section is the tail of the line between 3250 and 3900 m elevation. Accordingly, the first two sections represent the glacial valleys which are overemphasized in the second one. The third and the fourth sections, corresponds mainly to cirques most probably including the starting parts of the valleys. The last section stands for the summits at higher elevations.

The hypsometric curve of the southern part of the area is much simpler and resembles an ideal curve with some major deviations. The curve can be divided into three sections with certain generalizations. The first section shows a gradual decrease in slope from 1500 to 2950 m. From this point to 3300 m the curve is steep followed by a gentle slope to the end of the curve. These three parts represent the glacial valleys, the cirques and the summits, respectively.

The difference between the northern and southern parts is clear in the diagrams. Particularly, the maximum difference between 2200 m and 3050 m is noteworthy. In this section, the influence of the glaciers has been much more in the northern part of the area and truncated the surface.

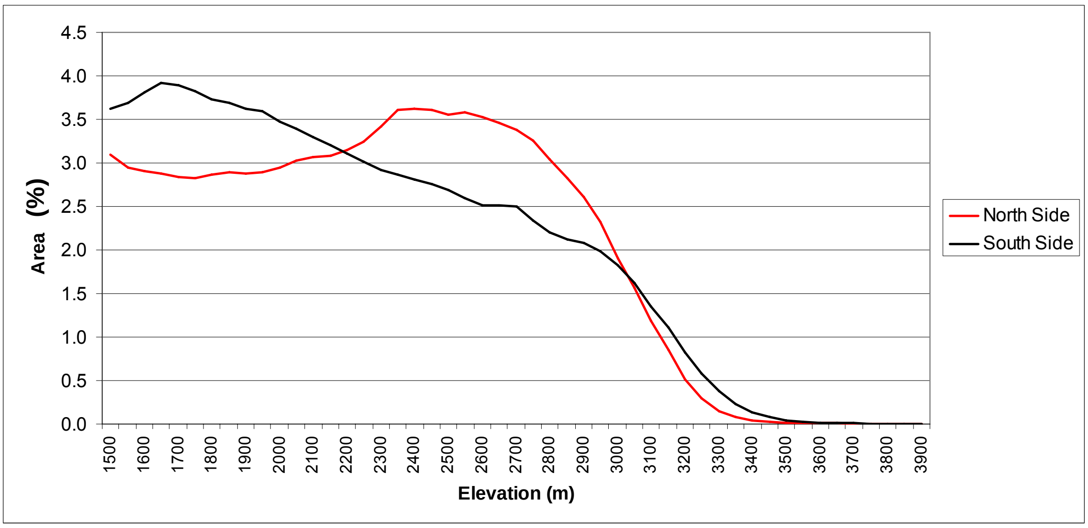

Figure 3.15: Comparison of North Side and South Side in respect of hypsometry.

3.6. Roughness Property of Study Area

A grid data was generated with size of 100 m by 100 m for each grid to investigate the roughness of the surface for the study area. By overlapping this grid layer with DEM, the standard deviation of each grid was computed. Since the initial DEM has pixel size of 10 m by 10 m, each grid contains 100 pixels. Standard deviation of these 100 pixels for each grid was assigned to that grid. Finally the roughness map is generated by coloring this grid map (Figure 3.16).

In general, the western part of study area has a smooth surface compared to the other parts. Therefore, the effect of glaciation is more powerful in the middle and eastern parts. A comparison between the last two sections suggests that in the middle part of the area the roughness has the maximum value.

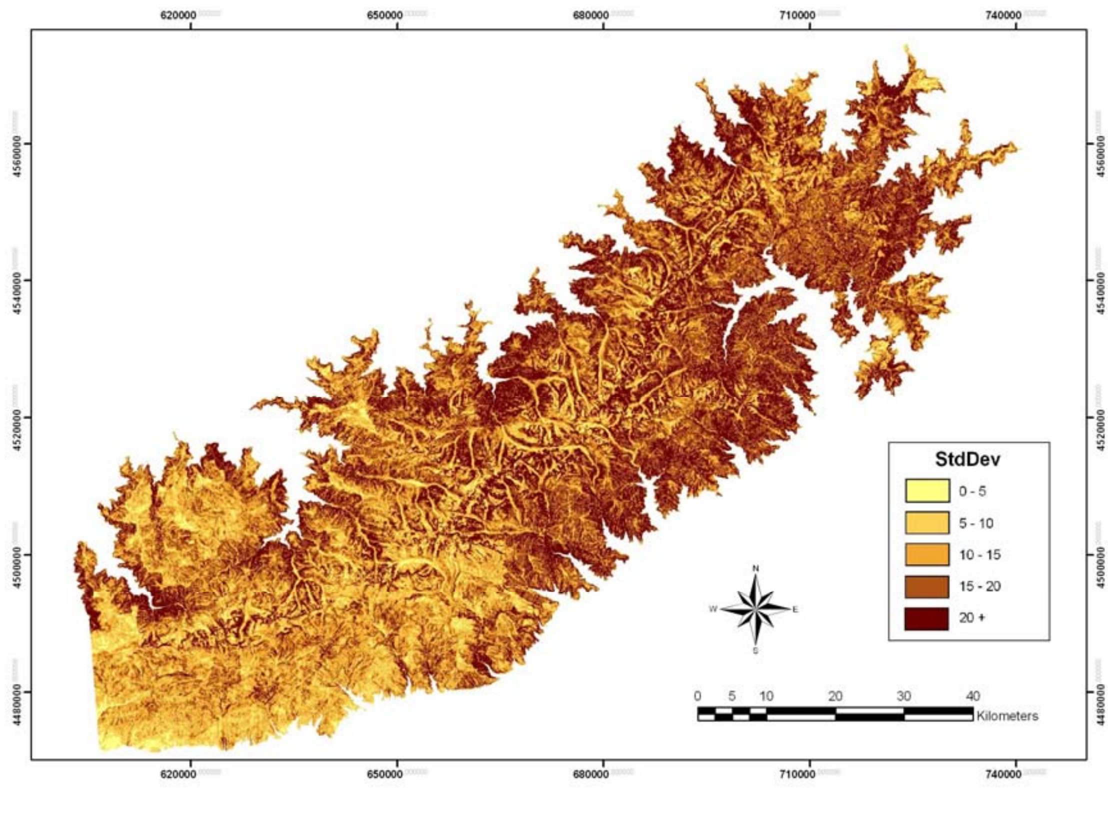

Figure 3.16: Roughness Map of study area.

CHAPTER 4

GLACIAL VALLEYS

4.1. Identification of Glacial Valleys

Glacial valleys located within the study area are digitized manually over the DEM. Digital topographic contour are displayed over the DEM in order to recognize the landscape. The main criterion in the identification of the glacial valley is the determination of the point where the glacial valley changes into a fluvial valley. This point, on the map, corresponds to the point that defines a difference between U-shape and V-shape valleys. Then from this point for each glacial valley the floor of valley has been traced backward up to start point of each valley where the valley joins a cirque. Therefore a glacial valley is confined to the section of a valley between a cirque and a fluvial valley. The valley floor is represented as line in order to use in GIS.

An example of valley determination is illustrated in Figure 4.1. The points A and B in the upper figure corresponds the start and the end of glacial valleys, respectively. The blue lines in the lower figure are the "main glacial valleys" with some "tributary glacial valleys" indicated by red color.

A total of 93 glacial valleys are detected and mapped in accordance with the criteria mentioned above (Figure 4.2). Among these 30 valleys are classified as the "main" and remaining 63 as "tributary". Considering total number of the valleys which is not suitable for GIS analyses, it is decided to concentrate only on the main valleys. Accordingly, 30 valleys are considered in the database (Figure 4.3) that will be mentioned in the next section.

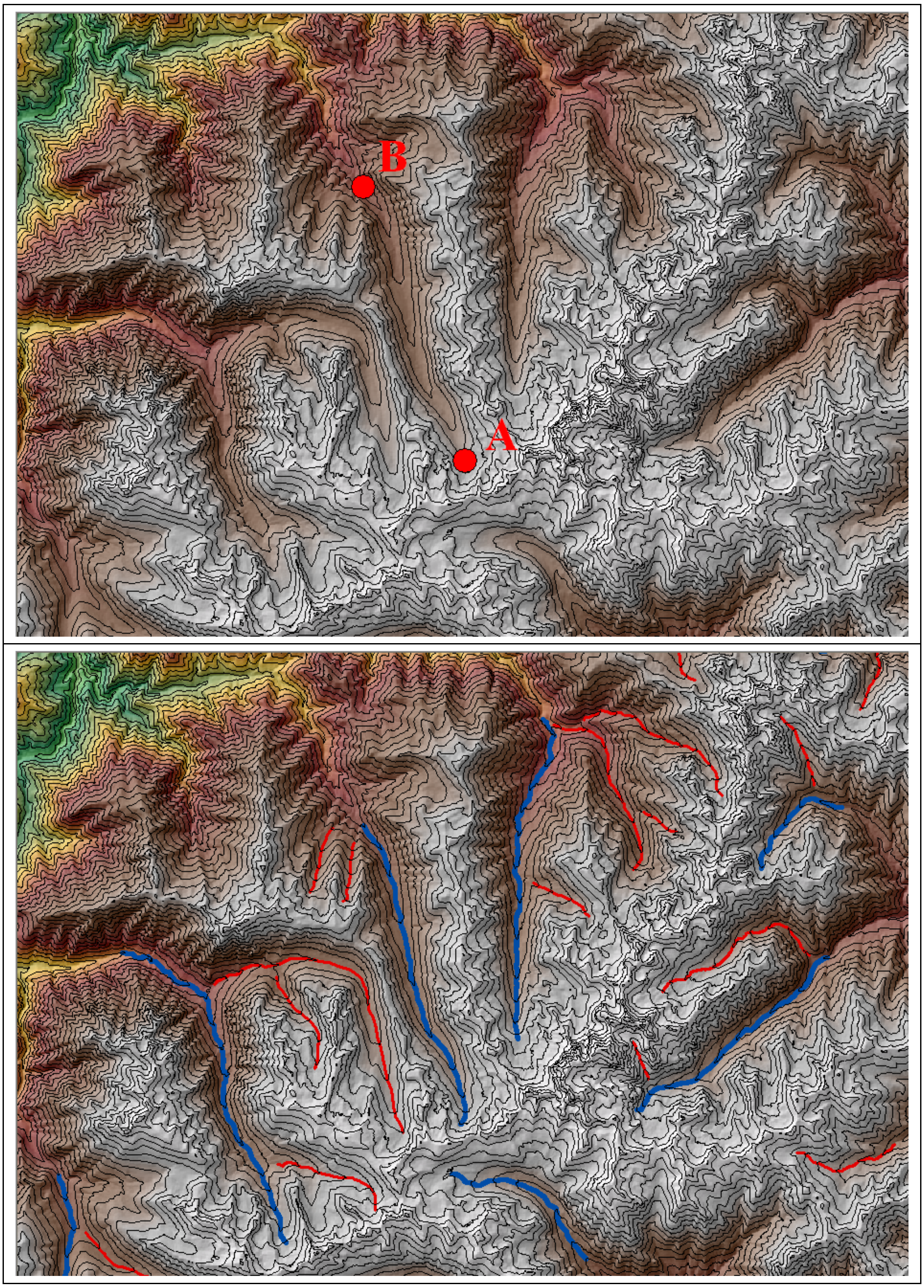

Figure 4.1: Determination of the glacial valleys over the DEM. The points A and B in the upper figure correspond to the starting and the ending points of the valley. The red and the blue lines are the glacial valleys (main and tributary) drawn for this example.

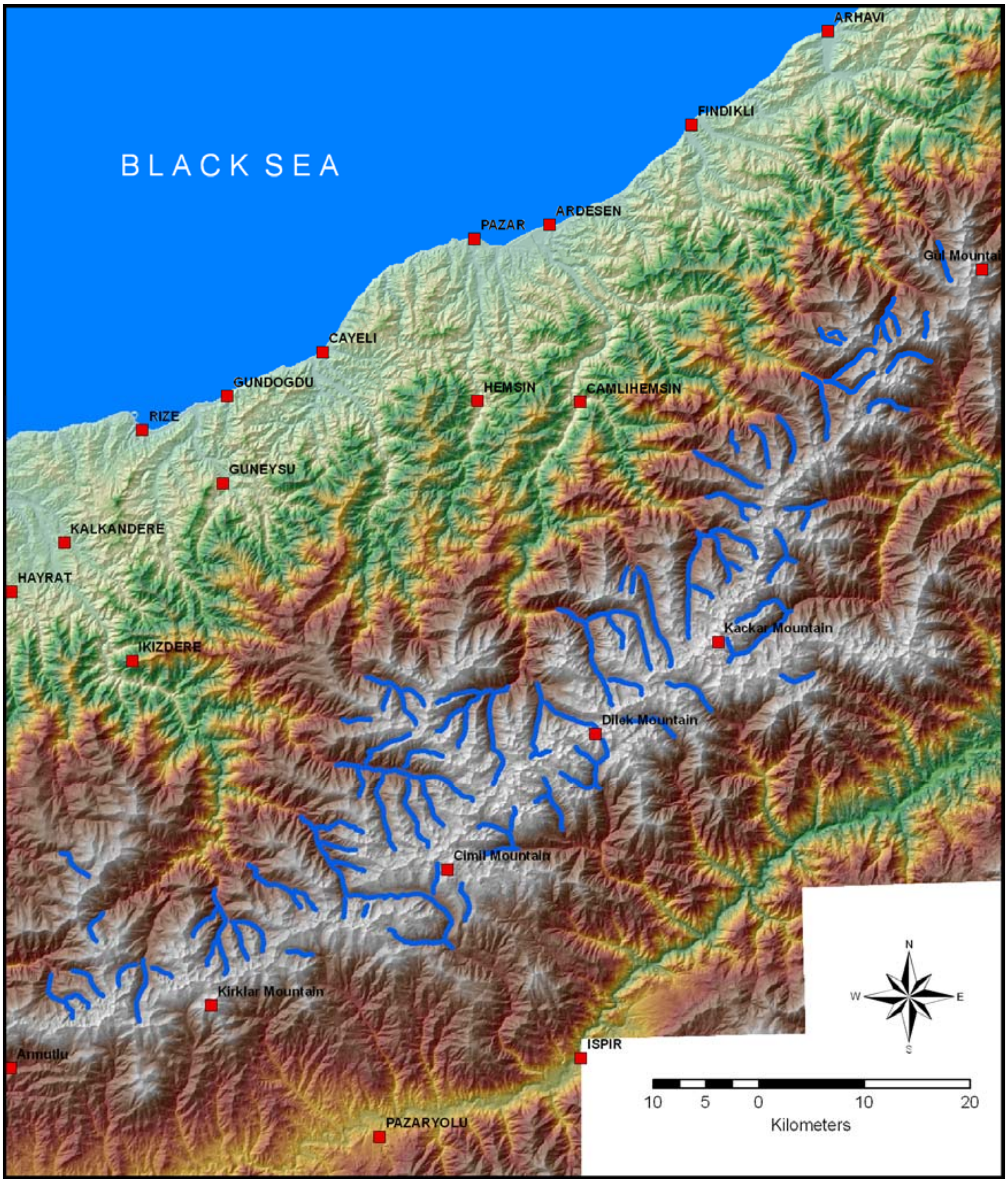

Figure 4.2: All glacial valleys determined in study area.

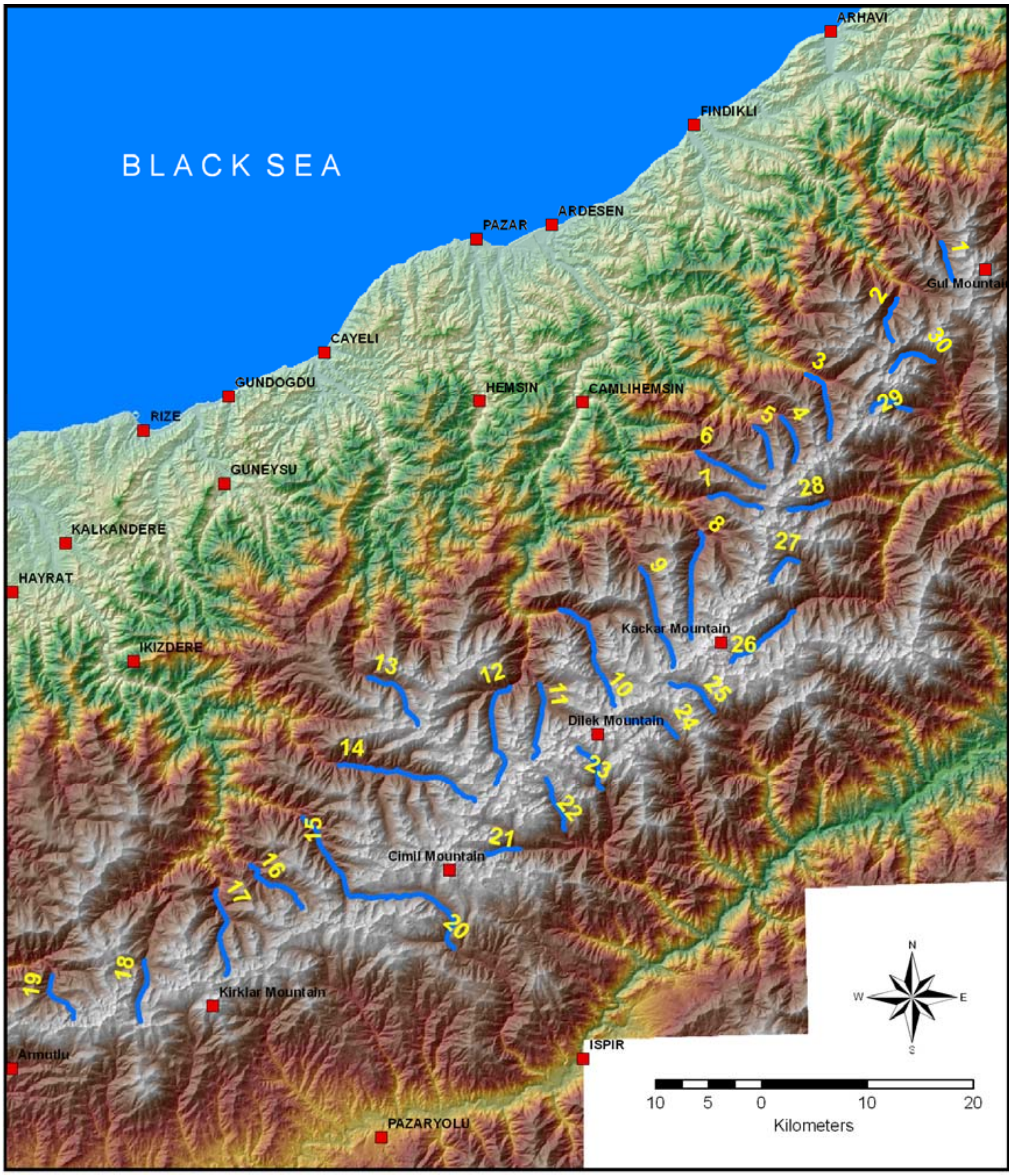

Figure 4.3: Main glacial valleys determined in study area.

Additionally, for each glacial valley an area around the river is digitized which is produced by intersecting the valley with a horizontal surface elevated 100 m above the valley floor (Figure 4.4). This area will be divided into two sections using the river to obtain two sub-areas as east and west to be used in the symmetry analyses. These two sub-basins are stored as two polygons in the database.

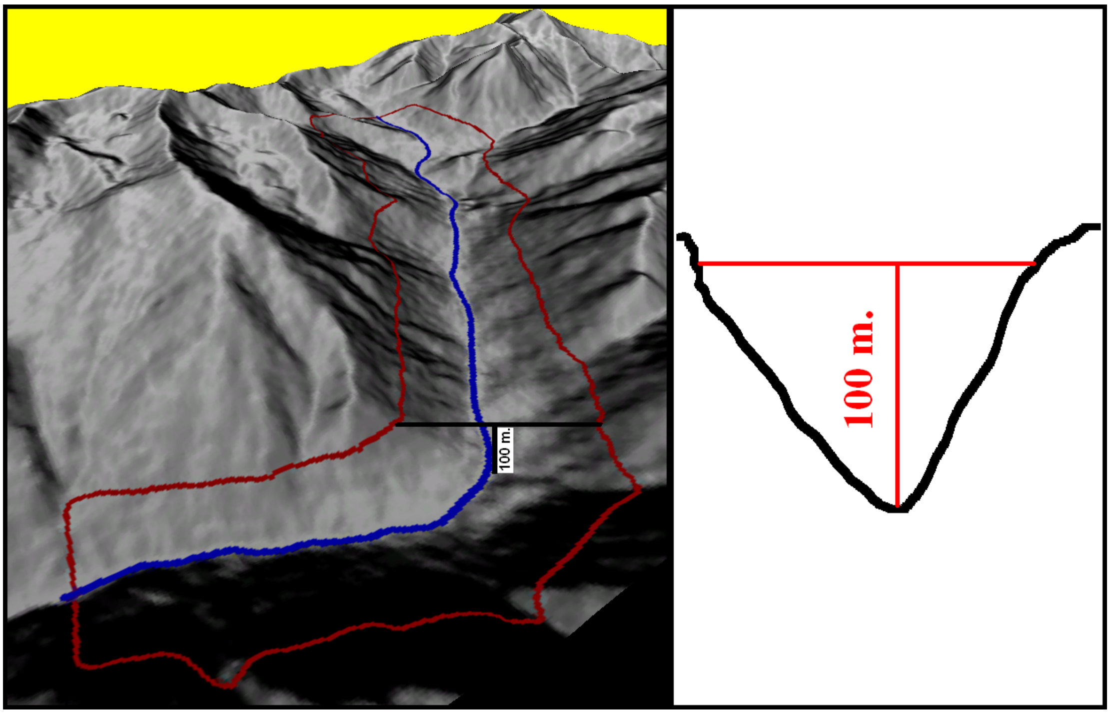

Figure 4.4: Determination of polygon by elevating the valley floor for 100 m.

As a last step the drainage basins (Figure 4.5.) of all glacial valleys are digitized to be used in further analysis. The divide that defines the boundary of the basin passes through the ridges that surround the glacial valley and its tributaries and intersects with the valley where the fluvial valley starts.

4.2 Creation of Database for Glacial Valleys

After digitizing the glacial valleys a database is created for the glacial valleys containing several properties (Table 4.1). Some properties are computed from the lines that represent the glacial valley floors, some other properties are computed from the basins of glacial valleys. A brief explanation of these properties is as follows:

ID: It is unique digital number for each glacial valley between 1 and 30. Starting from east of north side trough west 19 valleys were assigned from 1 to 19 and starting from west trough east on south side the valleys are numbered between 20 and 30.

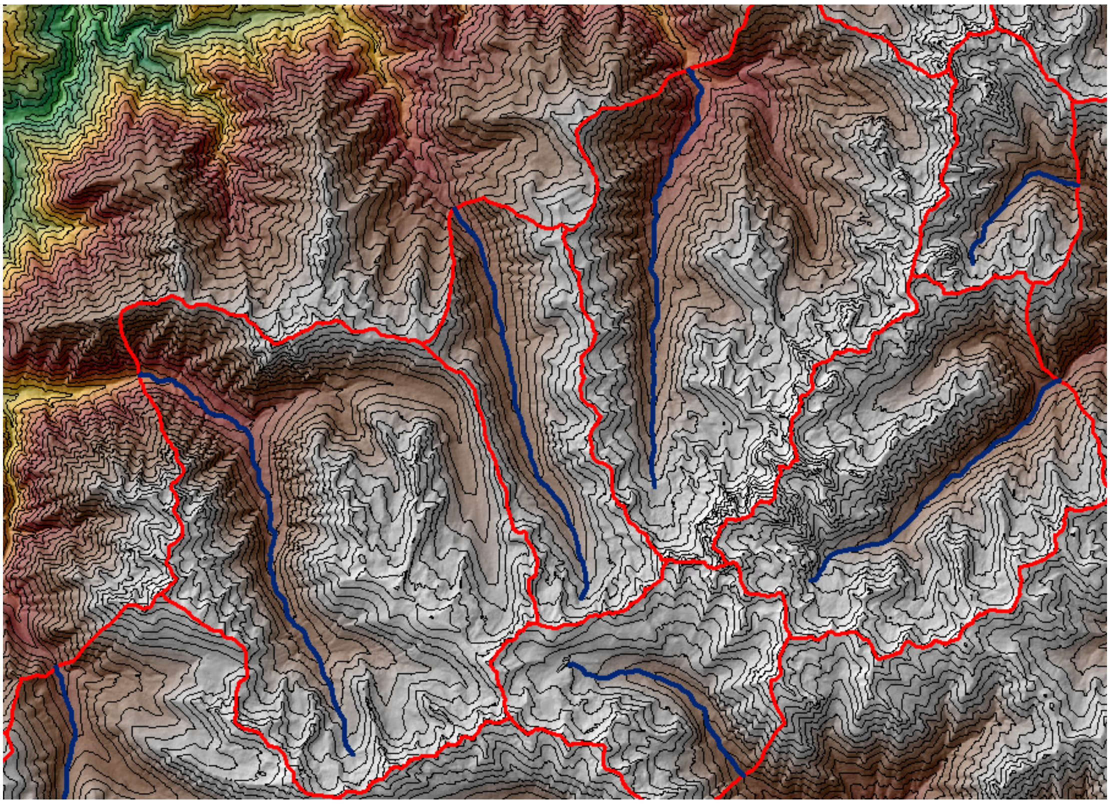

Figure 4.5: An example of drainage basins of the glacial valleys.

Name: It is name of each glacial valley. The names of valleys are mostly taken from previous studies. For the valleys that are not mentioned in the literature, a name is assigned in this study, simply adopting the name of the river flowing in that valley or the nearest settlement name.

Location: Study area is divided in to parts as north and side separated by the main drainage divide. Location refers to the location of the valley either to the north and south of the area in relation to this divide.

Length: Valleys start from cirques and end at change into fluvial valleys. Length for each glacial valley computed as true distance between these two points in metric unit as kilometer.

Shortest Length: This parameter is the shortest linear measurement of each valley between start point and end point in metric unit.

Table 4.1: Database of glacial valleys.

										Basins		Area			Lithology Area (km2)	
ID	Name	Location Side	Length	Shortest Length	Curviness	Max_Z	Min_Z	AVG_Slope	Basin Area (km2)	Basin Perimeter (m)	East	West	Symmetry	Intrusive Rocks	Volcanic and Sedimentary	Limestone
1	ALACAGOL	NORTH	4027.4	3823.6	1.05	2664.0	2051.0	15.2	13.3	15.2	1188803	948708	1.3	2.138	0.000	0.000
2	ABU	NORTH	4624.9	4022	1.15	2623.0	1723.6	19.4	17.7	17.6	1146572	1313219	1.0	2.460	0.000	0.000
3	TUNCA	NORTH	7005.3	6006.7	1.17	2463.0	1506.0	13.7	52.8	32.9	2333066	1559193	1.5	3.619	0.000	0.000
4	ERGUSU	NORTH	5997.3	5301.6	1.13	2558.0	1748.7	13.5	21.4	22.0	1315363	1049551	1.3	2.365	0.000	0.000
5	TOPLUCA	NORTH	5442.1	4967	1.10	2698.4	1791.9	16.7	14.0	17.4	1103163	1296518	1.0	2.400	0.000	0.000
6	KACKAR	NORTH	8968.1	8394.1	1.07	2805.4	1613.1	13.3	21.9	25.9	2079236	2038749	1.0	4.118	0.000	0.000
7	AVUCUR	NORTH	5486	5143.5	1.07	2642.6	1890.8	13.7	16.9	18.9	1519721	1653545	1.0	3.142	0.031	0.000
8	KAVRAN	NORTH	10700.9	10018.4	1.07	2854.0	1657.5	11.2	80.0	41.6	3616149	2861006	1.3	6.350	0.128	0.000
9	PALOVIT	NORTH	10172.8	9813	1.04	2902.2	1997.4	8.9	28.2	28.0	3103064	2974556	1.0	6.078	0.000	0.000
10	ELEVIT	NORTH	11678.7	10418.6	1.12	2915.0	1595.7	11.3	78.4	39.7	3895636	2904504	1.3	6.752	0.048	0.000
11	TATOS	NORTH	7621.2	7028.6	1.08	2928.8	2010.7	12.0	47.8	35.3	2617024	2158040	1.2	3.881	0.894	0.000
12	VERCENIK	NORTH	11174.2	9323.6	1.20	2900.3	1860.0	9.3	80.8	41.7	3063974	3768573	0.8	3.979	2.851	0.003
13	INCESU	NORTH	7461.2	6507.4	1.15	2836.3	1988.3	11.4	27.8	23.2	2236139	2031645	1.0	4.268	0.000	0.000
14	SALAR	NORTH	14390.3	13321	1.08	2829.4	1765.4	7.4	124.1	50.0	4533723	4507236	1.0	9.041	0.000	0.000
15	SEYTAN	NORTH	12683.3	10851.6	1.17	2686.0	1652.3	8.2	64.6	37.6	3108712	3702660	0.8	5.709	1.102	0.000
16	GOLPALA	NORTH	7395.8	6311.8	1.17	2582.1	1692.2	12.0	38.4	26.1	3036894	2172529	1.4	5.209	0.000	0.000
17	ARZAVAN	NORTH	8849.9	8043.1	1.10	2695.9	1635.0	12.0	62.5	35.1	2929132	2329029	1.3	5.258	0.000	0.000
18	ANZER	NORTH	6139.4	5809.7	1.06	2821.1	2237.0	9.5	37.4	29.8	1860377	1980619	1.0	2.303	1.538	0.000
19	BADIR	NORTH	5453.3	4579	1.19	2745.6	1887.0	15.7	29.2	24.7	1996691	2170493	1.0	0.474	3.693	0.000
20	BUYUKOVIT	SOUTH	10770.8	7999.2	1.35	2682.0	2186.0	4.6	62.7	35.7	4631173	3837662	1.2	7.232	1.237	0.000
21	GASURLUK	SOUTH	3466.6	3220.6	1.08	2610.6	2200.4	11.8	36.7	28.6	991739	780881	1.3	0.000	1.773	0.000
22	AKTAKAN	SOUTH	5528	5205.1	1.06	2877.3	2111.5	13.9	21.9	20.7	1653572	1581083	1.0	1.300	1.934	0.000
23	ANADAK	SOUTH	5204	4566.4	1.14	2894.6	2177.7	13.8	33.2	28.4	1585619	1137423	1.4	0.000	2.723	0.000
24	SOROH	SOUTH	5661.7	5047.8	1.12	2926.8	2366.0	9.9	21.6	20.8	2265589	1650547	1.4	3.916	0.000	0.000
25	DAVALT	SOUTH	5573.6	4948.3	1.13	2890.5	2301.0	10.6	27.7	23.5	2021661	1790317	1.0	3.812	0.000	0.000
26	HASTAF	SOUTH	7455.6	7140.7	1.04	2818.0	2085.1	9.8	52.2	33.8	2160274	2211129	1.0	3.217	1.155	0.000
27	BULUT	SOUTH	3899.7	3148.2	1.24	2807.6	2236.6	14.6	17.7	18.6	1084623	1057855	1.0	0.820	1.322	0.000
28	ONBOLAT	SOUTH	4030.2	3834.1	1.05	2669.4	1939.9	18.1	18.5	17.4	845486	1115213	0.8	1.828	0.133	0.000
29	OZGUVEN	SOUTH	4718	3675.4	1.28	2697.9	1962.4	15.6	15.5	16.1	1464805	1249074	1.2	2.361	0.353	0.000
30	BICAKCILAR	SOUTH	5323.7	4241.7	1.26	2794.0	2135.9	12.4	13.7	17.3	2006250	1216947	1.6	3.139	0.084	0.000

Curviness: Curviness of the valley is computed by dividing the length by the shortest length value of each glacial valley. If valley forms a straight line this parameter has value close to 1, otherwise the value becomes higher then 1.

Maximum Z: A glacial valley is considered to start at a cirque at higher elevations. This starting point is, therefore, the maximum elevation of the valley.

Minimum Z: A glacial valley is considered to end at a fluvial valley. This ending point is, therefore, the minimum elevation of the valley.

Average Slope: Average slope is the mean slope of each glacial valley computed by the equation: Average slope = [(Maximum Z – Minimum Z)/Length] * 100.

Basin Area: The basin of a valley corresponds to the area drained by this valley. The drainage divide of each valley is digitized and is represented by a polygon. This polygon includes all cirques and tributary valleys associated with the valley.

Basin Perimeter: This parameter refers to the length of the perimeter of the drainage basins of the glacial valleys.

Area of East Side: The area of the eastern part of the valley elevated for 100 m from the valley floor.

Area of West Side: The area of the western part of the valley elevated for 100 m from the valley floor.

Symmetry: Symmetry of the valley is obtained by dividing the “area of east” by the “area of west”. The reason for computing this property is to be able to comment on the symmetry/asymmetry of the valleys. Accordingly if this value is close to 1 that means the valley is symmetric. Otherwise is might be tilted to the east or west.

Lithology: This property is included in the database to see a probable control of the lithology on the formation of glacial valley. Three lithologic units exposed within the study area are 1) intrusive rocks, 2) volcano-sedimentary, and 3) limestone.

4.3 Properties of Glacial Valleys

Glacial valleys detected in study area are investigated for their properties listed in the database. The properties will be explained only for the main 30 glacial valleys in order not to complicate the description and make an efficient use of GIS. Some parameters, however, will already be included for the tributary valleys in the database. The properties mentioned here will include location, topographic properties, length, curviness, profile, symmetry, linearity and lithology.

4.3.1. Location

Location of the glacial valley in relation of the drainage divide in the area is believed to be an important feature because the divide passes almost in E-W direction which affects the direction of illumination in the area. This, in turn, controls the climatic properties such as temperature, precipitation etc.

Study area is composed of two belts located to the north and south of the drainage divide. Under normal conditions a similar number of glacial valleys are expected to exist on the both sides because the length of the two belts is the same. However, the number of the identified valleys shows great variation on different sides (Table 4.2.). There are 19 main glacial valleys out of 30 in the northern part whereas only 11 on the southern part. The difference in the spatial distribution of the tributary valleys, on the other hand, is much distinct as indicated by 49 and 14 for the northern and southern parts, respectively.

Table 4.2: Number of glacial valleys identified in the area.

	Number of main valleys	Number of tributary valleys
North of area	19	49
South of area	11	14

4.3.2. Length of the Valleys

Length of valleys refers to the distance between starting and ending point of valleys. These two points are connected by a line that runs parallel to the valley floor. The lengths for all 30 valleys are given in Table 4.3. These values are shown in the graphs in Figure 4.6 for the northern and southern parts separately.

Table 4.3: Lengths of the glacial valleys.

ID	Name	Length (m)
1	ALACAGOL	4027.4
2	ABU	4624.9
3	TUNCA	7005.3
4	ERGUSU	5997.3
5	TOPLUCA	5442.1
6	KACKAR	8968.1
7	AVUCUR	5486
8	KAVRAN	10700.9
9	PALOVIT	10172.8
10	ELEVIT	11678.7
11	TATOS	7621.2
12	VERCENIK	11174.2
13	INCESU	7461.2
14	SALAR	14390.3
15	SEYTAN	12683.3
16	GOLPALA	7395.8
17	ARZAVAN	8849.9
18	ANZER	6139.4
19	BADIR	5453.3
20	BUYUKOVIT	10770.8
21	GASURLUK	3466.6
22	AKTAKAN	5528
23	ANADAK	5204
24	SOROH	5661.7
25	DAVALT	5573.6
26	HASTAF	7455.6
27	BULUT	3899.7
28	ONBOLAT	4030.2
29	OZGUVEN	4718
30	BICAKCILAR	5323.7

The longest, the shortest and the average lengths are 14390.3, 4027.4 and 8172.2 for the northern part and 10770.8, 3466.6 and 5602.9 for the southern part respectively. It is very clear that the northern part valleys are longer than the southern part. Salar and Alacagöl valleys in the north; and Büyükovit and Gasurluk valleys in the south are the longest and the shortest valleys, respectively.

Spatial distribution of the valleys in the northern part suggests that the longer valleys are located in the central part of the area. The decrease in the length is much emphasized in the eastern part for the northern side. The southern part of the area, on the other hand display, more or less, a consistent length throughout the study area (Figure 4.6).

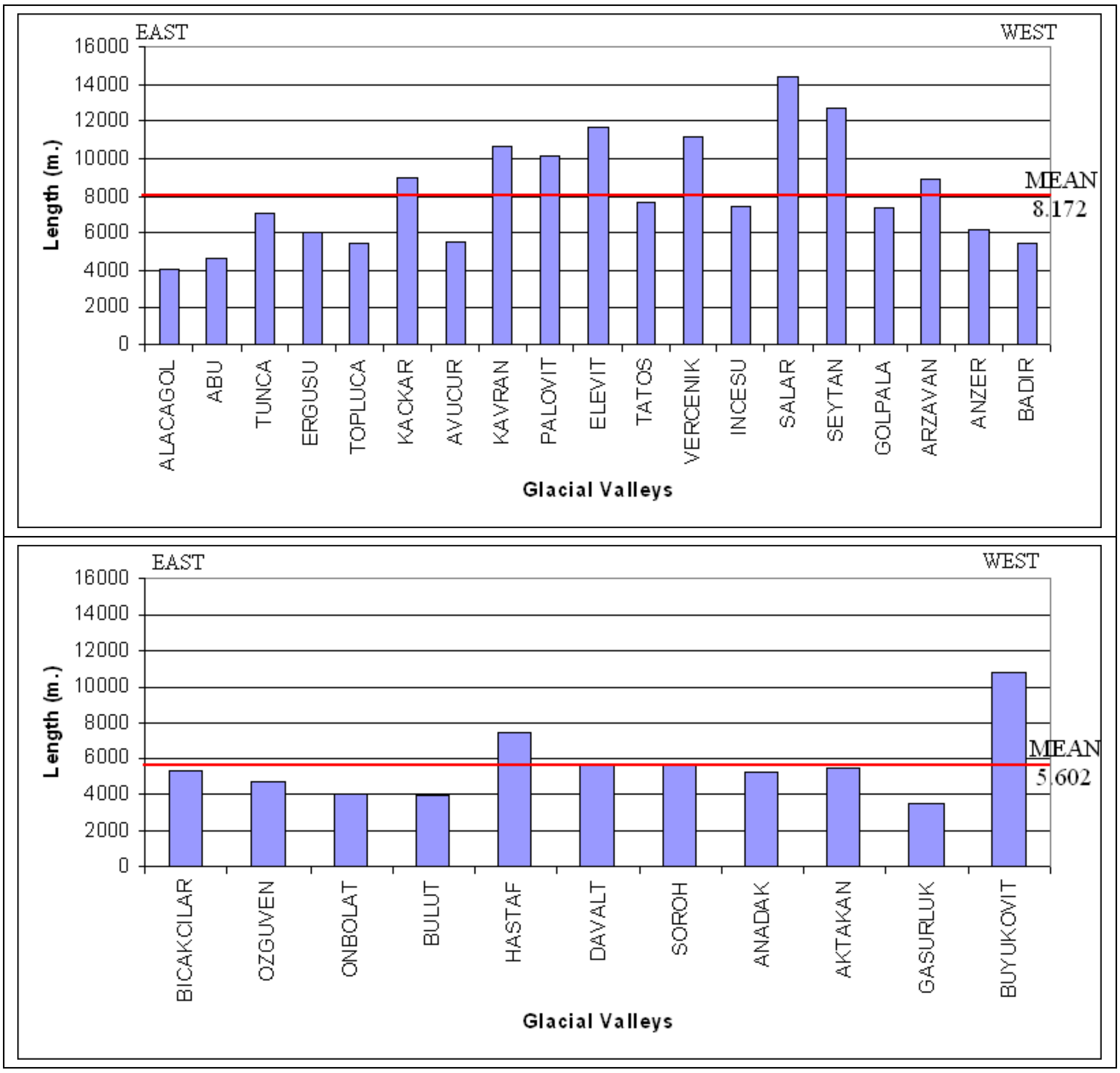

Figure 4.6: Length of glacial valleys on northern (upper) and southern (lower) sides.

4.3.3. Topographic Parameters

Topographic parameters include the properties of aspect, elevation and slope for 30 main glacial valleys separately. These properties are investigated based on the polygons drawn above 100 m above the valley floor as mentioned earlier.

Elevation values refer to the start (upper) and end (lower) points of polygons drawn for the valleys. These points are extracted from DEM and are listed in Table 4.4. The difference between these two elevations are computed and listed in the last column in the same table.

In the northern part, the maximum, minimum and average elevations of the upper points are 2928.8, 2425.4 and 2744.8 m, and of the lower points are 2237, 1506 and 1805.5 m respectively. These values for the southern part, in the same order, are 2926.8, 2610.6 and 2788 m for upper points and 2366, 1939.9 and 2154.8 for the lower points. Accordingly, the valleys in the southern start to develop at higher elevations compared to the northern part. This is best illustrated by the comparison of lower elevations on both parts. The lowest elevation in the northern part is 1506 m that belong to Tunca valley whereas in the southern part the lowest elevation is 1939.9 observed in Onbolat valley.

Elevations of the northern and southern part valleys are plotted on the graphs separately to investigate the general trend on both sides (Figure 4.7). The valleys in both graphs are in accordance with their geographic position located from east to west. The most characteristic feature of these graphs is that the starting elevations of the valleys, on both parts, is maximum in the middle part of the area which gradually decreases towards east and west.

The end points of the valleys do not display a regular trend. For the southern part there is slight decrease in elevation from west to east. The northern part, on the other hand, seems to be consistent in lower elevation around 1700 m with minor and sudden variations.

Table 4.4: Elevation properties of the main glacial valleys.

ID	Name	Start Point (m)	End Point (m)	Height (m)
1	ALACAGOL	2664.0	2051.0	613.0
2	ABU	2623.0	1723.6	899.4
3	TUNCA	2463.0	1506.0	957.0
4	ERGUSU	2558.0	1748.7	809.3
5	TOPLUCA	2698.4	1791.9	906.5
6	KACKAR	2805.4	1613.1	1192.3
7	AVUCUR	2642.6	1890.8	751.8
8	KAVRAN	2854.0	1657.5	1196.5
9	PALOVIT	2902.2	1997.4	904.8
10	ELEVIT	2915.0	1595.7	1319.3
11	TATOS	2928.8	2010.7	918.1
12	VERCENIK	2900.3	1860.0	1040.3
13	INCESU	2836.3	1988.3	848.0
14	SALAR	2829.4	1765.4	1064.0
15	SEYTAN	2686.0	1652.3	1033.7
16	GOLPALA	2582.1	1692.2	889.9
17	ARZAVAN	2695.9	1635.0	1060.9
18	ANZER	2821.1	2237.0	584.1
19	BADIR	2745.6	1887.0	858.6
20	BUYUKOVIT	2682.0	2186.0	496.0
21	GASURLUK	2610.6	2200.4	410.2
22	AKTAKAN	2877.3	2111.5	765.8
23	ANADAK	2894.6	2177.7	716.9
24	SOROH	2926.8	2366.0	560.8
25	DAVALT	2890.5	2301.0	589.5
26	HASTAF	2818.0	2085.1	732.9
27	BULUT	2807.6	2236.6	571.0
28	ONBOLAT	2669.4	1939.9	729.5
29	OZGUVEN	2697.9	1962.4	735.5
30	BICAKCILAR	2794.0	2135.9	658.1

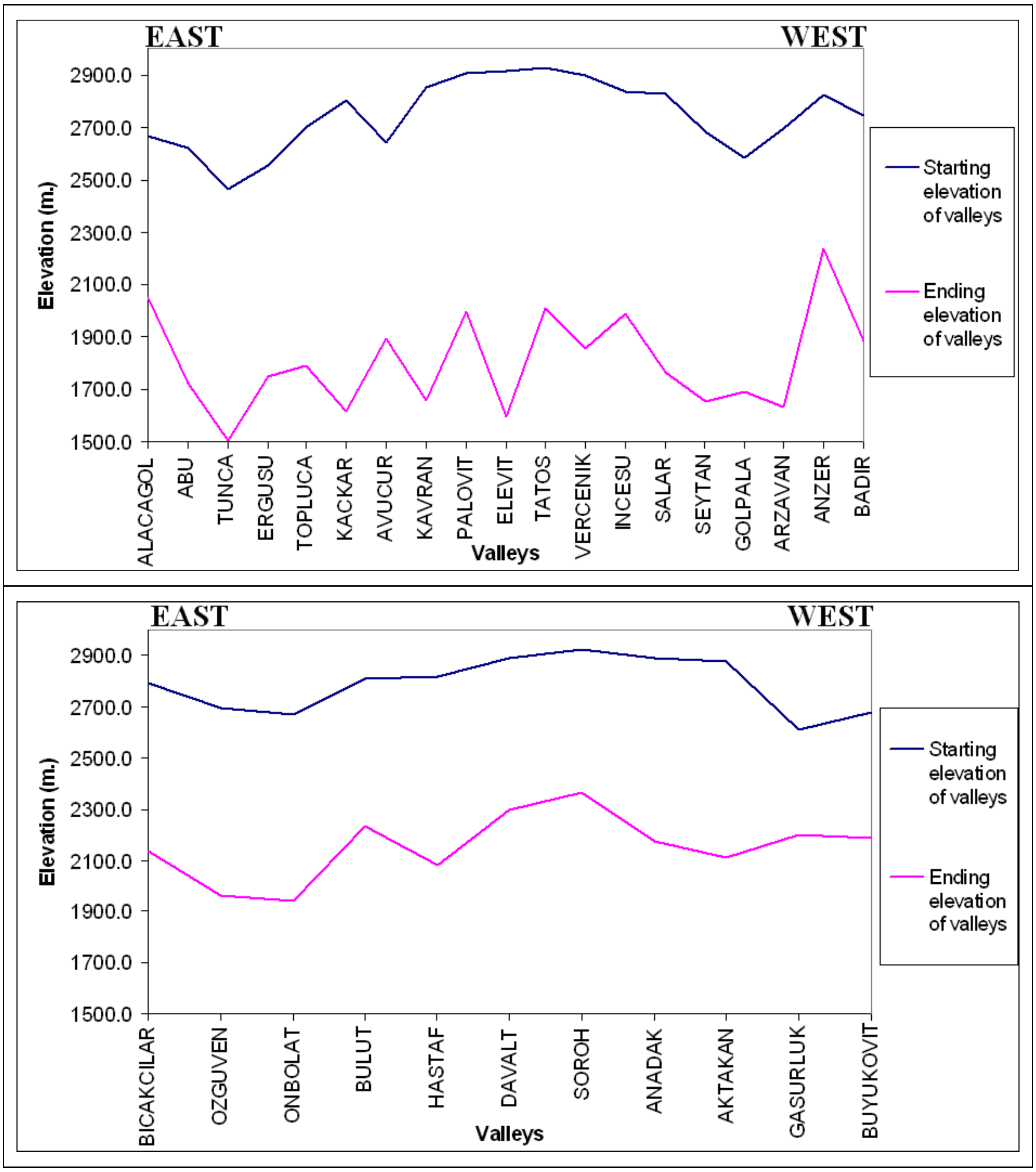

Figure 4.7: Start and End elevations of glacial valleys for the north (upper) and south (lower) parts of the area.

Elevation difference (height) shows a great variation in the southern and northern parts. These values are shown in the last column in Table 4.4. There is a difference of about 670 m between the averages of the northern and the southern part valleys. The valley with the maximum height difference is Elevit valley with 1319.3 m in the northern part. The valley with minimum difference is Gasurluk valley in the southern part with an elevation of 410.2 m.

Average slope values are computed using the height (elevation difference) and the length of the valley. Accordingly, the Slope = (Height / Length) * 100. The values for the average slopes are shown in Table 4.5. These values are shown in the graphs in Figure 4.8 separately for the northern and southern parts of the area.

Table 4.5: Average slopes of the valleys computed from the length and the height of the valleys.

ID	Name	Length (m)	Height (m)	Average Slope
1	ALACAGOL	4027.4	613.0	15.2
2	ABU	4624.9	899.4	19.4
3	TUNCA	7005.3	957.0	13.7
4	ERGUSU	5997.3	809.3	13.5
5	TOPLUCA	5442.1	906.5	16.7
6	KACKAR	8968.1	1192.3	13.3
7	AVUCUR	5486	751.8	13.7
8	KAVRAN	10700.9	1196.5	11.2
9	PALOVIT	10172.8	904.8	8.9
10	ELEVIT	11678.7	1319.3	11.3
11	TATOS	7621.2	918.1	12.0
12	VERCENIK	11174.2	1040.3	9.3
13	INCESU	7461.2	848.0	11.4
14	SALAR	14390.3	1064.0	7.4
15	SEYTAN	12683.3	1033.7	8.2
16	GOLPALA	7395.8	889.9	12.0
17	ARZAVAN	8849.9	1060.9	12.0
18	ANZER	6139.4	584.1	9.5
19	BADIR	5453.3	858.6	15.7
20	BUYUKOVIT	10770.8	496.0	4.6
21	GASURLUK	3466.6	410.2	11.8
22	AKTAKAN	5528	765.8	13.9
23	ANADAK	5204	716.9	13.8
24	SOROH	5661.7	560.8	9.9
25	DAVALT	5573.6	589.5	10.6
26	HASTAF	7455.6	732.9	9.8
27	BULUT	3899.7	571.0	14.6
28	ONBOLAT	4030.2	729.5	18.1
29	OZGUVEN	4718	735.5	15.6
30	BICAKCILAR	5323.7	658.1	12.4

Average Slope value for the glacial valleys on northern part is 12.34° whereas on the southern part is 12.27° which are very close to each other. However, individual investigation of the valleys displays certain differences. On north side from 19 glacial valleys, the slope values range between 7.4° (Salar valley) and 19.4° (Abu valley). In general the values first decrease and then again increase from east to west. The middle part valleys have low slope particularly towards the west.

In the southern part of the area, the slope values range between 4.6° (Buyukovit Valley) and 18.1° (Onbolat Valley). In general the slope is low in the central part and increases towards the both direction except the Büyükovit valley in the west.

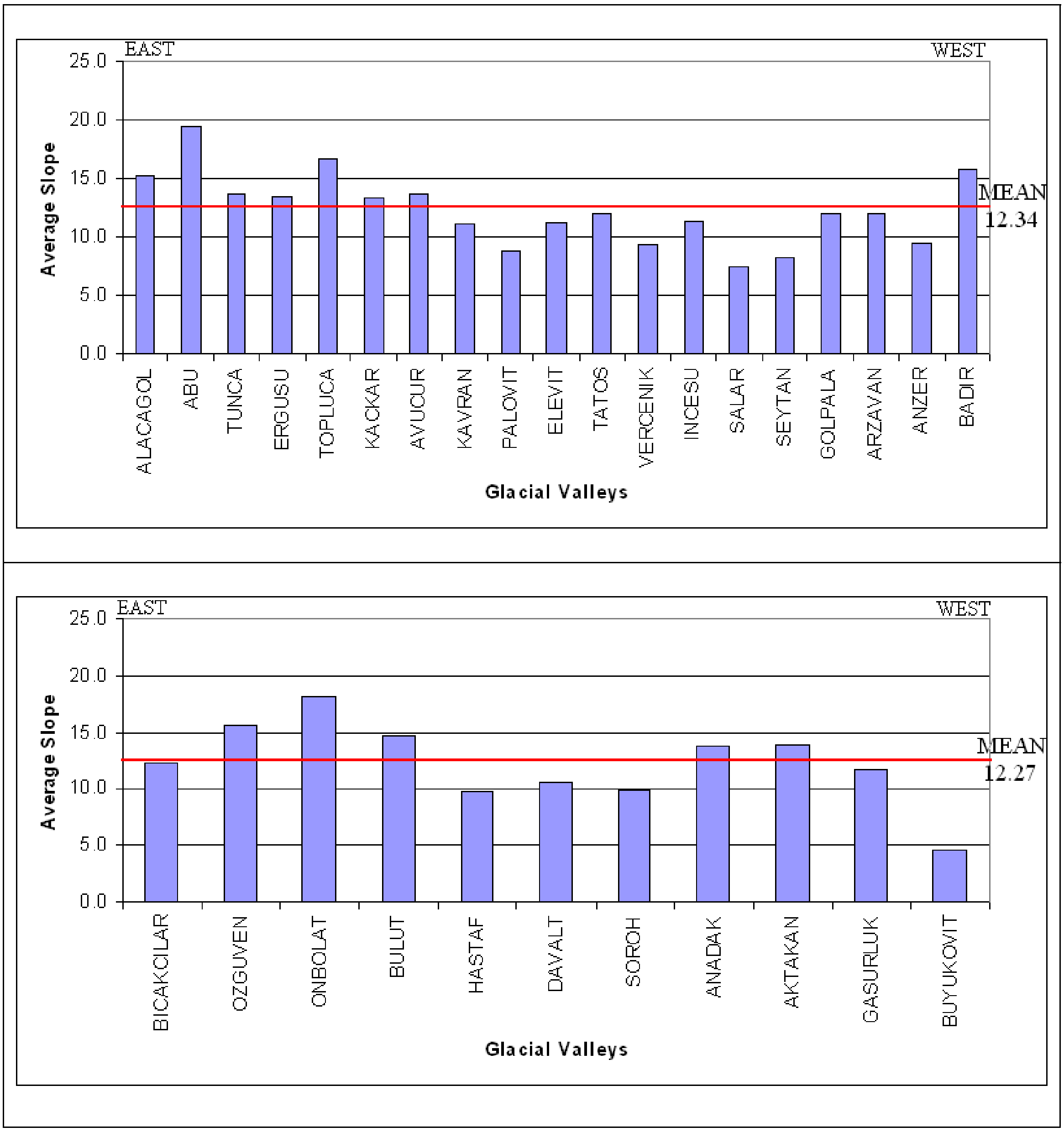

Figure 4.8: Average Slope of glacial valleys for the north (upper) and south (lower) parts of the area.

Aspect is calculated using the aspect values of pixels included in the polygons drawn for the valleys. For each valley a histogram is prepared for 15° intervals (Figure 4.9). Based on the visual analyses of these diagrams, two dominant aspect types are suggested for the aspect: 1) a bi-modal distribution, and 2) irregular variation of aspect. Bi-modal distribution should be considered an ideal valley because two slopes of the valley will have different aspect values with an average deviation angle of 150-180°.

Bi-modal type aspect is observed in 22 valleys. All the valleys in the northern part (a total of 19 valleys) show bi-modal distribution. Alacadağ, Tunca Avucur, Kavran, Elevit, and Tatos valleys are typical examples. The two peaks of the distribution in these valleys, however, may change from place to place. For example for Alacadağ valley, two peaks are at 30-45° and 270-285° whereas for Şeytan valley these are at 0-15° and 210-225°. This difference is due to the general orientation of the valley.

Another characteristic feature of the valleys with bi-modal distribution is the presence of an interval with almost 0 %. For example, in Tunca valley no aspect is recorded between 105 and 210°. This is good evidence either for the lack of a tributary valley linked to the main valley or the linear trend of the main valley. This is the case observed almost for all valleys in the northern part except the Verçenik and Badır valleys.

The second type of the aspect shape (irregular distribution) is commonly observed in the southern part of the area. Except three valleys in the south (Gasurluk, Aktakan and Hastaf) all the valleys have an irregular pattern of the aspect. Büyükovit, Davalt, Bulut and Bıçakçılar are the typical examples. In this type, generally there is not a concentration at certain intervals but rather an equally distributed histogram throughout the scale.

Maximum frequency of the bi-modal and irregular types is another characteristic feature observed in the diagrams. Bi-modal distribution can reach to a value of 14 % whereas the irregular one is mostly confined to 6-8 %.

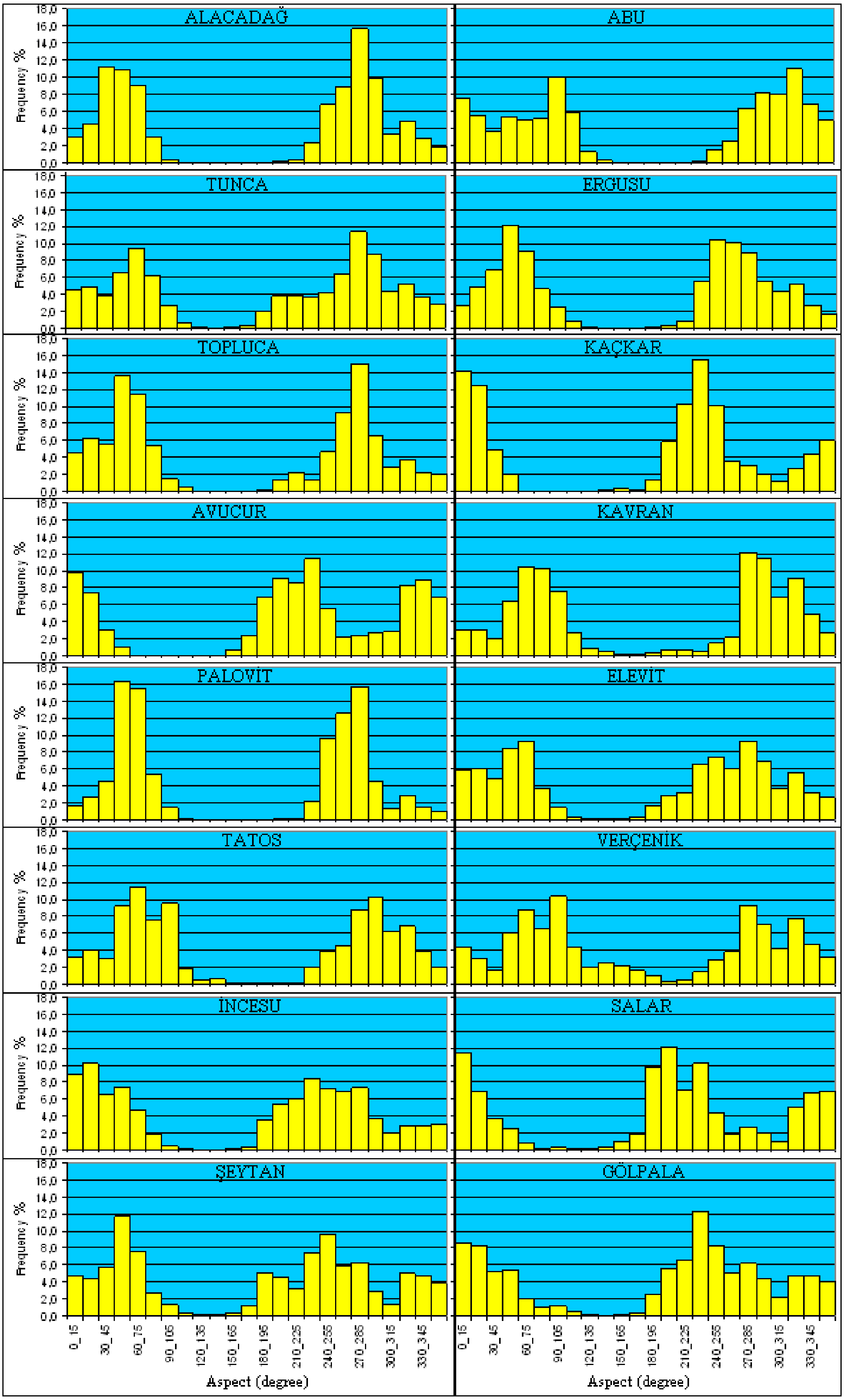

Figure 4.9: Histograms prepared for the aspect values of valleys.

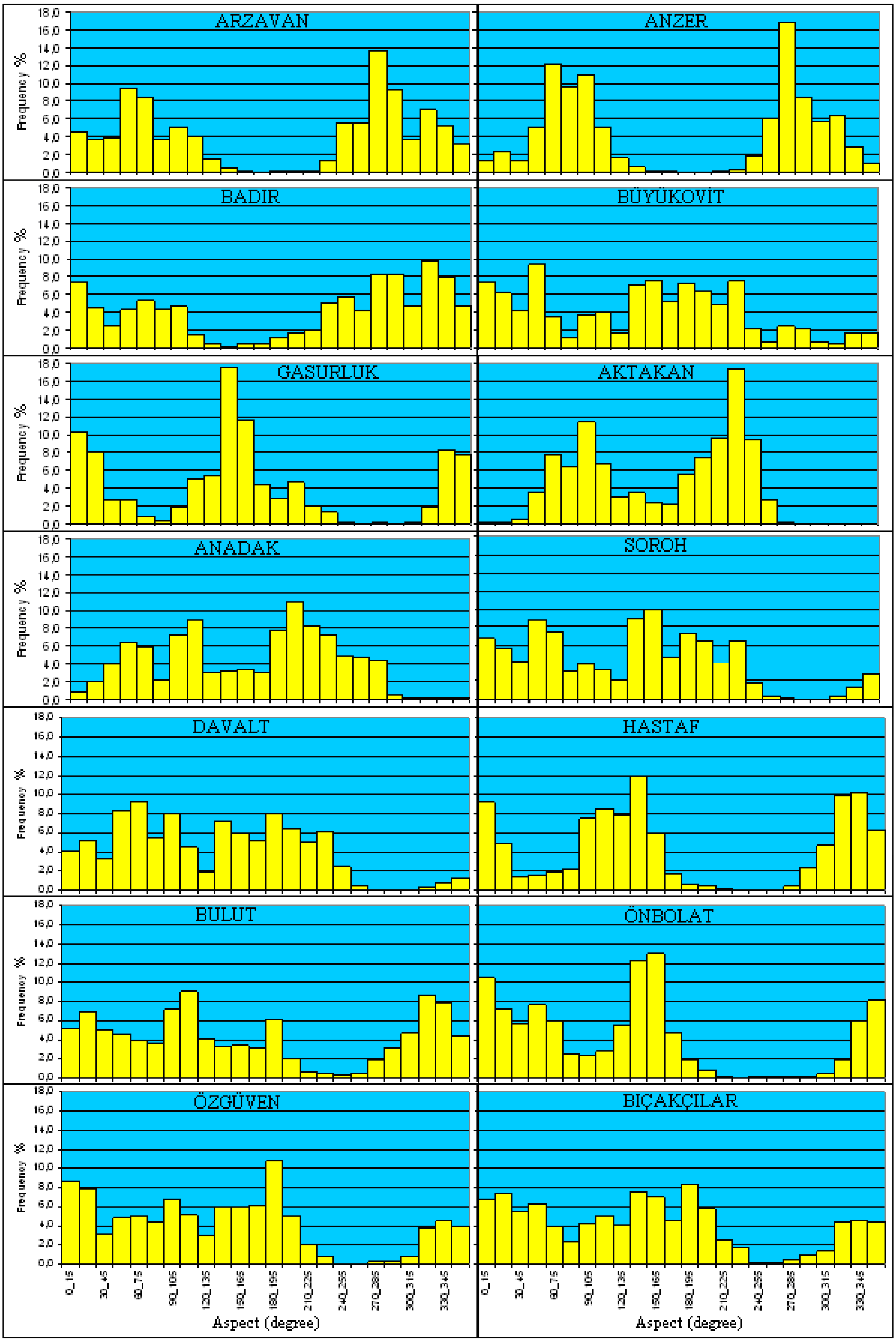

Figure 4.9: (continued).

4.3.4. Sinuosity

Sinuosity determines if the trend of the valley is straight or curved. In order to compute the curviness the length mentioned above and the shortest length between starting and ending points computed. Sinuosity is determined by rationing these two parameters (Sinuosity = Length / Shortest length). The result is shown in Table 4.6. The values start from 1 and increase depending on its curviness. If the value is equal to 1 this indicates a straight trend for the valley. As the value higher than 1 the valley becomes curved and the sinuosity increases.

Table 4.6: Sinuosity of the valleys computed using the length and the shortest length.

ID	Name	Length (m)	Shortest Length (m)	Sinuosity
1	ALACAGOL	4027.4	3823.6	1.05
2	ABU	4624.9	4022	1.15
3	TUNCA	7005.3	6006.7	1.17
4	ERGUSU	5997.3	5301.6	1.13
5	TOPLUCA	5442.1	4967	1.10
6	KACKAR	8968.1	8394.1	1.07
7	AVUCUR	5486	5143.5	1.07
8	KAVRAN	10700.9	10018.4	1.07
9	PALOVIT	10172.8	9813	1.04
10	ELEVIT	11678.7	10418.6	1.12
11	TATOS	7621.2	7028.6	1.08
12	VERCENIK	11174.2	9323.6	1.20
13	INCESU	7461.2	6507.4	1.15
14	SALAR	14390.3	13321	1.08
15	SEYTAN	12683.3	10851.6	1.17
16	GOLPALA	7395.8	6311.8	1.17
17	ARZAVAN	8849.9	8043.1	1.10
18	ANZER	6139.4	5809.7	1.06
19	BADIR	5453.3	4579	1.19
20	BUYUKOVIT	10770.8	7999.2	1.35
21	GASURLUK	3466.6	3220.6	1.08
22	AKTAKAN	5528	5205.1	1.06
23	ANADAK	5204	4566.4	1.14
24	SOROH	5661.7	5047.8	1.12
25	DAVALT	5573.6	4948.3	1.13
26	HASTAF	7455.6	7140.7	1.04
27	BULUT	3899.7	3148.2	1.24
28	ONBOLAT	4030.2	3834.1	1.05
29	OZGUVEN	4718	3675.4	1.28
30	BICAKCILAR	5323.7	4241.7	1.26

The values of sinuosity are plotted on the graphs for the northern and southern parts of the area separately (Figure 4.10). The average values are similar to each other which are 1.11 for the northern and 1.16 for the southern part. These high values for both parts indicate that all the valleys in the study area have almost straight trends.

In the northern part, the valleys located on middle part have straight trend. The typical examples are Kaçkar, Palovit, Kavran, and Avucur valleys with sinuosity value of about 1.05.

The valleys on the southern part, on the other hand, have a similar pattern to the northern part as indicated by straight valleys in the central part. The minimum sinuosity values in both east and west of the area is obvious in this part. Buyukovit valley in the west; Özgüven and Bıçakçılar valleys in the east have maximum sinuosity values in the whole area indicating maximum curvature.

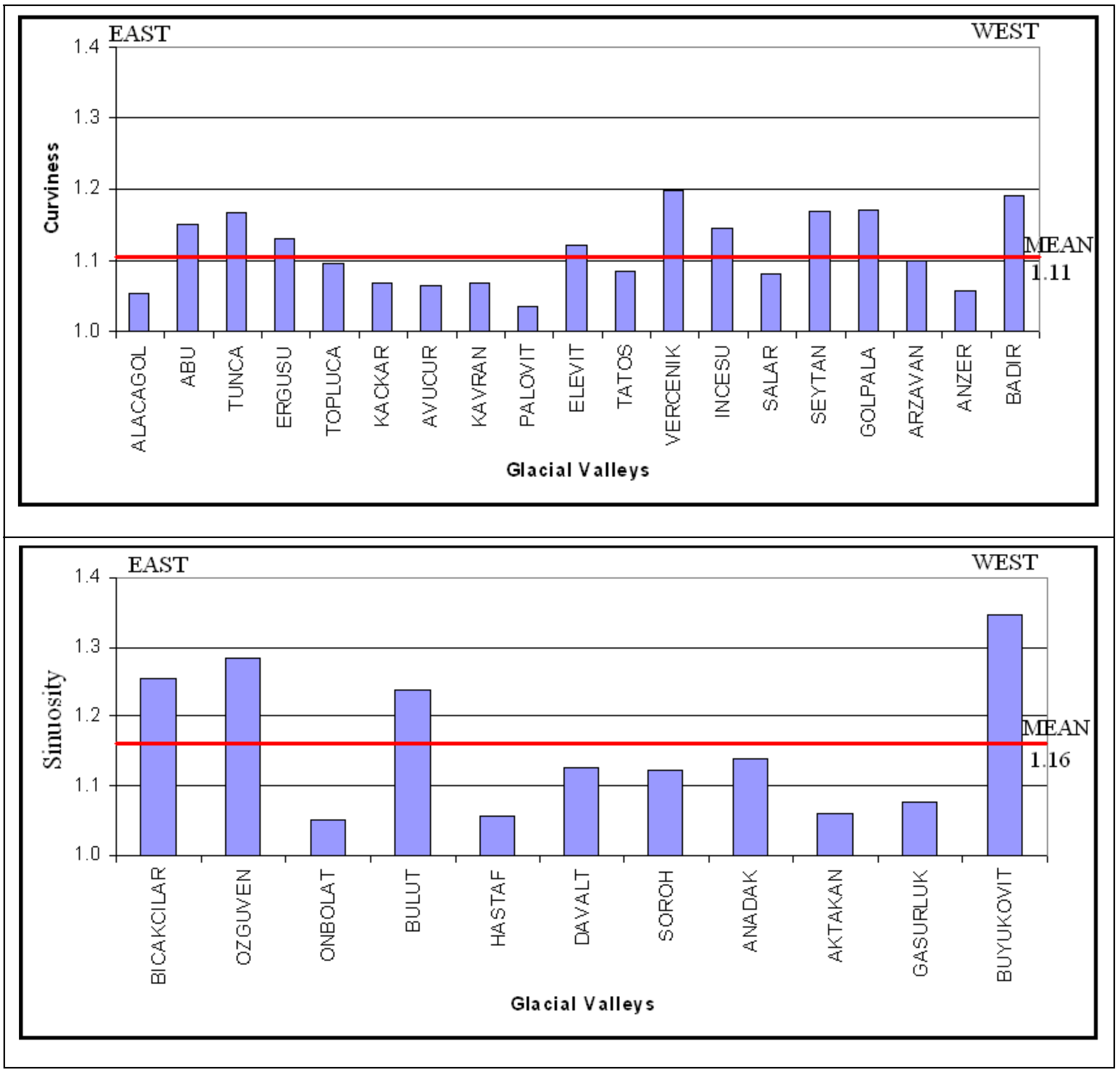

Figure 4.10: Curviness of glacial valleys for the north (upper) and south (lower) parts of the area.

4.3.5. Longitudinal Profiles of Glacial Valleys

Longitudinal profiles of valleys show the change in the elevation in their floor base from the starting point to ending point. Under normal conditions, in a glacial valley the elevation decreases rapidly at the starting part indicated by a step line for this part. This is followed by a gentle slope that corresponds to the middle of the valley. At the end of the valley the profile changes to flat line where the moraine is accumulated. From this point the fluvial valley starts characterized by steep slope. In the diagrams the fluvial valleys are not illustrated because the end of the line represents the end of the glacial valley.

The profiles are grouped into three categories based on the visual observation. These are 1) linear profiles, 2) profiles with a steep section at the start, and 3) profiles with a nick-point in the middle of the curve.

The profiles prepared for all valleys are illustrated in Figure 4.11. Using the classification mentioned above, 21 valleys fall into the first, 5 into the second and 4 into the third category. Typical examples of the first category are Tatos, İncesu, Kavran, Elevit, Büyükovit and Hastaf valleys. The second category valleys are Abu, Ergusu, Avucur, Anzer and Aktakan. The four valleys of the third category are Anadak, Önbolat, Özgüven and Bıçakçılar.

The profiles are overlapped for northern and southern parts of the area and are shown in Figure 4.12. Following observation can be made using Figures 4.11 and 4.12.

- The third category valleys are observed only in the southern part. Three of these are located in the eastern part of the area adjacent to each other.
- Four of the five valleys of the second category are located in the northern part of the area. Spatial investigation of these valleys indicates that the valleys are located in the eastern and western parts of the area.
- Fifteen valleys of the first category valleys are located in the northern and six in the southern part.
- In general the length of the valley is greater and the slope is gentler in the northern part as already confirmed by the length and slope analyses mentioned above.

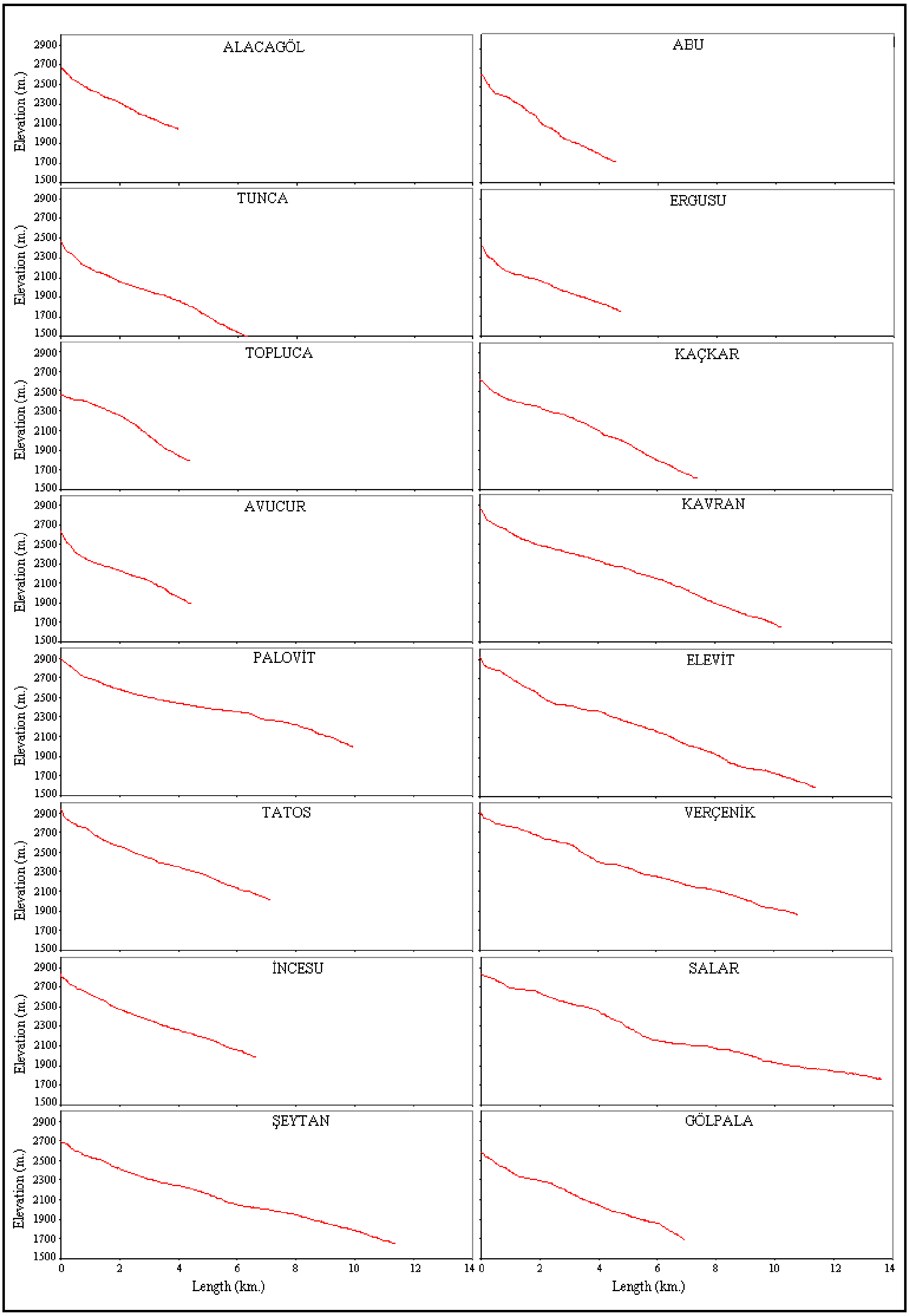

Figure 4.11: Longitudinal profiles of glacial valleys.

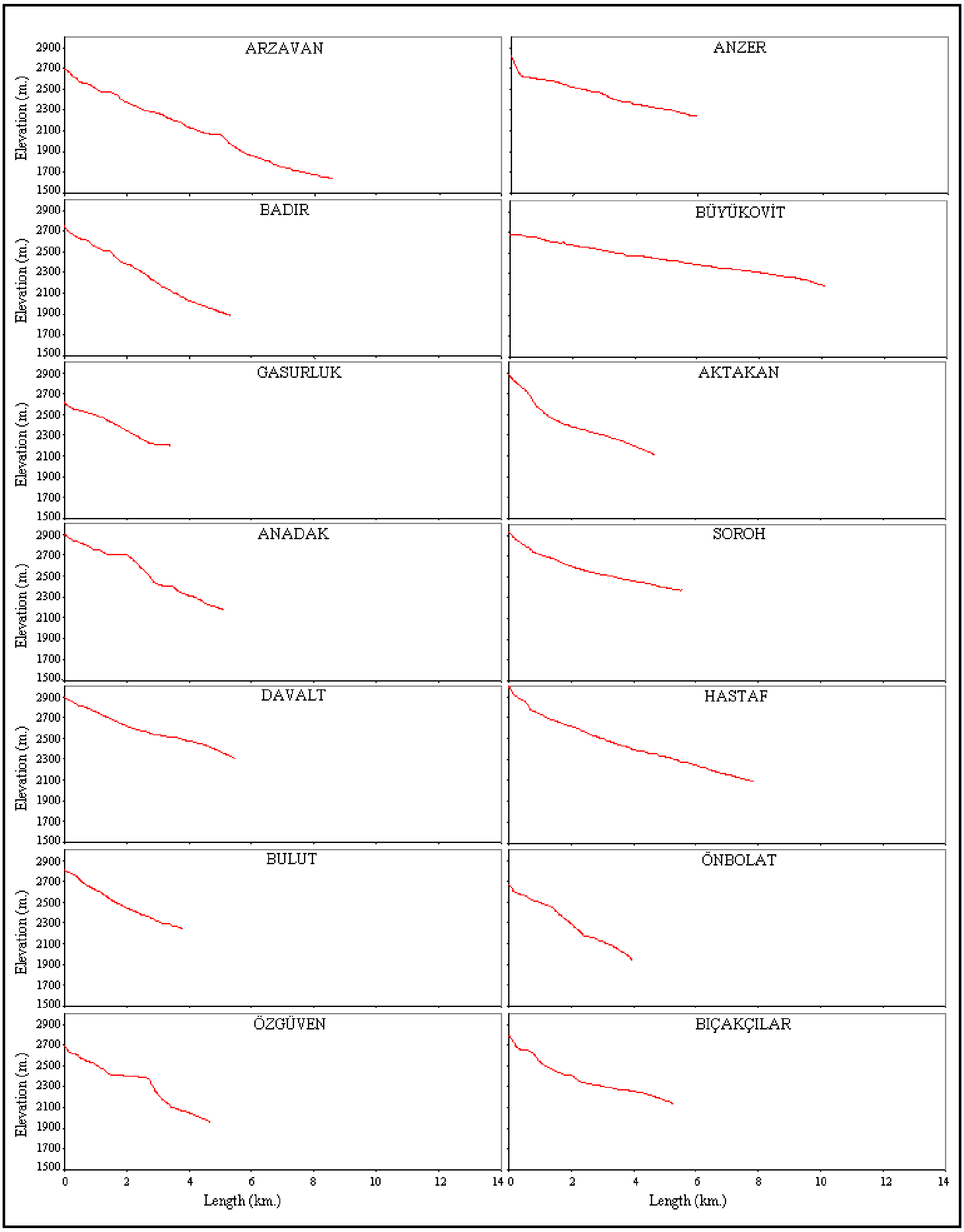

Figure 4.11: (continued).

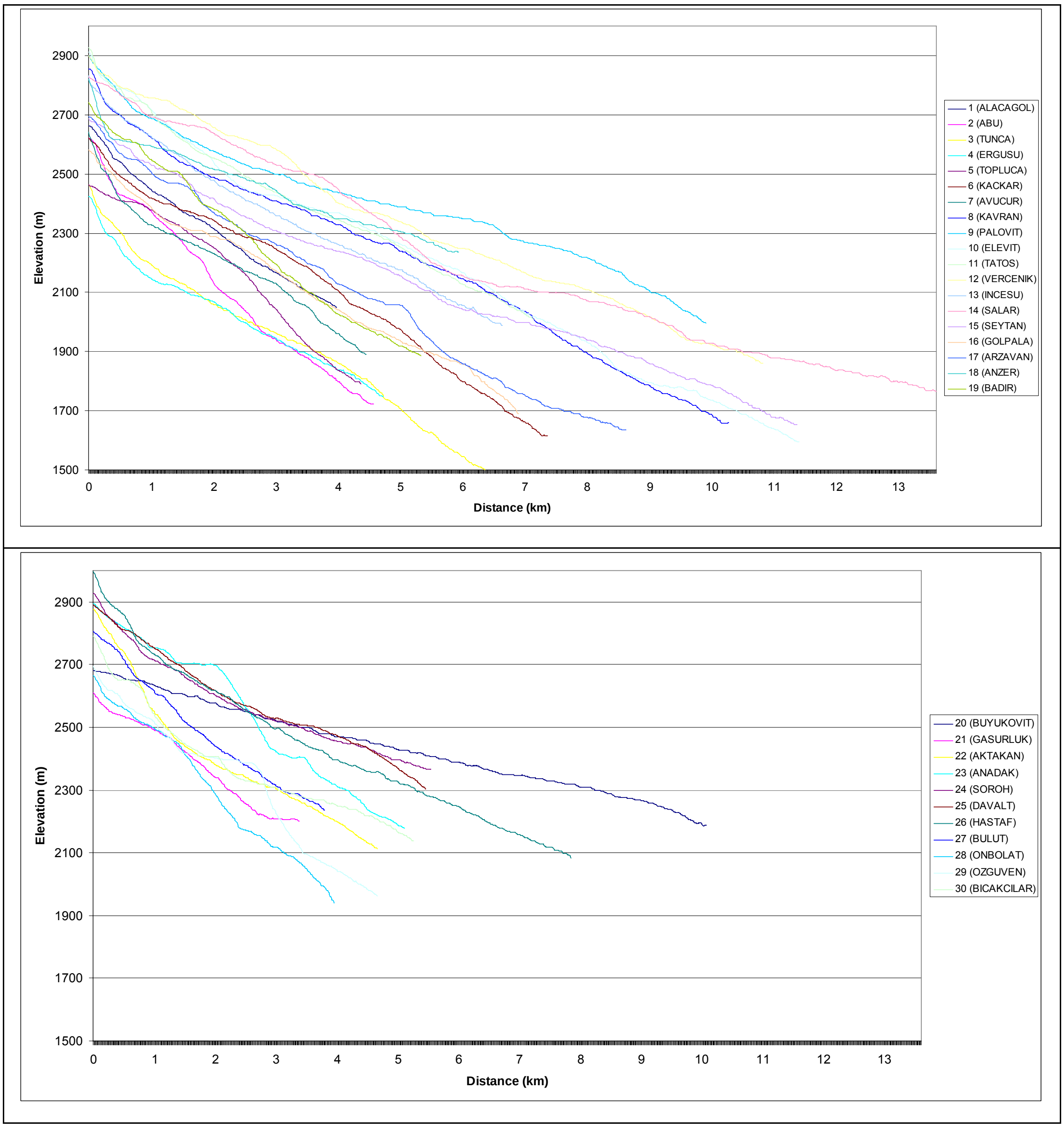

Figure 4.12: Longitudinal profiles of the valleys of the northern (upper) and the southern (lower) parts of the area.

4.3.6. Symmetry of the Valleys

Symmetry of the valleys is investigated in two methods. In both methods the polygon drawn 100 m above the valley floor is used. This polygon is divided into two regions as “east” and “west” using the river. In the first method the ratio of the surface area of two regions is computed which is believed to be an indicator of the symmetry. In the second method, a histogram is prepared by subtracting the slope values of all pixels in each sub-region.

The result of the first method is given in Figure 4.13. The values close to 1 indicate a symmetric valley. The number greater than 1 indicates an asymmetric valley with steep western slope; similarly a value less than 1 indicates an asymmetric valley with steep eastern slope. As the number deviates from 1, the amount of asymmetry increases. Accordingly, 13 valleys have values very close to 1 and can be classified as symmetric valleys. These are Abu, Topluca, Kaçkar, Avucur, Pavolit, İncesu, Salar, Anzer, Badır, Aktakan, Davalt, Hasnaf and Bulut valleys. The first 8 valleys are in the nortern parth of the area and the 5 in the southern.

Fourteen valleys have values above 1 indicating that the western slopes are steep. These are Alacagöl, Tunca, Ergusu, Kavran, Elevit, Tatos, Gölpala, Arzavan, Büyükovit, Gasurluk, Anadak, Soroh, Özgüven and Bıçakçılar. The first 8 valleys are located in the northern and the rest in the southern part of the area. The most asymmetric valley is Bıçakçılar followed by Tunca valley.

Three valleys with eastern steep valleys are Verçenik, Şeytan and Önbolat. The first two valleys are in the northern part and the last in the southern part of the area.

A comparison between different steep sides clearly indicate that the asymmetric valleys with eastern steep valleys are "slightly asymmetric" compared with western steep valleys.

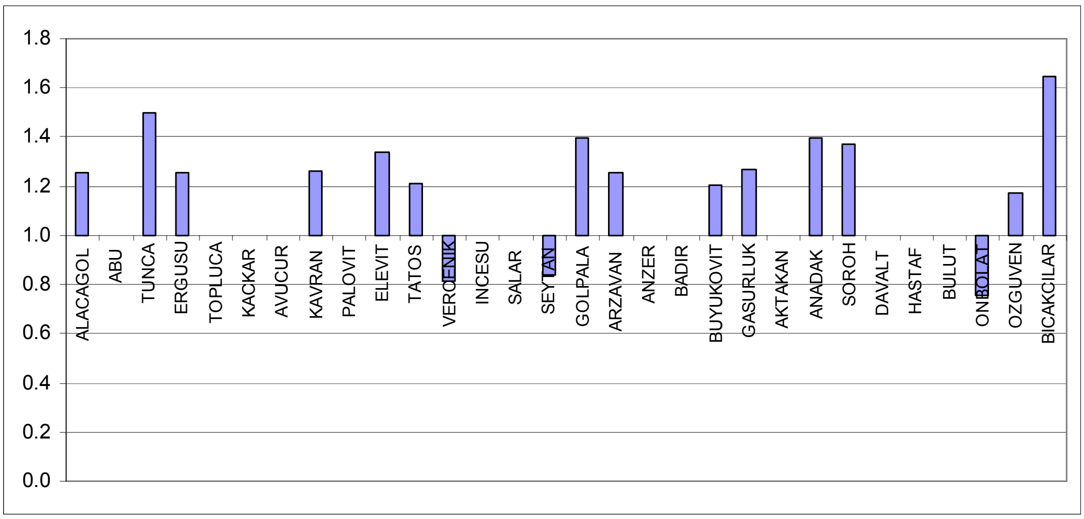

Figure 4.13: Symmetry of main glacial valleys.

The results of the second method for the investigation of the asymmetry are given in 30 histograms in Figure 4.14. Each histogram in this figure is provided by subtracting the slope values of all pixels in the western polygon from the eastern polygon of the valley. Accordingly the values close to 0 indicate a symmetric valley. Positive values represent asymmetric valleys with steep eastern slopes and, vice versa, a negative value implies an asymmetric valley with steep western valley.

Visual analysis of the patterns in the histogram leads to the classification of the valleys into 5 categories. These categories are illustrated in Figure 4.15 and briefly explained as follows:

A) Symmetric valley: There is not an obvious positive or a negative value. Most of the values are scattered around 0-line
B) Asymmetric valley with steep eastern slope: This pattern is represented by a negative region at low slope values followed by a positive region at high slope values.
C) Asymmetric valley with steep western slope: This pattern is represented by a positive region at low slope values followed by a negative region at high slope values.
D) Easterly asymmetric valley with a break in the steep slope: The graph of this valley has three regions in the histogram represented by a gentle, a medium and a steep slope. If the first and the third sections are positive, the eastern slope is first characterized first by a gentle slope followed by a steep slope indicating a sudden break in the slope.
E) Westerly asymmetric valley with a break in the steep slope: The pattern of the plot is similar to previous one with opposite signs in the three sections.

Based on this classification following observations are made using the histograms:

- There are 10 symmetric valleys (type A). These are Kaçkar, Avucur, Palovit, Tatos, Verçenik, İncesu, Salar, Şeytan, Davalt and Hastaf. Although some of these valleys have a distinct sections of positive and negative values such as Verçenik and Avucur valley, these are considered as symmetric because the values are very close to 0. The first 8 valleys are in the northern and the last two in the southern part of the area.

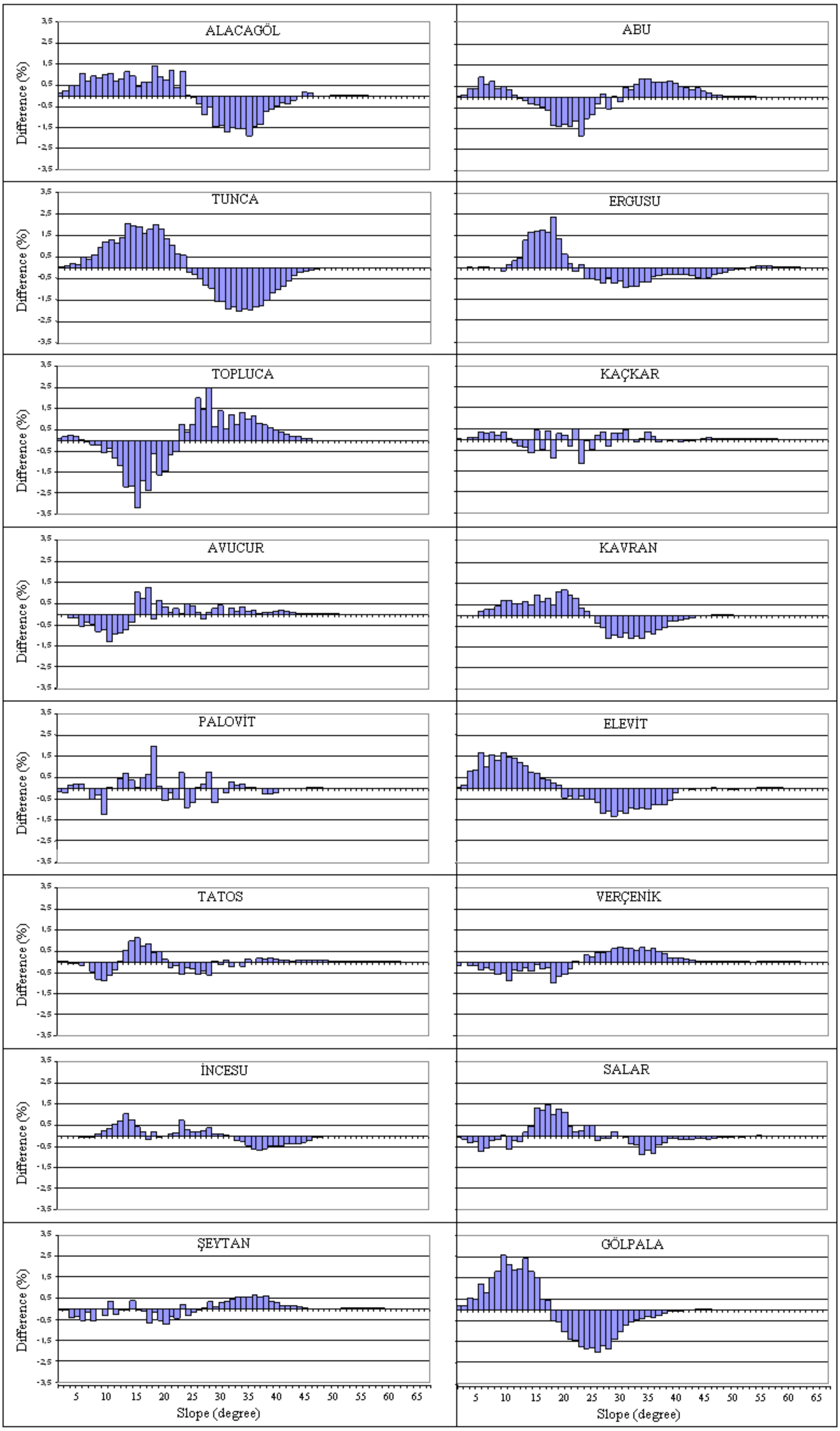

Figure 4.14: Histograms used to investigate the symmetry of glacial valleys by subtracting the western pixels from eastern ones.

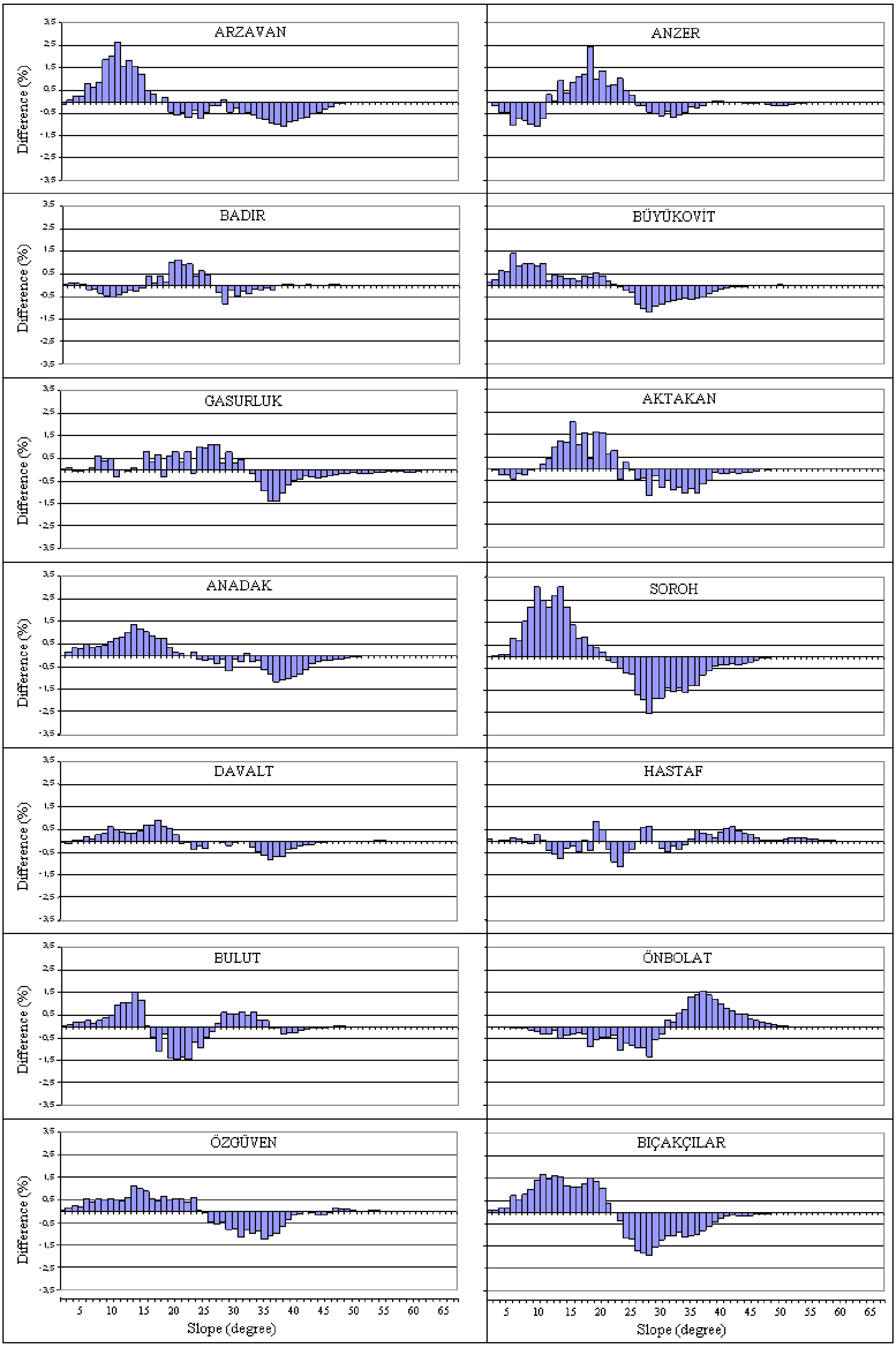

Figure 4.14: (continued).

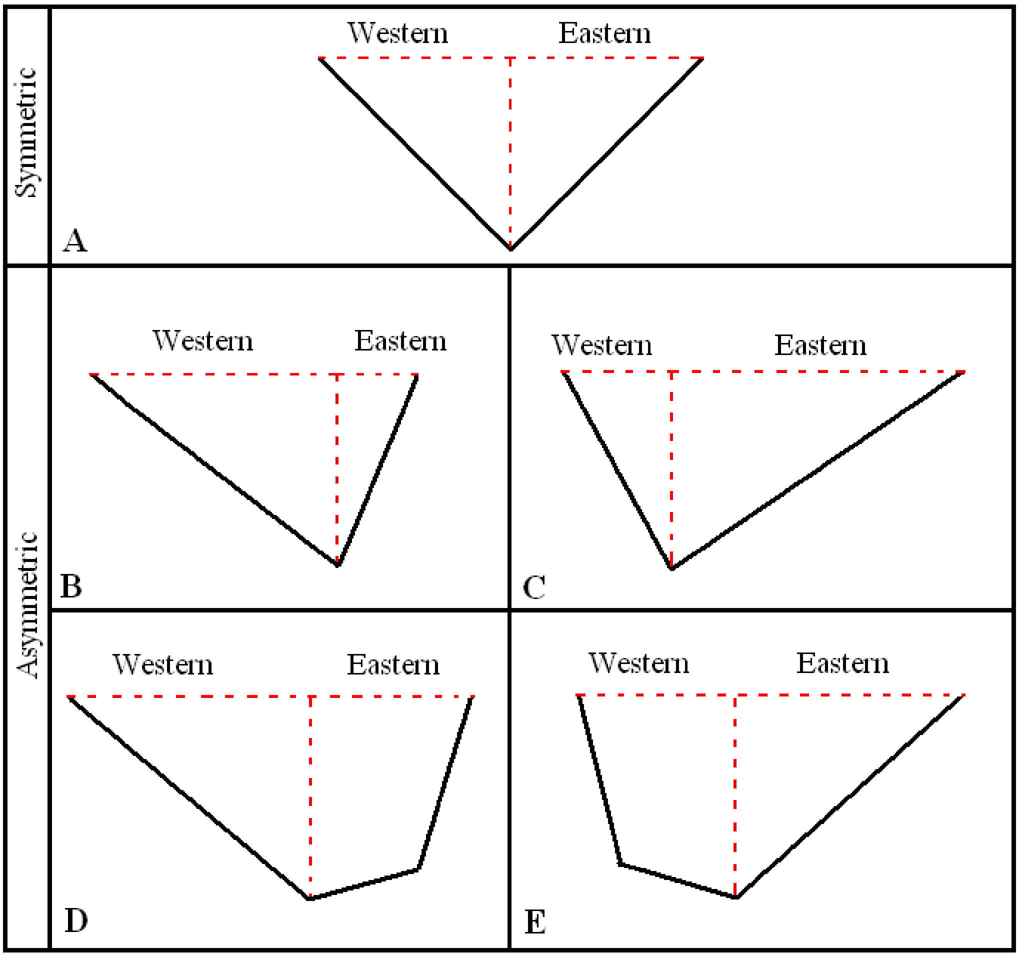

Figure 4.15: Five classes of asymmetric valleys identified in the study area.

- The second type (B) is represented by two valleys namely, Topluca and Önbolat. The first one is in the northern and the second one is in the southern part of the area.
- The third type (C) is represented by 13 valleys which are Alacagöl, Tunca, Ergusu, Kavran, Elevit, Gölpala, Arzavan, Büyükovit, Gasurluk, Anadak, Soroh, Özgüven and Bıçakçılar. Seven of these valleys are located in the northern and 6 in the southern part of the area.
- The fourth type (D) is represented by two valleys namely Abu and Bulut. The first is in the northern and the second in the southern part of the area.
- The fifth type (E) is represented by three valleys namely Anzer, Badır and Aktakan. The first two are located in the northern part of the area and the last one in the southern part.

4.3.7. Orientation of the Valleys

Orientation refers to the direction of the valley. A rose diagram is prepared for 30 valleys each measurement representing a valley. The rose diagram is bi-directional therefore is missing information on the sense of the valley. An average value is computed for each valley based on the starting and ending coordinates of the valley.

The result is shown in Figure 4.16. The overall pattern of the orientations forms an ellipse in NNW-SSE direction. The main gap interval is developed almost perpendicular to the dominant direction. This gap interval is parallel to the general orientation of Eastern Black Sea mountain chain. Therefore the NNW-SSE direction is expected to be the general trend of the glacial valleys.

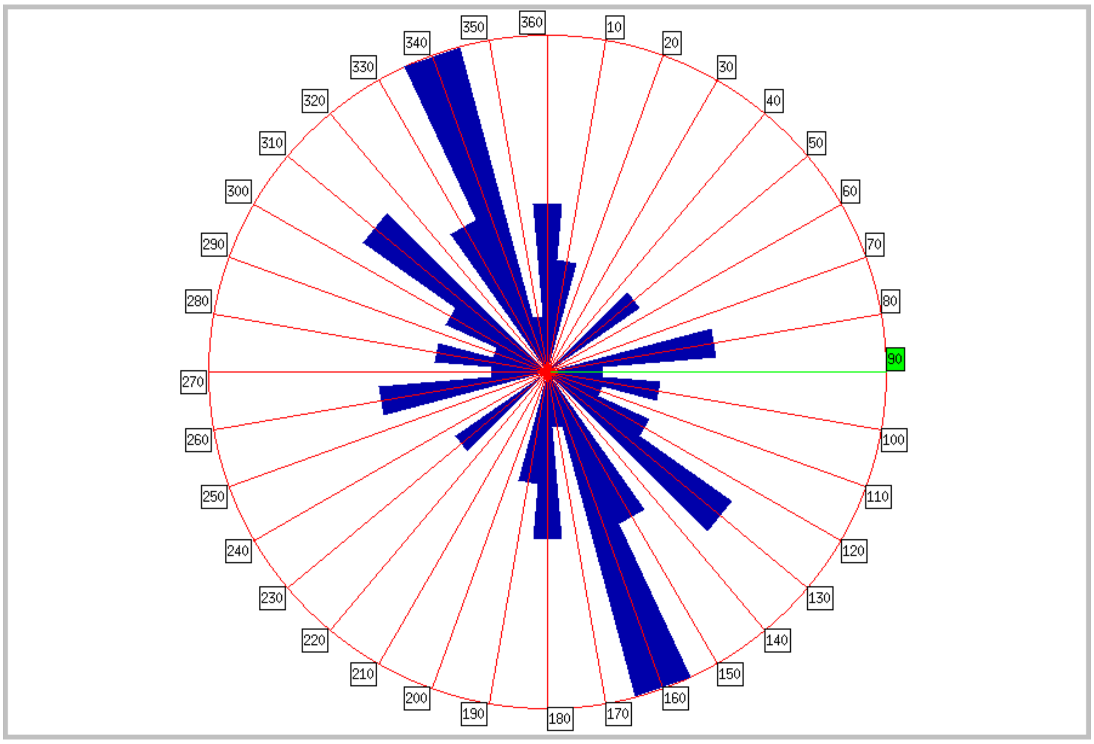

Figure 4.16: Rose Diagram of the orientation of the valleys.

4.3.8. Relationships with Rock Units

The relationship between the valley and the rock type is investigated by intersection of geology map with the valley map. The area covered in percentage for each valley is calculated. The results are tabulated in Table 4.7 and are illustrated in Figure 4.17.

Table 4.7: Areas of the rock types covered by the valleys in the study area.

ID	Name	Intrusive Rocks (km^2)	Volcano-sedimentary Rocks (km^2)	Limestone (km^2)
1	ALACAGOL	2,138		
2	ABU	2,460		
3	TUNCA	3,619		
4	ERGUSU	2,365		
5	TOPLUCA	2,400		
6	KACKAR	4,118		
7	AVUCUR	3,142	0,031	
8	KAVRAN	6,350	0,128	
9	PALOVIT	6,078		
10	ELEVIT	6,752	0,048	
11	TATOS	3,881	0,894	
12	VERCENIK	3,979	2,851	0,003
13	INCESU	4,268		
14	SALAR	9,041		
15	SEYTAN	5,709	1,102	
16	GOLPALA	5,209		
17	ARZAVAN	5,258		
18	ANZER	2,303	1,538	
19	BADIR	0,474	3,693	
20	BUYUKOVIT	7,232	1,237	
21	GASURLUK		1,773	
22	AKTAKAN	1,300	1,934	
23	ANADAK		2,723	
24	SOROH	3,916		
25	DAVALT	3,812		
26	HASTAF	3,217	1,155	
27	BULUT	0,820	1,322	
28	ONBOLAT	1,828	0,133	
29	OZGUVEN	2,361	0,353	
30	BICAKCILAR	3,139	0,084	
	Total Percentage (%)	83,61408	16,38358	0,002341

There area three rock types included in the valleys. These are intrusive rocks, volcano-sedimentary rocks and limestone. The presence of limestone can be ignored because it is included in Verçenik valley with a very small amount together with other two lithologies. Therefore, the valleys are located in mainly two rock units namely the intrusive rocks and the volcano-sedimentary rocks. Half of 30 valleys are located in a single rock unit. Among these, 13 valleys are developed within intrusive rocks and 2 within volcano-sedimentary. On the other hand, 14 valleys comprise both of these rock units. Similarly, Verçenik valley that contains a little portion of limestone is dominantly covered by two units (Table 4.7 and Figure 4.17).

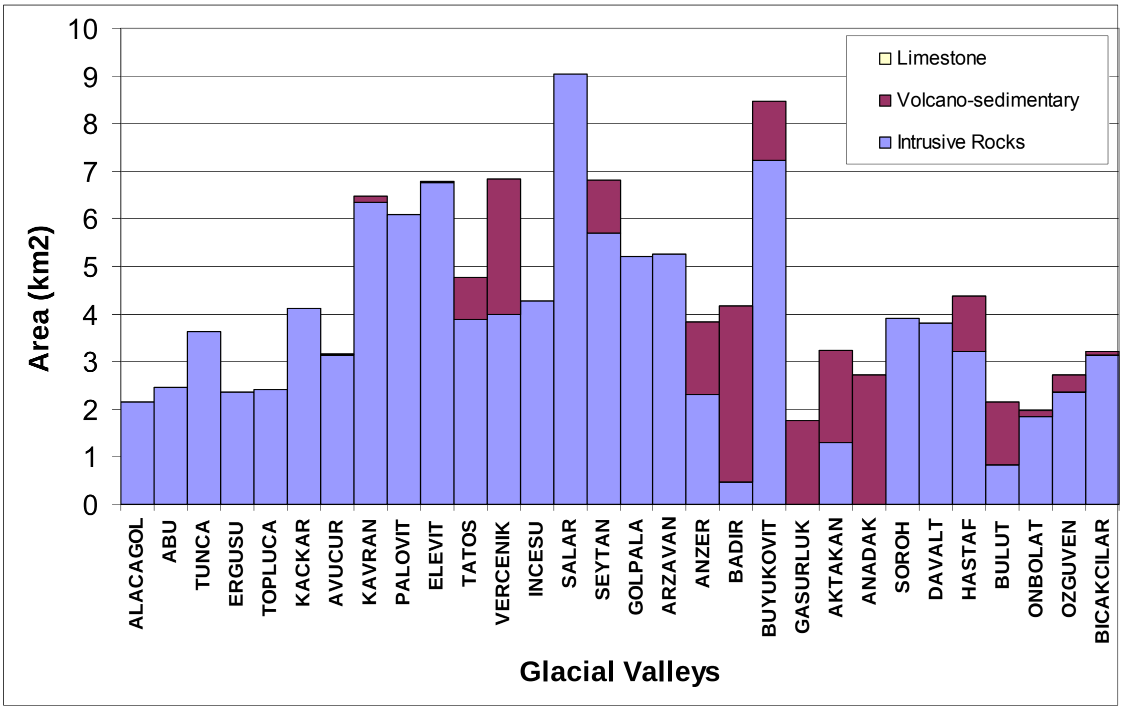

Figure 4.17: Histogram showing the areas covered by the rocks in the glacial valleys.

CHAPTER 5

GLACIAL CIRQUES

5.1. Identification of Cirques

Cirque is steep bowl-shaped hollow occurring at the upper end of a mountain valley, especially one forming at the head of a glacier or stream. They can be easily seen from contours map and DEM. Cirques in study area are digitized manually using the DEM and digital contour map. For each cirque a gate point of bowl is determined and starting from this point the cirque is digitized manually backward to crest or divide. A close up view of some cirques is shown in Figure 5.1 as an example. A total of 1222 cirques are digitized and saved as new layer (Figure 5.2).

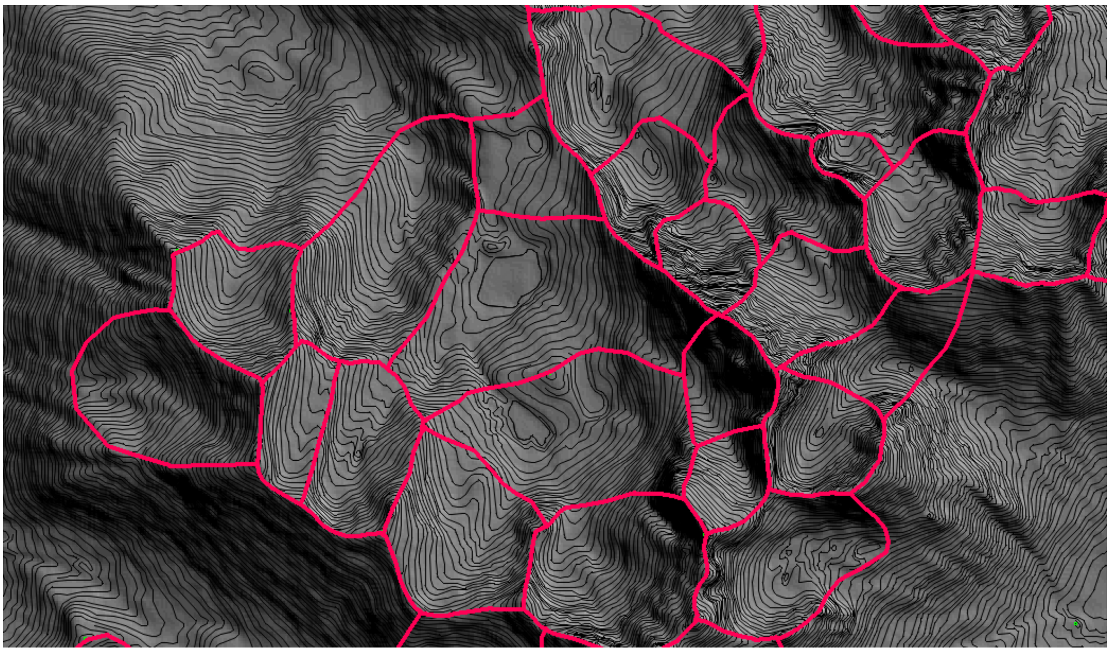

Figure 5.1: A close up view of the area showing digitization of glacial cirques.

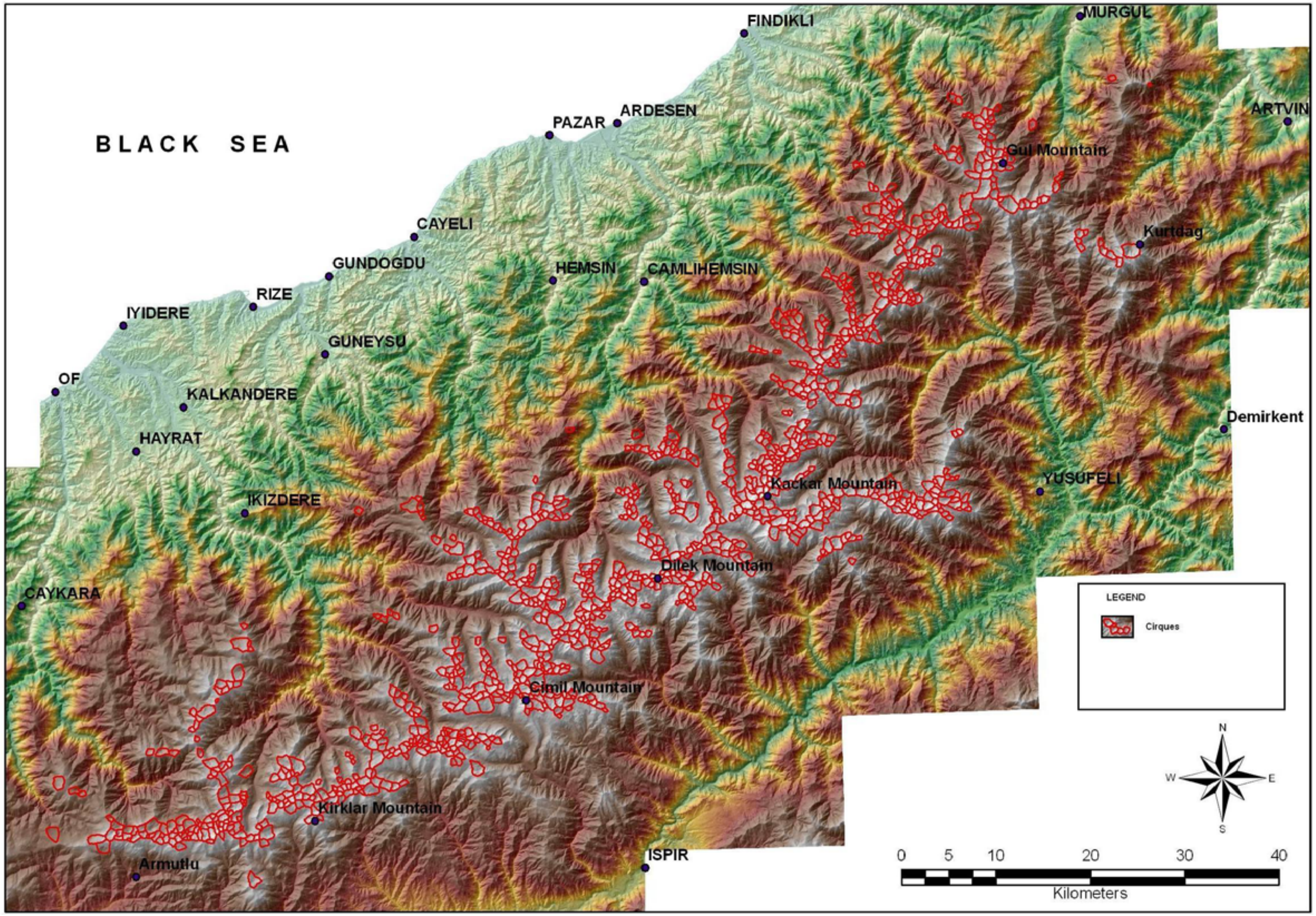

Figure 5.2: All cirques existing on study area

5.2. Creation of Database for Cirques

A database is created for the digitized the glacial cirques containing several properties (Table 5.1). Some properties are computed from the polygons that represent the boundary of the cirques, while some other properties are computed from the polygons of the cirques. A brief explanation of these properties is as follows:

ID: Digital numbers from 1 to 1222 were assigned to each glacial cirque as ID. This digital number is unique for each cirque, and contributes the key for database.

Location: Study area is divided in to parts as north and side separated by the main drainage divide. Location refers to the location of the cirque either to the north and south of the area in relation to this divide.

Valley name: The cirque is located in one of the drainage basins of the glacial valleys. This column represents the name of the valley to which this cirque belongs.

Central_X: Easting coordinate of the center of cirque stored UTM coordinate systems, ED 50 datum, Zone 37.

Central_Y: Northing coordinate of the center of cirque stored UTM coordinate systems, ED 50 datum, Zone 37.

Basal Elevation: Elevation is the height of cirques measured from sea level. It is measured at minimum elevation value representing the cirque base.

Slope: Cirques polygons are intersected with slope map and statistics are computed for each polygon. The mean value is assigned as slope value for each cirque.

Area: Area for each glacial cirque was computed from the polygon drawn for the cirque.

Perimeter: Length of glacial cirque polygons. This parameter will be used in order to define shape properties of Glacial Lakes.

Table 5.1: A part of the database negated for glacial cirques

ID	Location	Valley	Central_X	Central_Y	Basal Elevation	Average Slope	Area	Perimeter	Ideal Perimeter	Roundness	Lithology
1	South	Aktakan	664733	4510161	3112	43	223497	1903	1675	0.88	Volcano-sedimentary
2	South	Hastaf	684402	4524014	2968	29	970165	4275	3491	0.82	Volcano-sedimentary
3	South	Aktakan	663769	4510122	3153	37	290272	2073	1909	0.92	Volcano-sedimentary
4	North	Vercenık	663226	4510277	2957	38	560413	3207	2653	0.83	Volcano-sedimentary
5	North	Golpala	644908	4496576	2973	27	112367	1440	1188	0.83	Intrusive Rocks
6	North	-	640980	4510218	2450	11	297535	2317	1933	0.83	Intrusive Rocks
7	North	-	644521	4521866	2369	12	1840726	5966	4808	0.81	Volcano-sedimentary
8	North	-	642934	4510238	2454	22	413505	2451	2279	0.93	Intrusive Rocks
9	North	-	641628	4509904	2471	14	404688	2588	2255	0.87	Intrusive Rocks
10	North	Vercenık	662481	4510479	2839	21	660264	3822	2880	0.75	Volcano-sedimentary
11	North	Golpala	644856	4498112	2686	26	855147	3564	3277	0.92	Intrusive Rocks
12	North	Golpala	644908	4497024	2861	23	189373	1790	1542	0.86	Intrusive Rocks
13	North	Salar	658768	4510492	2958	28	540082	2855	2605	0.91	Intrusive Rocks
14	North	Seytan	645540	4499064	2605	25	1189449	4466	3865	0.87	Intrusive Rocks
:	:	:	:	:	:	:	:	:	:	:	:
:	:	:	:	:	:	:	:	:	:	:	:
:	:	:	:	:	:	:	:	:	:	:	:
1217	North	Tunca	692368	4541719	2458	32	518163	2966	2551	0.86	Volcano-sedimentary
1218	North	Ergusu	689909	4539569	2645	28	182413	1720	1514	0.88	Intrusive Rocks
1219	North	Ergusu	690273	4539118	2805	32	226394	2072	1686	0.81	Volcano-sedimentary
1220	North	Tunca	693128	4541455	2585	31	1275868	5260	4003	0.76	Volcano-sedimentary
1221	North	Ergusu	690950	4539914	2979	40	41872	874	725	0.83	Intrusive Rocks
1222	North	Tunca	691770	4541456	2799	29	155804	1534	1399	0.91	Volcano-sedimentary

Ideal Perimeter: Beside the real perimeter of the cirques an ideal perimeter is measured that represents the length of perimeter if the cirque has pure circular shape using the equation (2*pi*square (Area/pi)).

Roundness: This parameter is calculated by dividing the ideal perimeter by perimeter for each glacial cirque.

Lithology: Geology map is overlaid with glacial cirques layer and the lithologic unit which contains cirque is assigned to that cirque.

5.3. Properties of Cirques

The parameters that exist in the database are used to investigate the basic properties of the cirques. Analyses made here include the location, topographic properties, size, roundness, relation with lithology and density.

5.3.1. Location of the Cirques

Location refers to the site of the cirque in relation to the main drainage divide that separates the study area into two as north and south. This analysis therefore shows the distribution of the cirques in two parts of the area. According to the diagram prepared from the location of the cirques (Figure 5.3) 820 are located on northern part, and remaining 402 on the southern part.

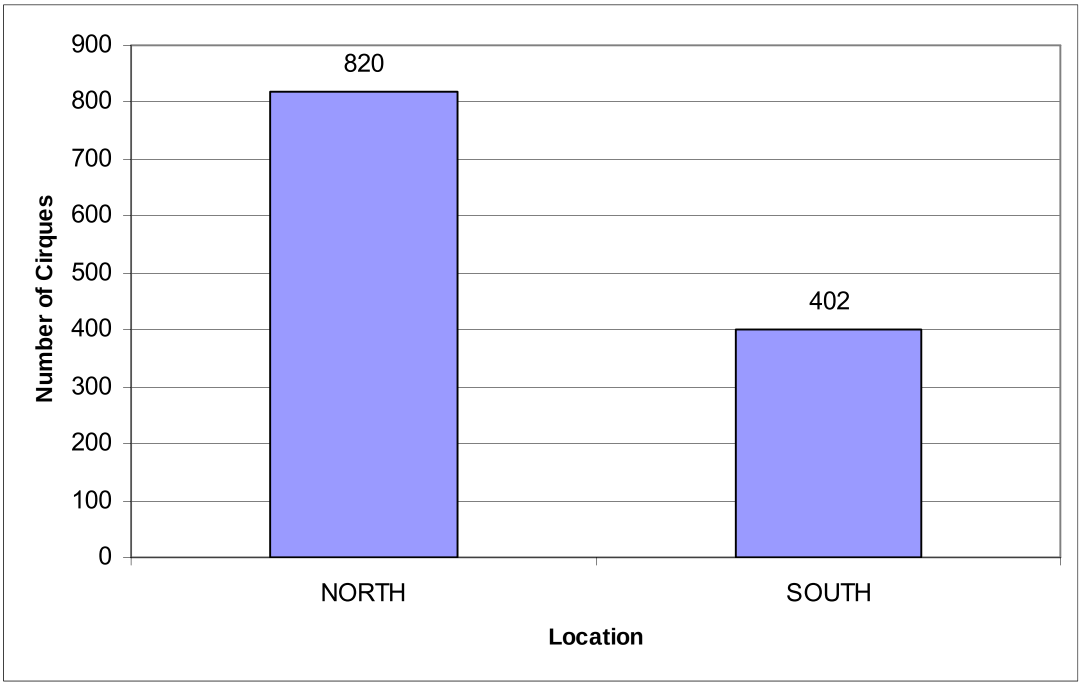

Figure 5.3: Distribution of cirques according to main aspect sides.

5.3.2. Topographic Properties of the Cirques

Topographic properties of the cirques are extracted from the DEM. Aspect is not taken into consideration because of their bowl shapes of the cirques. Therefore, here only two topographic properties, namely, basal elevation and slope will be dealt.

In order to examine dispersion of cirques in respect of their elevation, investigated area is divided into elevation zones of 100 m intervals and number of cirques for each zone is computed (Figure 5.4). Cirques start from 1700-1800 meters zone and go on to 3400-3500 m with different quantity. About 75 percent are located between 2600 and 3000 m. The cirques exist rarely below 2400 m and above 3200 m.

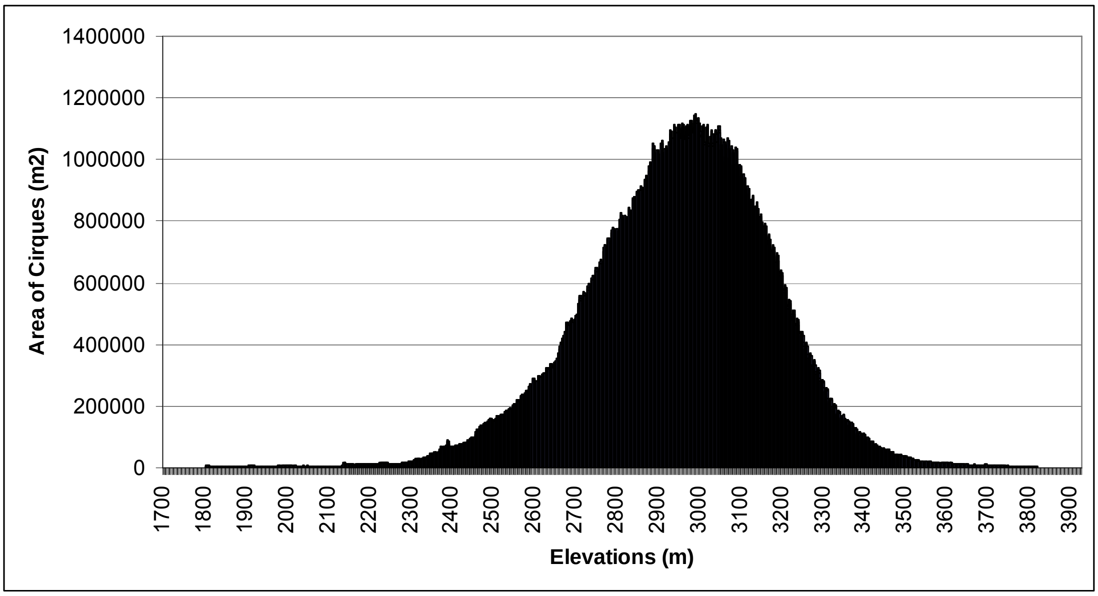

Figure 5.4: Distribution of cirques according to elevation.

Distribution of cirques according to elevation zones differs in both parts of the area (Figure 5.5). They start from 1700-1800 m zone on north side; while at south side the lowest ones exists at 2300-2400 m zone. In addition, cirques have maximum density between 2900-3000 m on north side whereas the density on south side is between 3050-3150 m. Therefore, the cirques in the southern part are exposed at higher elevations. This is best highlighted in the difference histogram in Figure 5.6 indicating that the cirques are developed more in the northern part up to elevation of about 3000 m after which is more dominant in the south side.

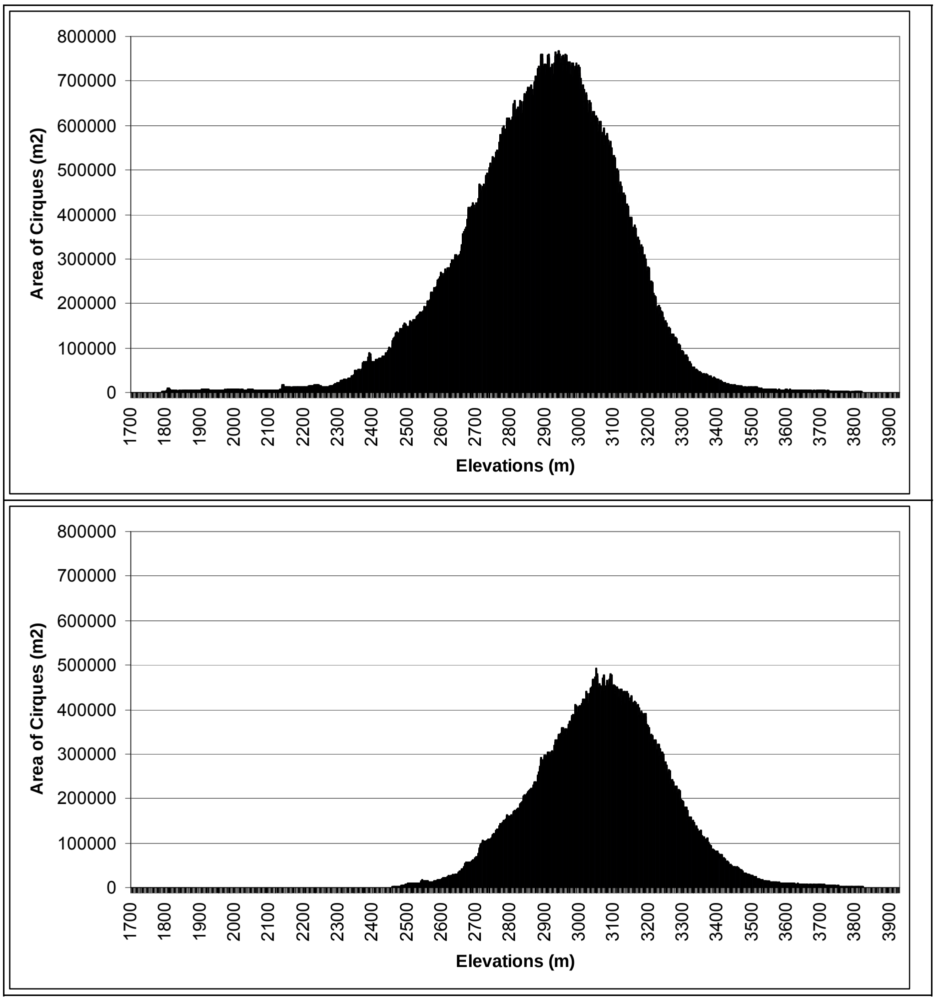

Figure 5.5: Distribution of cirques according to elevation zones in the north (above) and the south (below) sides.

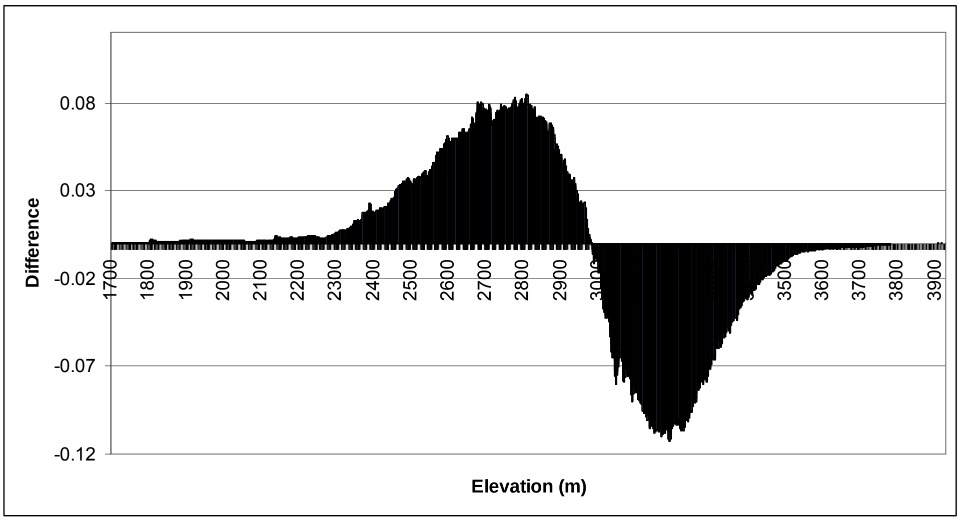

Figure 5.6: The difference histogram prepared by subtracting the percentage areas of cirques on the south side from north side.

A single slope value is assigned for each cirques polygon which is the mean value of the pixels in this polygon. These values are illustrated in Table 5.2 at 5-degree interval for the northern and southern parts separately. A histogram is given in Figure 5.7 for the whole area. Accordingly, the slope values range from 10 to 45° with a maximum concentration at 25-30°.

Table 5.2: Distribution of cirques according to slope groups with five degree intervals.

	Number of Cirques			Percentage		
Slope Intervals	Whole Area	North Side	South Side	North Side	South Side	North Side - South Side
0_5	0	0	0	0.0	0.0	0.0
5_10	0	0	0	0.0	0.0	0.0
10_15	11	11	0	1.3	0.0	1.3
15_20	56	39	17	4.8	4.2	0.5
20_25	261	185	76	22.6	18.9	3.7
25_30	438	301	137	36.7	34.1	2.6
30_35	313	197	116	24.0	28.9	-4.8
35_40	110	62	48	7.6	11.9	-4.4
40_45	29	21	8	2.6	2.0	0.6
45+	4	4	0	0.5	0.0	0.5

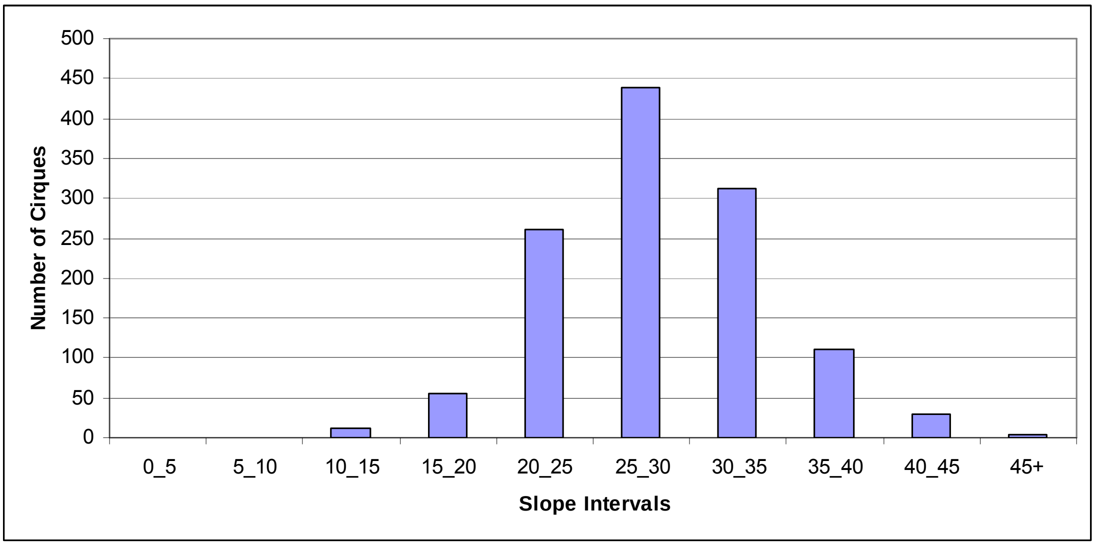

Figure 5.7: Distribution of cirques according to slope groups with five degree intervals.

The slope percentages of the southern cirques are subtracted from the northern ones to see a probable difference (Figure 5.8). Positive region in the diagram indicates the abundance in the northern part and vice versa the negative region indicates the abundance in the southern part. Accordingly, the cirques with slope values lower then 30° and higher then 40° are more on north side (Table 5.2 and Figure 5.8).

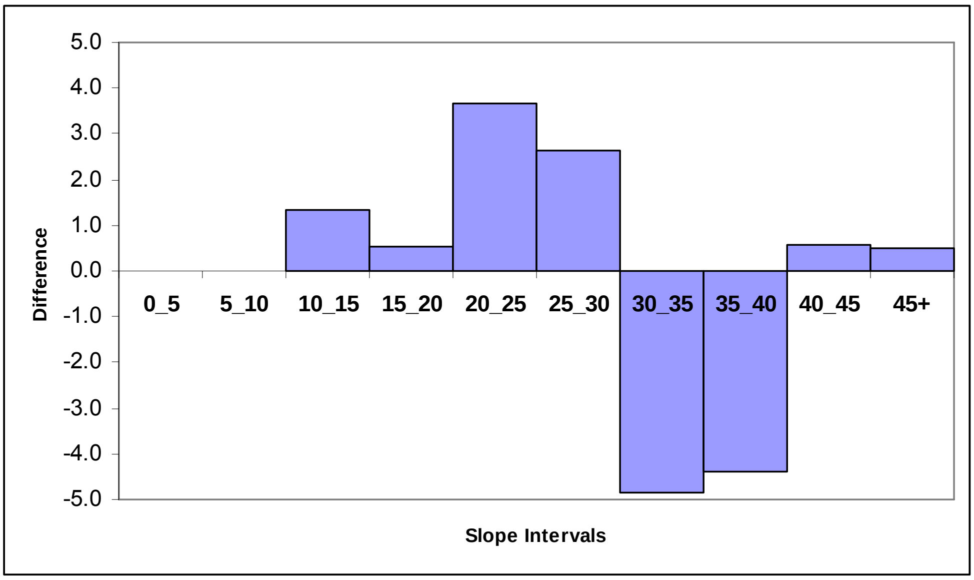

Figure 5.8: Differences between cirques on north and south sides with respect to slope property (percent of cirques on north – percent of cirques on south side).

5.3.3. Size of the Cirques

The area of each polygon that represents the cirques object is computed as a parameter and saved into database. Here the size of cirques and their distribution according to topographic properties are examined.

The area of cirques is investigated at intervals of 0.5 km^2 (Figure 5.9). The areas change between 0.03 km^2 (the smallest) and 2.93 km^2 (the largest). Majority of cirques (1116 of 1222 cirques) have area less then 1 km^2. The areas of 794 cirques (about 70 %) are less then 0.5 km^2. Remaining 106 cirques are larger the 1 km^2.

To compare the size of the cirques located in the northern part of the area with the southern part two scatter plots are prepared using the areas of the cirques versus elevation (Figure 5.10). The cirque in these plots is represented by the elevation of its center. The trend lines are added to the plots in red color. The trend lines in both areas gradually decreases as the elevation increases. This means, the larger cirques are located at lower elevations while the smaller ones occur at the upper elevations. This relation is more emphasized in the southern part as indicated by a steeper slope of the trend line.

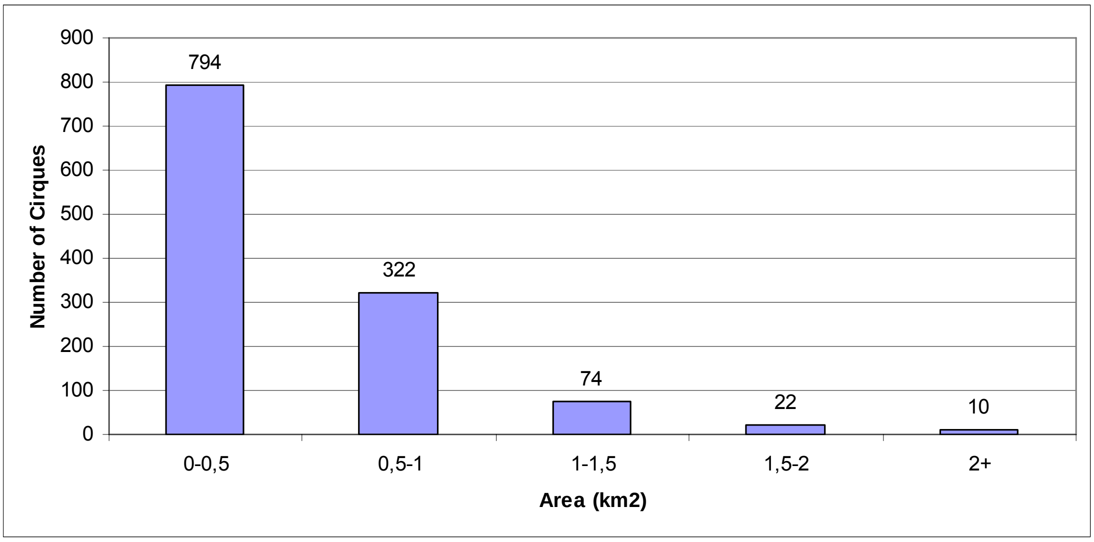

Figure 5.9: Distribution of cirques according to their size.

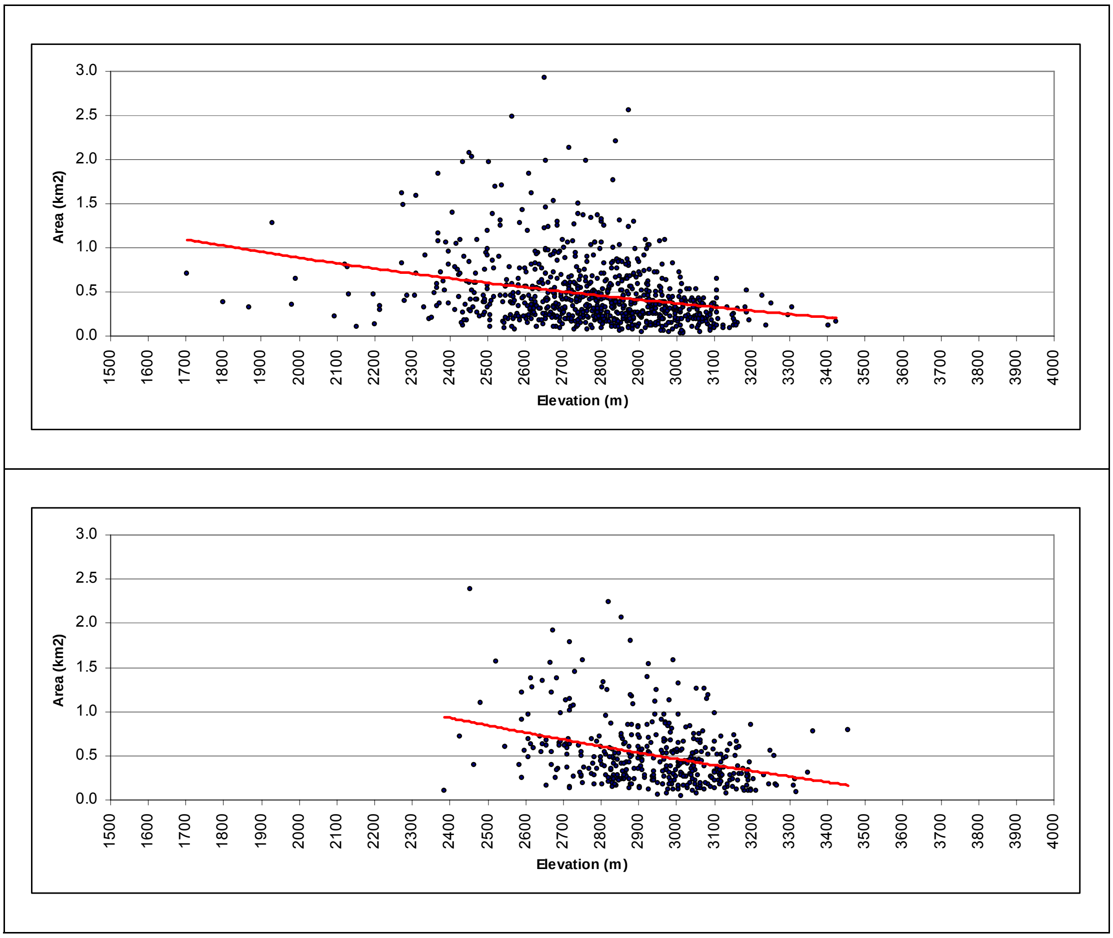

Figure 5.10: Scatter plots of elevation versus area of cirques for the northern (above) and southern (below) parts of the area.

5.3.4. Roundness of the Cirques

The roundness of the cirque is calculated by dividing the ideal perimeter by true perimeter that gives a range between 0 and 1. The plot for all roundness values given in Figure 5.11 indicates that most of the cirques have a roundness value close to 0.9. Therefore, the boundaries of the cirques are usually smooth without any major irregularity. In order to test the variation of roundness against elevation a scatter plot is generated at 100 m interval (Figure 5.12). Accordingly, there is a slight variation in the roundness indicated by a negative trend line. As the elevation increases, the roundness of cirques decreases implying that the cirques at lower elevations are smoother..

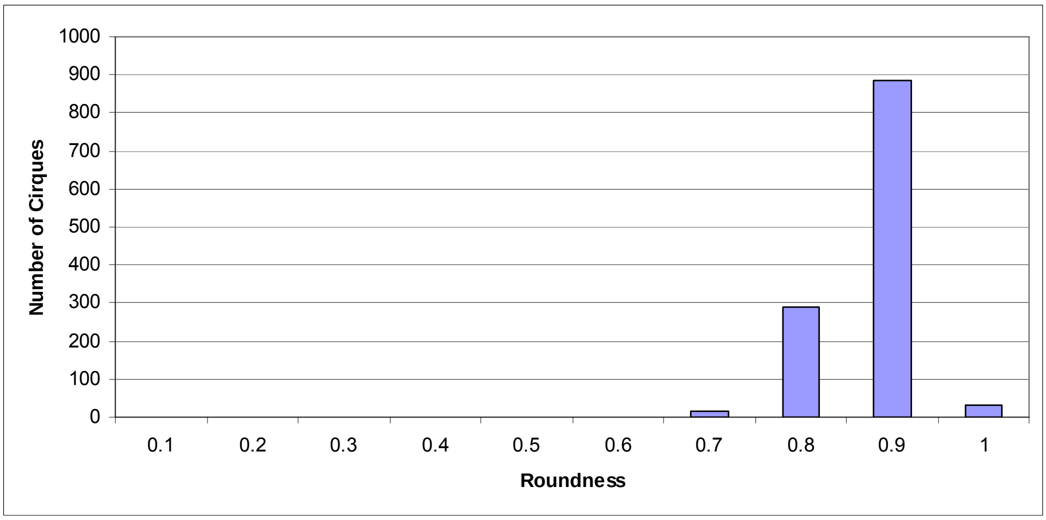

Figure 5.11: Distribution of cirques according to roundness.

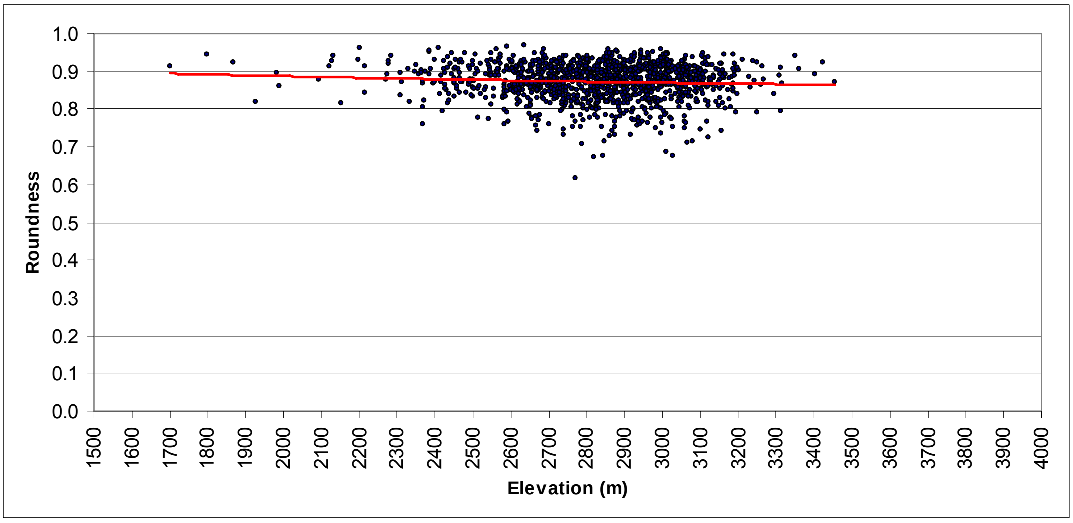

Figure 5.12: Scatter plots of elevation versus roundness of cirques for the whole area.

5.3.5. Lithologic Properties of Cirques

It is necessary to consider the lithologic properties during the investigation of the cirques because certain properties of rocks such as hardness, flexibility, permeability etc may affect the development of cirque in any particular rock type.

The relationship between the cirques and the lithologies is investigated on the parameters given in Table 5.3 and Figure 5.13 which are extracted by intersection of lithology and cirque layers. Although there are six lithologic units in the area they do not show an equivalent distribution. The half of study area consists of intrusive rocks, and 46 percent of volcano-sedimentary rocks. The remaining 4 percent of area consists of other four lithologic units namely limestone, clastic sedimentary rocks, volcanic rocks, and clastic and carbonate rocks.

Table 5.3: Properties of cirques according to lithologic units.

Lithologic Unit	Area of Lithologic Units (km^2)	Area of Cirques (km^2)	% Area of Lithologic Units	% Area of Cirques	Difference
Volcano-sedimentary Rocks	2466	296	45.9	49.9	4.0
Intrusive Rocks	2701	290	50.3	48.9	-1.4
Limestone	51	3	0.9	0.5	-0.4
Clastic Sedimentary Rocks	19	3	0.4	0.5	0.2
Volcanic Rocks	108	1	2.0	0.2	-1.8
Clastic & Carbonate Rocks	29	0	0.5	0.0	-0.5

The percentage area of lithologic unit is subtracted from the percentage of cirques total area to investigate the suitability of the lithologies (Figure 5.14). Accordingly, volcano-sedimentary rocks and with a low value the clastic sedimentary rocks have positive score that indicates these rocks are more suitable for cirque development compared to others.

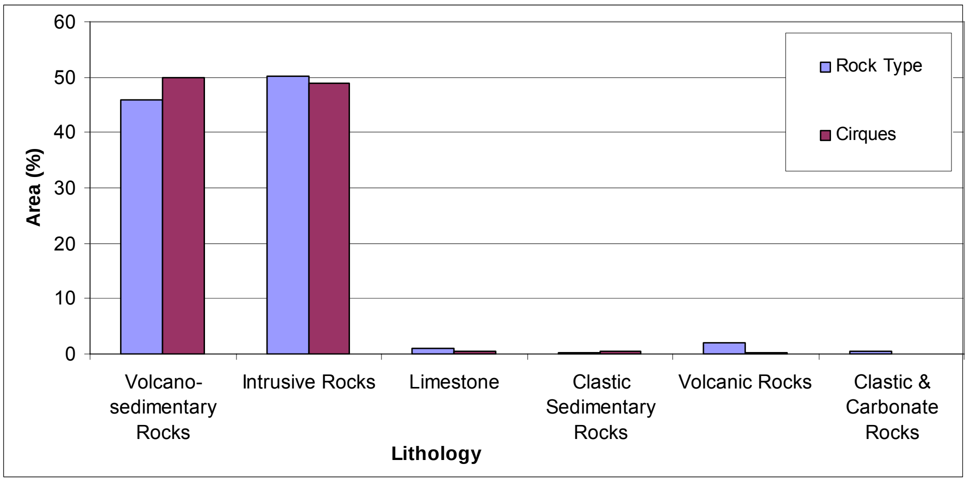

Figure 5.13: The percent areas distribution of lithologic unit classes' and cirques within each lithologic unit.

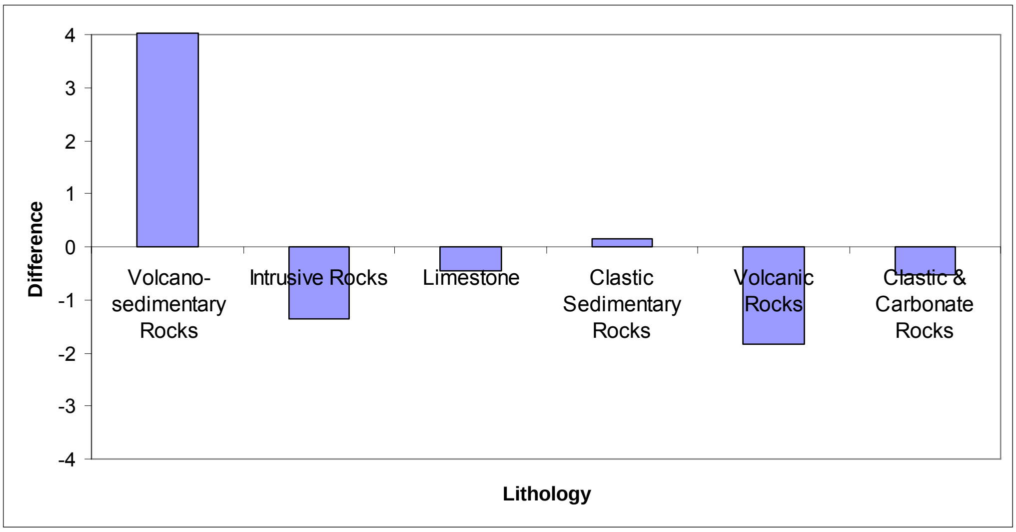

Figure 5.14: Differences between percent area of cirques and percent area of lithologic units.

5.3.6. Density of the Cirques

The density of the cirques through the study area is interpolated by applying the Kriging method with a search radius of 5 km (Figure 5.15). Two observations made based on this figure are 1) High density region is consistent with the regional drainage divide of the area; 2) The distribution is denser especially on north side of the study area.

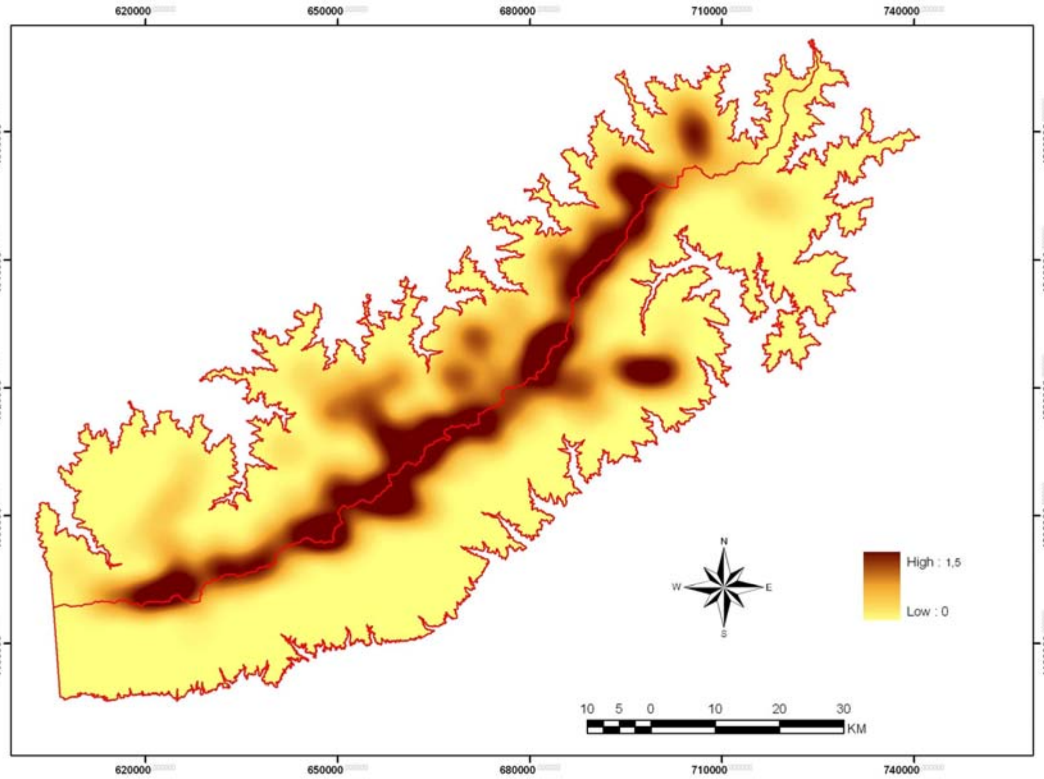

Figure 5.15: Distribution of cirques through study area.

CHAPTER 6

GLACIAL LAKES

6.1. Identification of Glacial Lakes

A glacial lake is a hollow formed by glaciers as it moves. The lakes are classified into two types as abrasion and deposition lakes based on the mode of glacier movement either vertical or horizontal. The movement of glacier in a cirque area usually is vertical to sub-vertical excavating the floor of the cirque. After glaciers melt and retreat, this hollow is filled by water from the glaciers or by other sources such as precipitation or groundwater. The depositional lakes, on the other hand, are formed by moraine carried by glaciers. Glaciers rupture and transport material in the valley as they move. At the end point of the movement these materials settle down and form a barrier. Behind this barrier water is accumulated forming a depositional lake. In this study all hollows existing in the area are considered as lakes whatever the origin is.

The lakes are identified from the DEM by the help of contour and hydrologic maps and are manually digitized (Figure 6.1). The highest elevation of the hollow is accepted as boundary of the lake. A new GIS vector layer is generated containing the digitized lakes. In order to test the accuracy, this vector layer is overlaid on analog topographic map and all digitized lake objects are reviewed.

The total number of the glacial lakes identified in this study is 685 (Figure 6.2). Some of the lakes are dry while some others are filled with water. This property is not investigated; therefore the depths of the dry lakes are not measured. Other properties which are believed to contribute to the study are measured or computed and kept in a database.

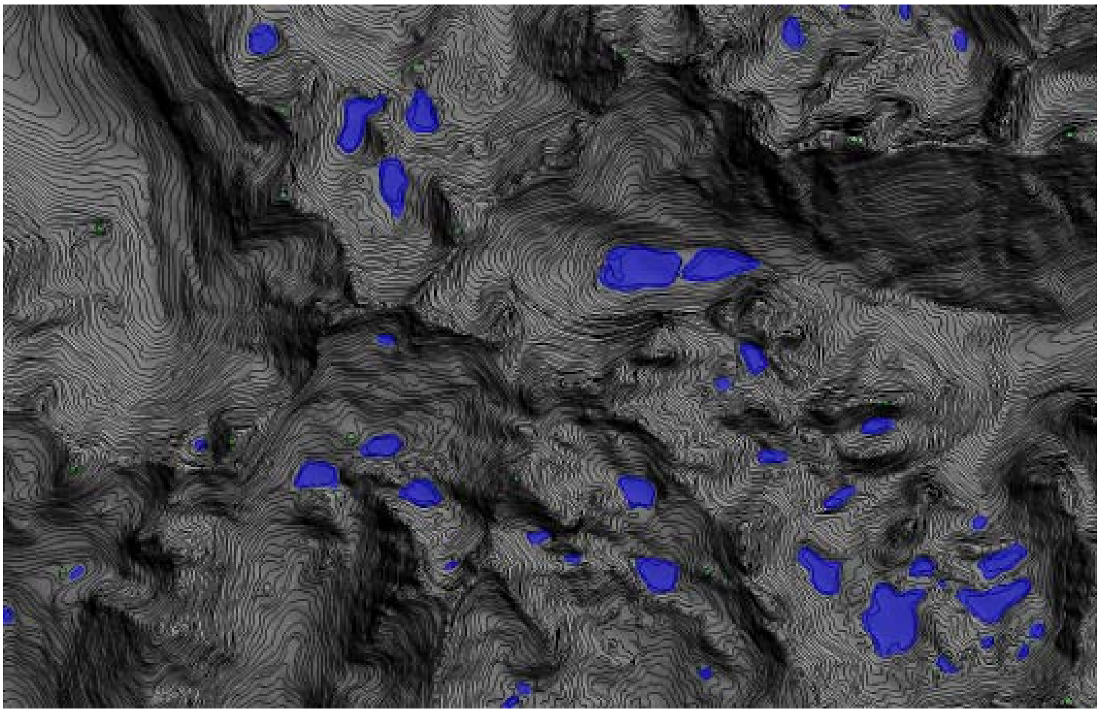

Figure 6.1: An example of digitization of glacial lakes over the DEM.

6.2. Creation of Database for Glacial Lakes

The database created for the lakes include the parameters to be used in the analysis. A section of the database is illustrated in Table 6.1 as an example. A short description of the parameters in the database is as follows:

ID: A total of 685 glacial lakes are detected and for each one an integer value between 1 and 685 is assigned as ID number. This ID column constitutes a key for database and has unique value for each object.

Location: Location of the lake in relation to the main drainage divide that separates the study area into two as north and south. Therefore, this attribute will get a value of either north or south.

Central X: Easting coordinate of the center of the lake stored in UTM ED50 projection system.

Central Y: Northing coordinate of the center of the lake stored in UTM ED50 projection system.

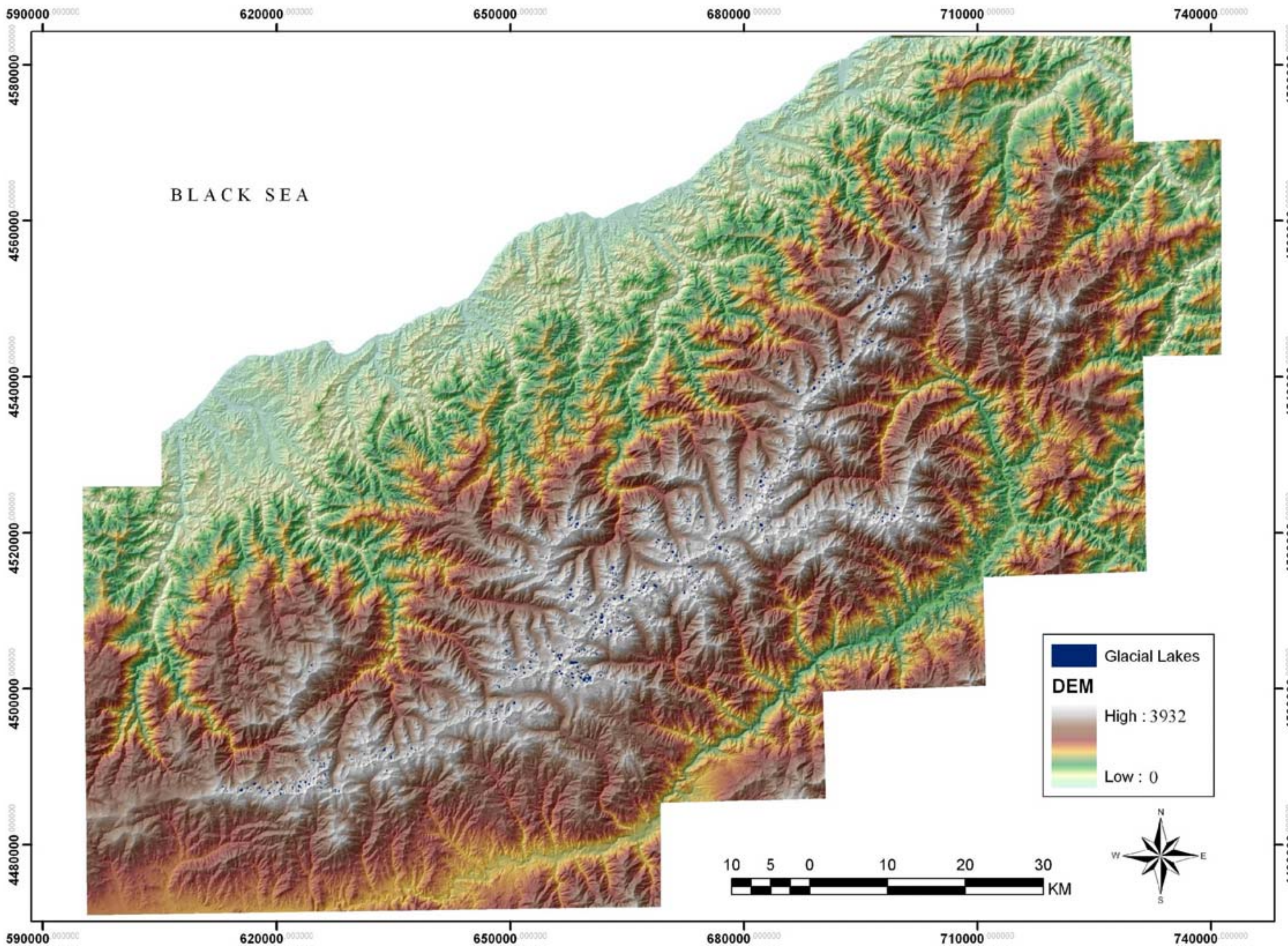

Figure 6.2: Glacial lakes identified in this study.

Table 6.1: A sample section of the database created for glacial lakes.

ID	Location	Center_X	Center_Y	Elevation (m)	Orientation (degree)	Area (m^2)	Perimeter (m)	Ideal Perimeter (m)	Roundness	Length (m)	Width (m)	Elongation	Lithology
1	South	665159	4509112	2951	276	23681	668	545	0.8	282.0	126.0	0.4	Volcano-sedimentary
2	South	665359	4511400	3158	51	25653	580	567	1.0	197.4	175.9	0.9	Volcano-sedimentary
3	North	657052	4519533	3028	268	949	118	109	0.9	45.6	27.4	0.6	Intrusive Rocks
4	North	620084	4487982	2647	324	17629	531	470	0.9	205.6	107.1	0.5	Volcano-sedimentary
5	North	626073	4489987	2881	261	1576	183	140	0.8	79.2	27.6	0.3	Volcano-sedimentary
6	North	652799	4520142	2873	117	1627	151	143	0.9	57.5	35.4	0.6	Volcano-sedimentary
7	North	622815	4486864	3026	24	8244	337	321	1.0	98.9	67.4	0.7	Volcano-sedimentary
8	North	659756	4520863	2950	257	10492	397	363	0.9	138.8	107.1	0.8	Volcano-sedimentary
9	South	659162	4501889	2950	58	11913	492	386	0.8	216.5	72.5	0.3	Volcano-sedimentary
10	South	649760	4497197	2868	214	4031	284	225	0.8	122.2	48.4	0.4	Volcano-sedimentary
11	North	650968	4514837	2999	2	4454	254	236	0.9	96.7	56.6	0.6	Intrusive Rocks
:	:	:	:	:	:	:	:	:	:	:	:	:	:
:	:	:	:	:	:	:	:	:	:	:	:	:	:
680	South	678612	4516696	3128	122	260	60	57	1.0	20.0	15.5	0.8	Intrusive Rocks
681	South	679313	4516164	3005	188	1391	160	132	0.8	68.5	25.7	0.4	Intrusive Rocks
682	South	681267	4521160	3486	123	1246	130	125	1.0	47.4	34.6	0.7	Volcano-sedimentary
683	South	685082	4519942	3125	48	637	93	89	1.0	32.2	27.3	0.8	Volcano-sedimentary
684	South	688845	4520890	3109	117	1034	123	114	0.9	48.2	29.9	0.6	Volcano-sedimentary
685	South	689017	4528543	2923	178	737	98	96	1.0	31.3	29.1	0.9	Volcano-sedimentary

Elevation: Elevation of the boundary line of the lake that defines the boundary of lake. This line represents the upper surface of the lake. Other elevations within the polygon are not taken into consideration.

Area: Area of the lake calculated by computer software represented by the area of the polygon.

Perimeter: Length of the lake polygon computed by the software. This parameter will be used to evaluate the shape of the lake.

Ideal Perimeter: Ideal perimeter is a parameter computed from the perimeter assuming a pure circular shape for the lake using the equation Ideal Perimeter=2*pi*square (Area/pi). This parameter together with true perimeter will be used to interpret the shape of the lake.

Roundness: Roundness is a measure of the roughness of the lake boundary. This parameter is calculated is dividing the Ideal Perimeter by Perimeter of each Glacial Lake (Figure 6.3). The result is a number between 0 and 1 like. If the number is close to 1, it means the lake has smooth boundary; if the value is close to 0, that means the lake has rough boundary.

Length: This is a straight line that represents the long axis of the lake. It is drawn manually over the lake polygon.

Width: This is a straight line that represents the long axis of the lake. It is drawn manually over the lake polygon.

Elongation: Elongation means the ratio between of the width and length (Elongation=Width/Length). These two lines normally should be perpendicular to each other. The result is a number between 0 and 1. At a value of 1, the lake is circular; as the number decreases to 0 the lake gets more elongated (Figure 6.4).

Lithology: Name of the rock unit in which the lake is formed.

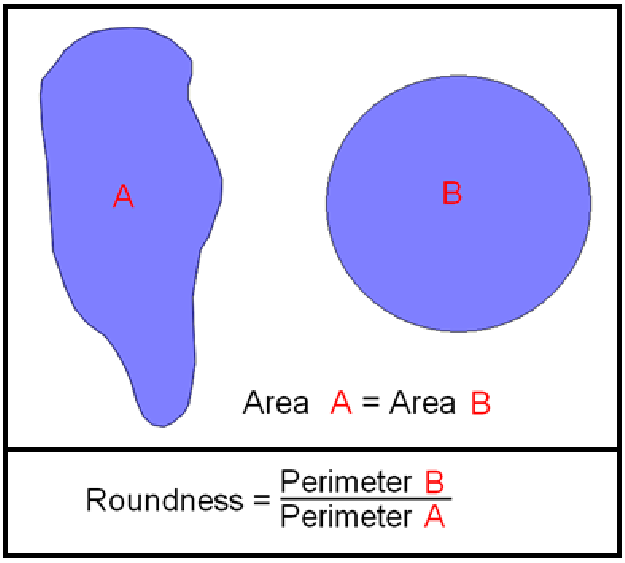

Figure 6.3: Computation of roundness for glacial lakes.

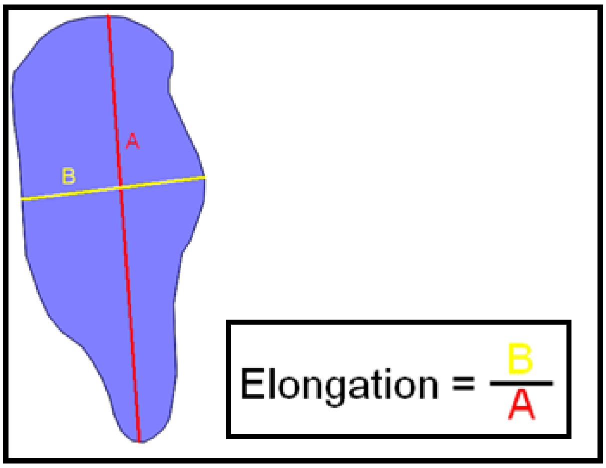

Figure 6.4: Computation of elongation for each glacial lake.

6.3. Properties of Glacial Lakes

Parameters listed in the database are used to investigate the basic properties of the lakes. Analyses made here include the location, topographic properties, size, elongation, roundness, orientation, lithology and density.

6.3.1. Location of the Lakes

Distribution of the lakes is analyzed by plotting a) number, b) area of the lakes for the northern and southern parts separately (Figure 6.5). Accordingly, 431 lakes (63 %) are located on the northern and 254 lakes (37 %) on the southern. The distribution according to the area gives, more or less, the same distribution.

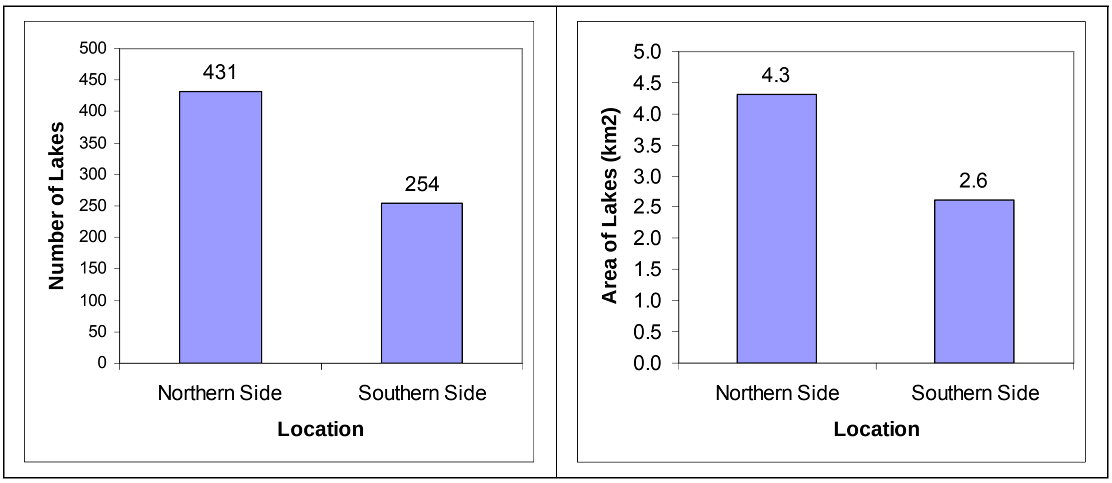

Figure 6.5: Distribution of number and area glacial lakes according to aspect sides.

6.3.2. Topographic Properties of Lakes

The only topographic property investigated for the lakes is elevation. Since the surface of the lake is horizontal there is no slope value; and therefore there is no aspect. For analysis of the elevation, the area is divided into elevation zones with interval of 100 m and number of lakes and area of lakes for each elevation zone is counted (Table 6.2). Distribution shown in Figure 6.6 indicates that approximately 85 percent of lakes are occurred between 2700 and 3200 m elevations.

The comparison of the lakes of the northern and southern parts is given in Figure 6.7. The lowest lake on south is located between 1700-1800 m whereas on north side the lowest one is located between 1500-1600 m. Great portion of lakes on north side are distributed between 2700 and 3100 m while on south side between 2900 and 3300 m. Therefore, south side lakes are developed at higher elevation than the north side.

Table 6.2: Frequency of lakes according to elevation zones.

Elevation Zone (m)		Number of Lake		
Min.	**Max.**	**Whole Area**	**North Side**	**South Side**
1500	1600	1	1	0
1600	1700	0	0	0
1700	1800	1	0	1
1800	1900	2	2	0
1900	2000	1	1	0
2000	2100	2	0	2
2100	2200	1	1	0
2200	2300	1	1	0
2300	2400	5	5	0
2400	2500	17	14	3
2500	2600	25	24	1
2600	2700	42	38	4
2700	2800	94	75	19
2800	2900	110	86	24
2900	3000	152	95	57
3000	3100	122	60	62
3100	3200	77	23	54
3200	3300	26	5	21
3300	3400	4	0	4
3400	3500	2	0	2
Total		**685**	**431**	**254**

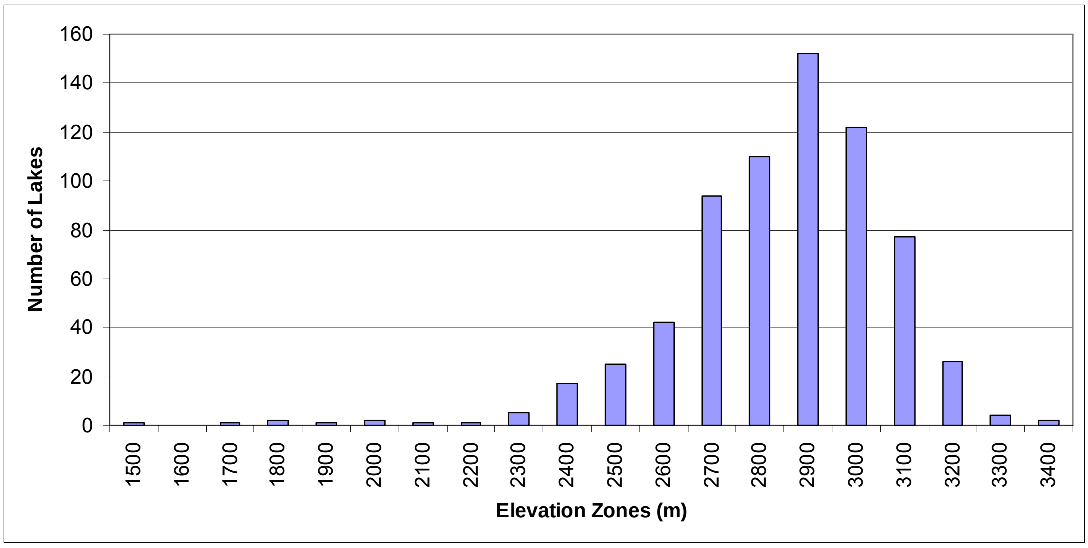

Figure 6.6: Distribution of number of glacial lakes according to elevation zones.

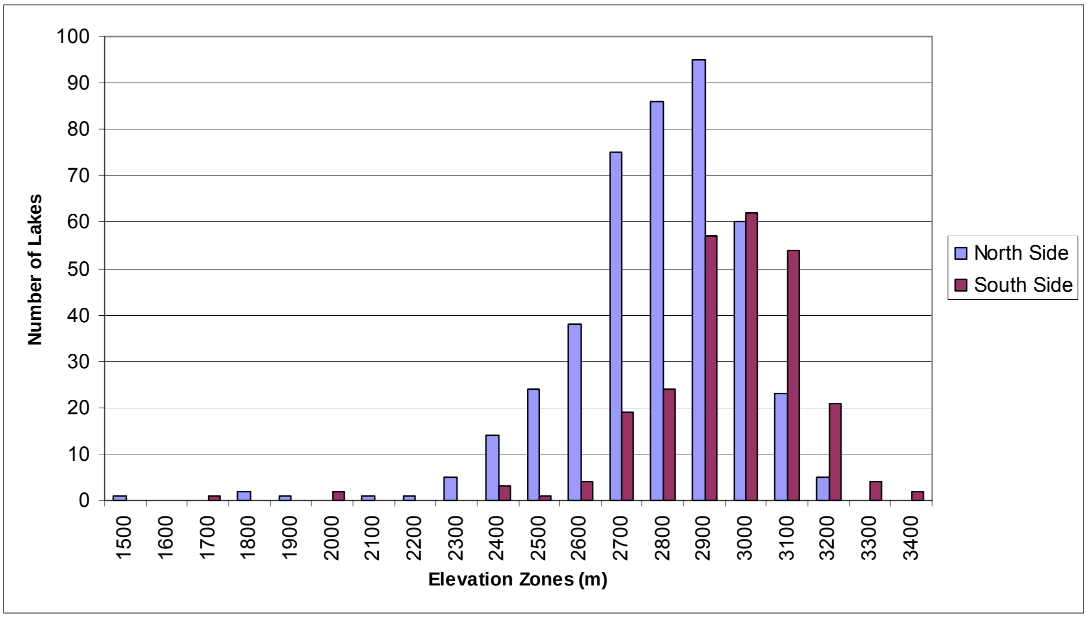

Figure 6.7: Distribution of glacial lakes according to elevation zones comparing North and South sides.

6.3.3. Size of Lakes

The size of the lakes is usually represented by its area which is already a parameter existing in the database. The smallest lake has an area of 114 m^2, while the largest one 115509 m^2. The lakes in the database are classified into 6 classes with interval of 10000 m^2 area (Figure 6.8). The great portion of lakes has area lower than 10000 m^2. However, it should be noted that 24 lakes have area more than 50000 m^2 area.

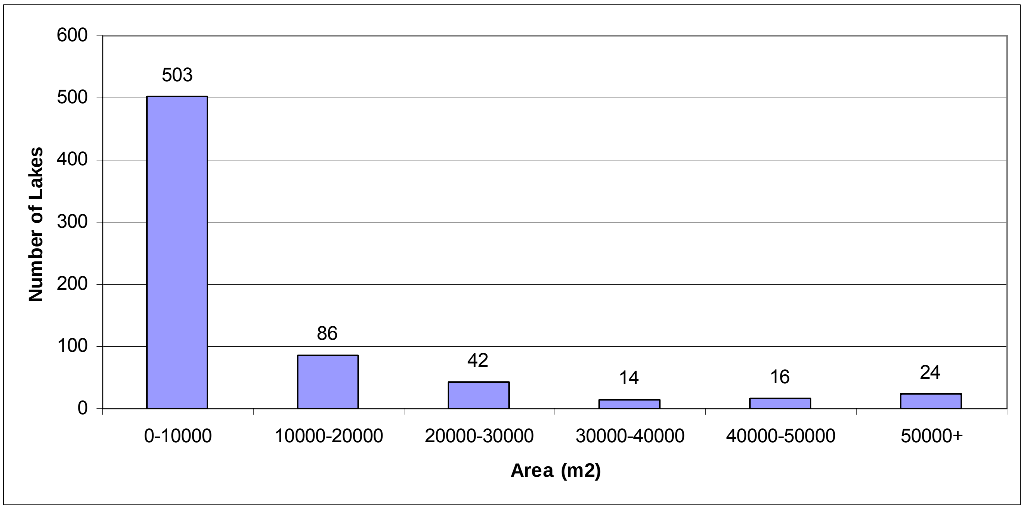

Figure 6.8: Distribution of glacial lakes according to size.

Areas of lakes are plotted against elevation separately for north and south to seek a probable difference (Figure 6.9). Based on the trend line drawn for each cluster, a slight change across the elevation can be observed. This is the case valid for both sides. Therefore, as the elevation increases the size of the lake decreases.

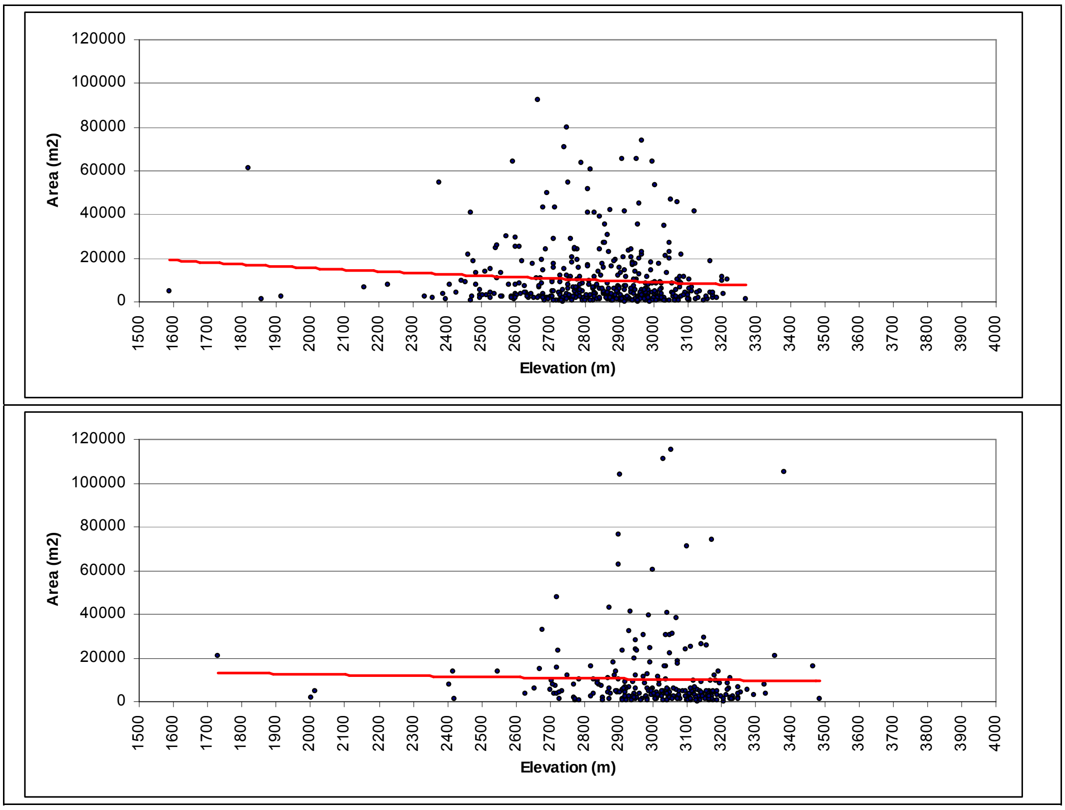

Figure 6.9: Scatter plots of elevation versus area of lakes for the northern (above) and southern (below) parts of the area.

6.3.4. Elongation of Lakes

Elongation is a parameter used to investigate the shape of glacial lakes. For each lake two perpendicular axes are drawn, one for the long axis the other for the short axis that represent the length and the width, respectively. Length of these axes are measured and saved into database of lakes.

Elongation parameter is computed by dividing width by length value of each lake which will range between 0 and 1. The lakes having value close to "1" have circular shape whereas that having value close to "0" have elongated shape. This range is divided into five classes as Well Elongated, Elongated, Semi Circular, Circular, and Well Circular. According to this classification distribution of lakes are shown in Table 6.3. Frequency of these values is illustrated in Figure 6.10. Accordingly, majority of lakes in the area have value between 0.4 and 0.8.

Table 6.3: Distribution of glacial lakes according to elongation.

		Number of Lakes		
Elongation	Whole Area	North Side	South Side	
0.1	2	1	1	Well Elongated
0.2	7	4	3	
0.3	46	23	23	Elongated
0.4	106	61	45	
0.5	105	68	37	Semi Circular
0.6	141	98	43	
0.7	120	81	39	Circular
0.8	93	54	39	
0.9	60	37	23	Well Circular
1.0	5	4	1	

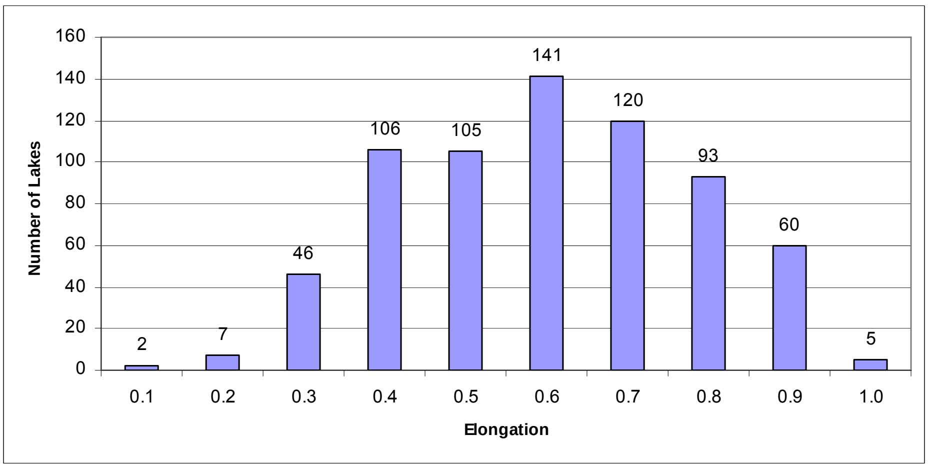

Figure 6.10: Distribution of glacial lakes according to elongation.

The elongation frequency of northern and southern lakes is shown separately in Figure 6.11. Although both sides show similar distribution a small difference can be noticed. The lakes on north side have a normal distribution with a peak at middle part of graph (at 0.6). The southern part, on the other hand, is characterized by high frequency between 0.4 and 0.8 elongation values.

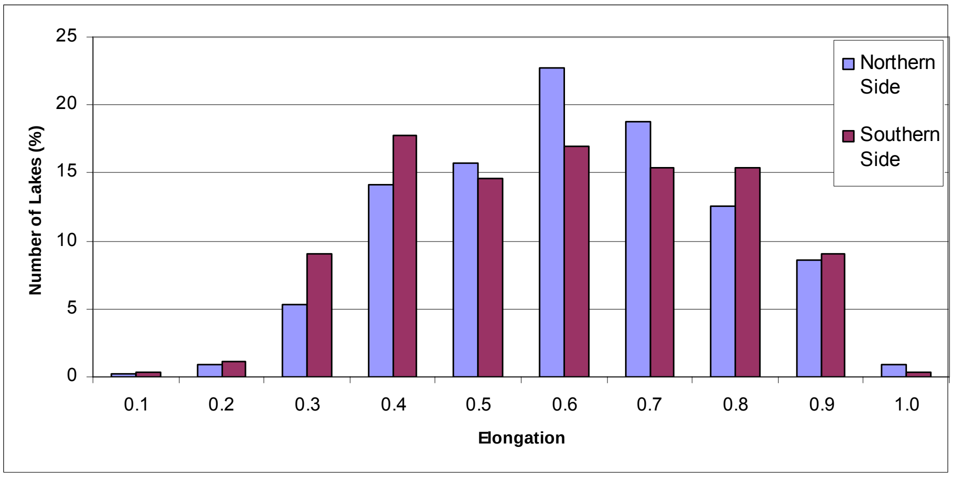

Figure 6.11: Percentage distribution of lake elongation according to their location sides.

6.3.5. Roundness of Lakes

The roundness is computed by dividing the ideal perimeter of the lake by its true perimeter. Accuracy of this parameter depends on resolution of DEM and Contours map. In this study, digital topographic map of 1:25000 scale are used with contour interval of 10 m. On the other hand, the lakes investigated generally have depths less then 10 m.

Roundness values for the lakes are tabulated in Table 6.4 and plotted in Figure 6.12. Almost all glacial lakes show smooth boundary properties. This is confirmed by 220 of 685 lakes having value of 1 and 313 value of 0.9. Number of lakes with a roundness value less than 0.8 is only 31.

Comparison of the lake roundness on the northern and southern parts of the area is shown in Figure 6.13. In general, the roundness properties of lakes located on both sides show similar properties.

Table 6.4: Distribution of glacial lakes according to roundness.

		Number of Lakes	
Roundness	Whole Area	North Side	South Side
0.1	0	0	0
0.2	0	0	0
0.3	0	0	0
0.4	1	1	0
0.5	0	0	0
0.6	3	1	2
0.7	27	18	9
0.8	121	65	56
0.9	313	208	105
1.0	220	138	82

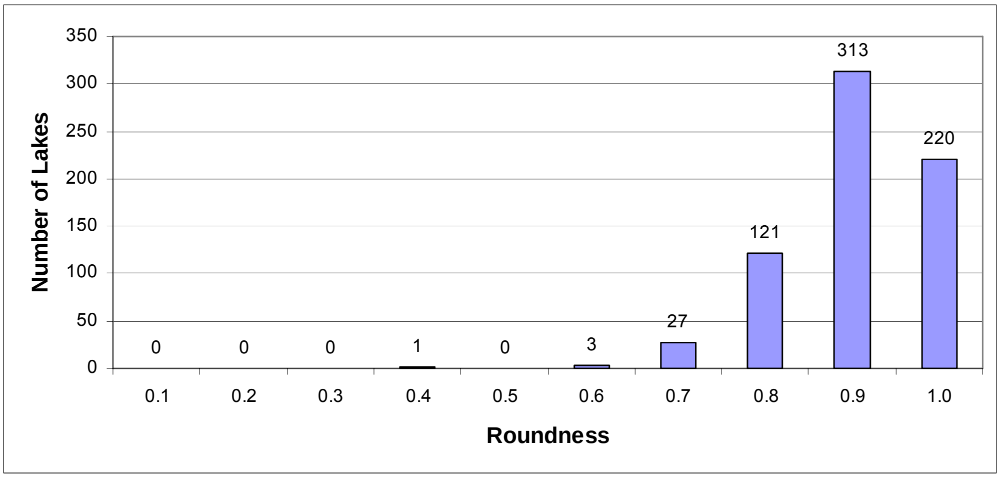

Figure 6.12: Distribution of glacial lakes according to roundness.

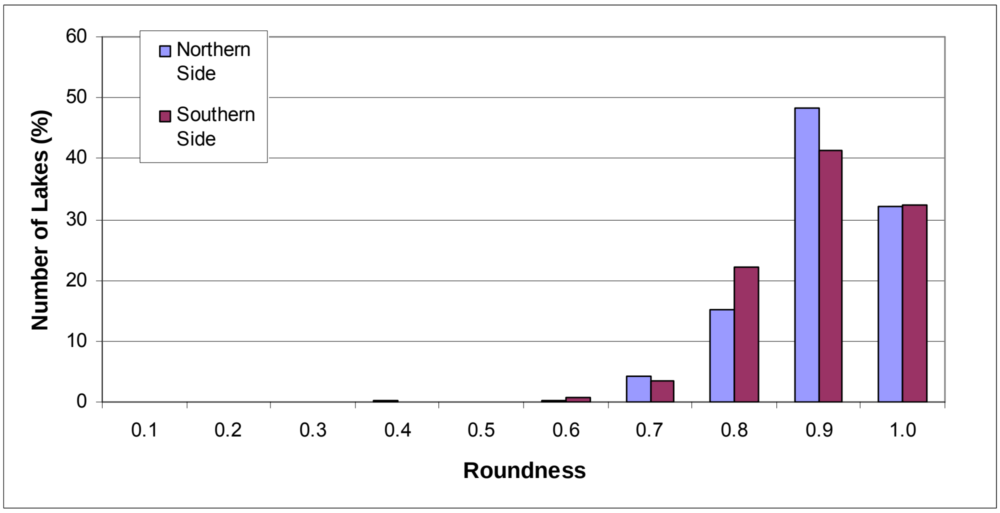

Figure 6.13: Distribution of glacial lakes according to roundness on different aspect sides.

6.3.6. Orientation of Lake Elongation

Orientation of the lake is computed using the direction of its long axis. Since the upper surface of the lake is horizontal, there is no sense of this direction. Therefore the direction is confined to the interval between 0 and 180°. An orientation in NW direction, for example, is the same as SE. The graph prepared from the orientations is given in Figure 6.14 for 10-degree interval. According to diagram there is not a dominant direction for the orientation as indicated by an equalized histogram.

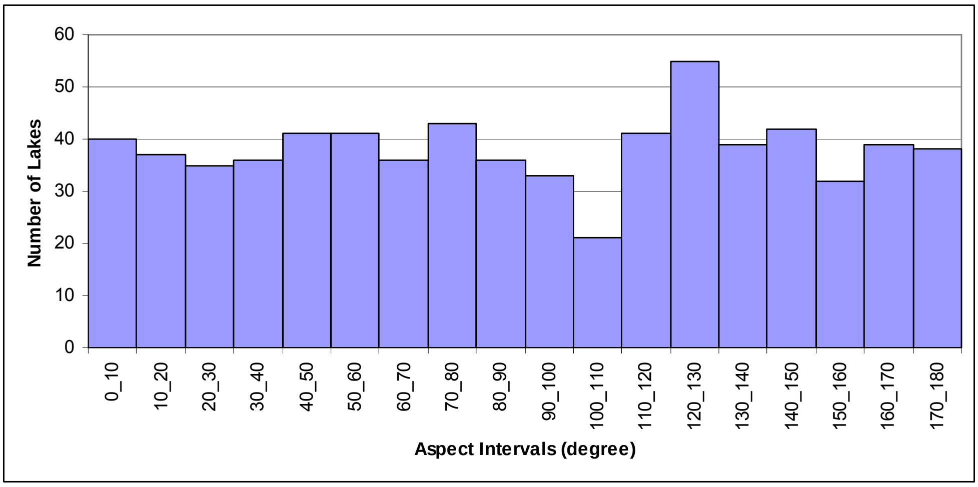

Figure 6.14: Histogram showing the frequency of the orientation of lake elongations.

6.3.7. Lithologic Properties of Lakes

The relationship between the lakes and the rock units in the area is investigated by intersecting the lithology and lake layers. The parameters measured during this process are given in Table 6.5 and Figure 6.15. Two rock types out of six, volcano-sedimentary and intrusive rocks cover most of the area. The area covered by these two lithologies is more than 96 %. The rest of the area is covered by limestone, clastic sedimentary rocks, volcanic rocks, and clastic and carbonate rocks.

Lithologic units are investigated for suitability of lake development by subtracting the percentage of area of lithologic unit from percentage of lakes total area within each unit (Figure 6.16). Consequently, volcano-sedimentary, clastic sedimentary rocks and to some extend the limestone have positive scores (suitable), whereas the intrusive rock and volcanic rocks have negative

Table 6.5: Properties of cirques according to lithologic units.

Lithologic Units	Area of Lithologic Units (km^2)	Area of Lakes (km^2)	% Area of Lithologic Units	% Area of Lakes	Difference
Volcano-sedimentary Rocks	2466	3.40	45.9	49.1	3.2
Intrusive Rocks	2701	3.27	50.3	47.2	-3.1
Clastic Sedimentary Rocks	19	0.12	0.4	1.7	1.4
Limestone	51	0.08	0.9	1.1	0.2
Volcanic Rocks	108	0.06	2.0	0.9	-1.1
Clastic & Carbonate Rocks	29	0.00	0.5	0.0	-0.5

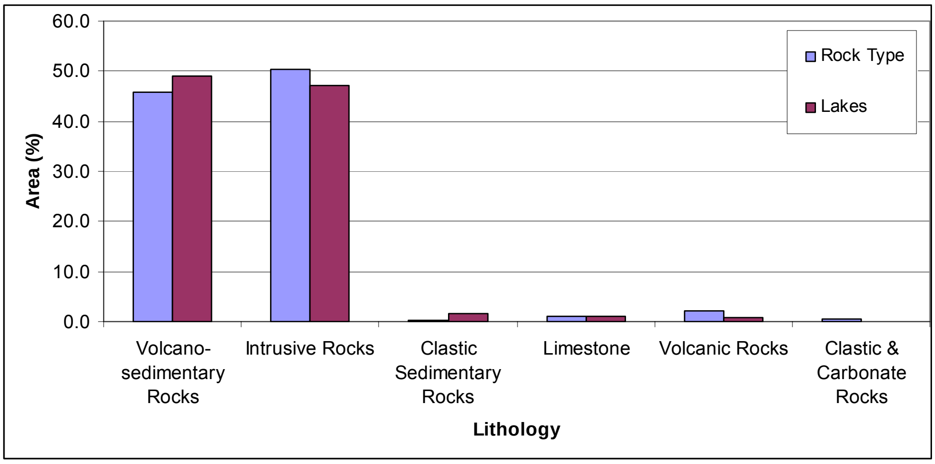

Figure 6.15: The percent area distribution of lithologic unit classes, and lakes within each lithologic unit.

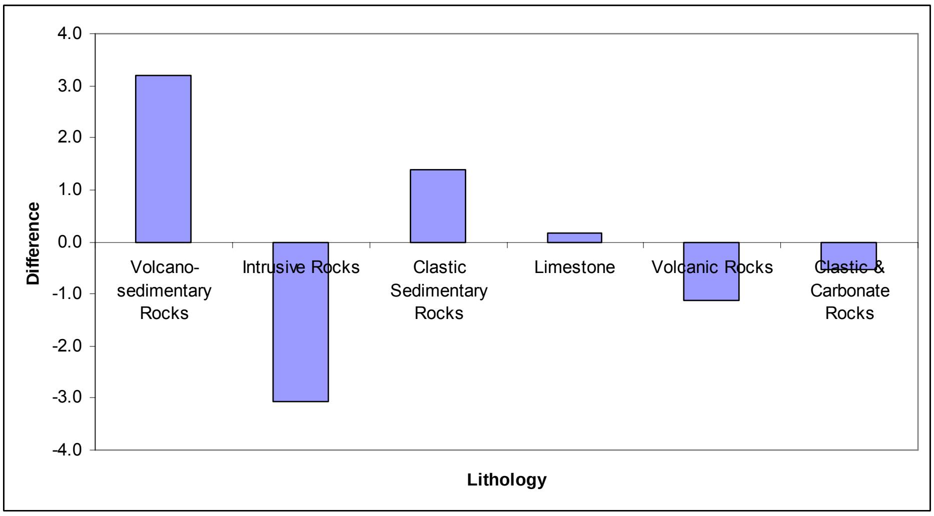

Figure 6.16: Differences between percent area of lakes and percent area of lithologic units.

6.3.8. Density of Lakes

The density of the lakes exposed in the study area is interpolated by applying the Kriging method with a search radius of 5 km (Figure 6.17). Two observations made based on this figure are 1) High density region is consistent with the regional drainage divide of the area; 2) The distribution is symmetric in the middle part of the area with respect to the drainage divide; however, in the eastern and western parts of the area the lakes are more in the northern part of the area.

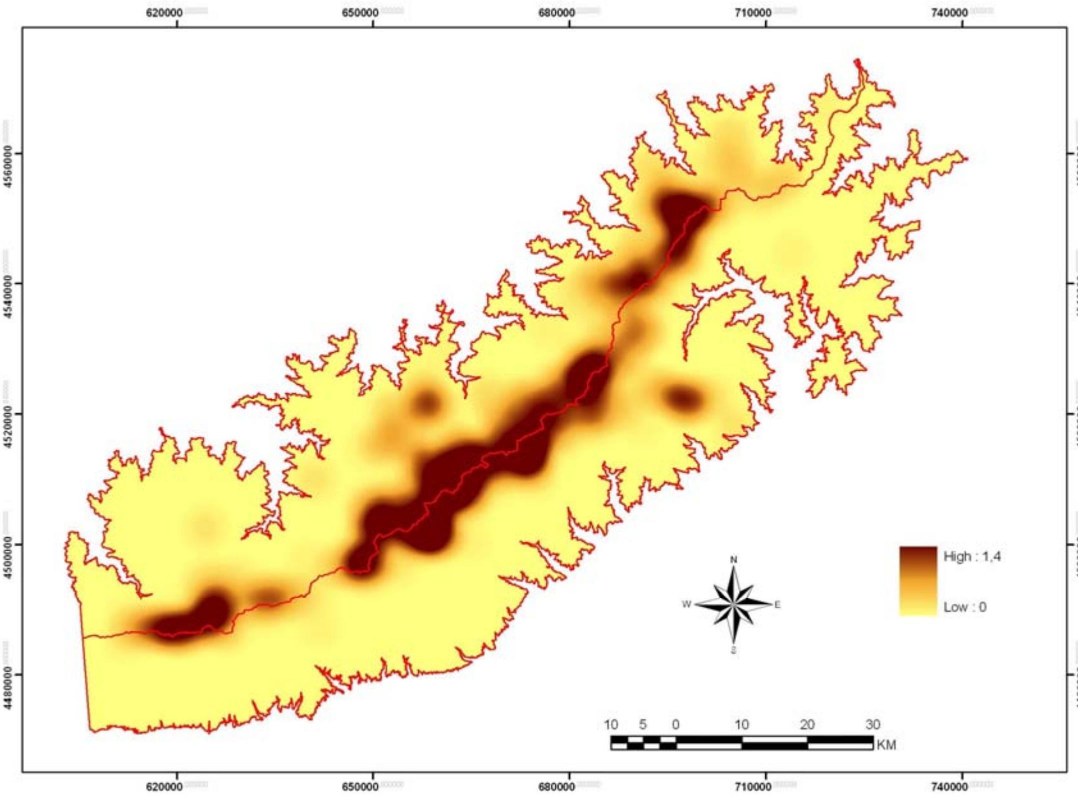

Figure 6.17: Distribution of glacial lakes through study area.

CHAPTER 7

CONDITION OF ACTIVE GLACIERS

In this study the glaciation and the landscapes of glaciers have constituted the main purpose. Glaciation is a continuous action that grows and shrinks depending on climate conditions. The study area is exposed by glaciation especially in Pleistocene. During Holocene the glaciers started to melt and retreated. Recently because of Global Warming, the glaciers shrank and became smaller in size.

This chapter focuses on the present conditions of glaciers that exist in the area. Their existence, size and distribution are investigated using Remote Sensing applications. First of all satellite images of study area are obtained. Two frames of Landsat images (172-031 and 172-32) are acquired covering the study area (Figure 7.1).

The glaciers can be confused with snow, so the date of images is very important for studies of glaciations. The last year snow should be melt, and the new year's snow should not fell down. For this reason images that belong to September are selected. The year of the image, on the other hand, is also important. It should be a recent image because the actual glaciers will be investigated. The most recent image available belongs to the year of 2007. Based on the criteria the Landsat 7 ETM images taken 8 September 2007 are obtained.

7.1. Preparation of Satellite Images

The images acquired geometrically and atmospherically are already corrected. Histogram Matching analysis is conducted, because the images belong to two different paths. The coincident bands in both frames are merged to create new seven bands containing two frames. Finally seven bands were cropped by boundary of study area (above 1500 m) and all bands are spectrally enhanced (Figure 7.2).

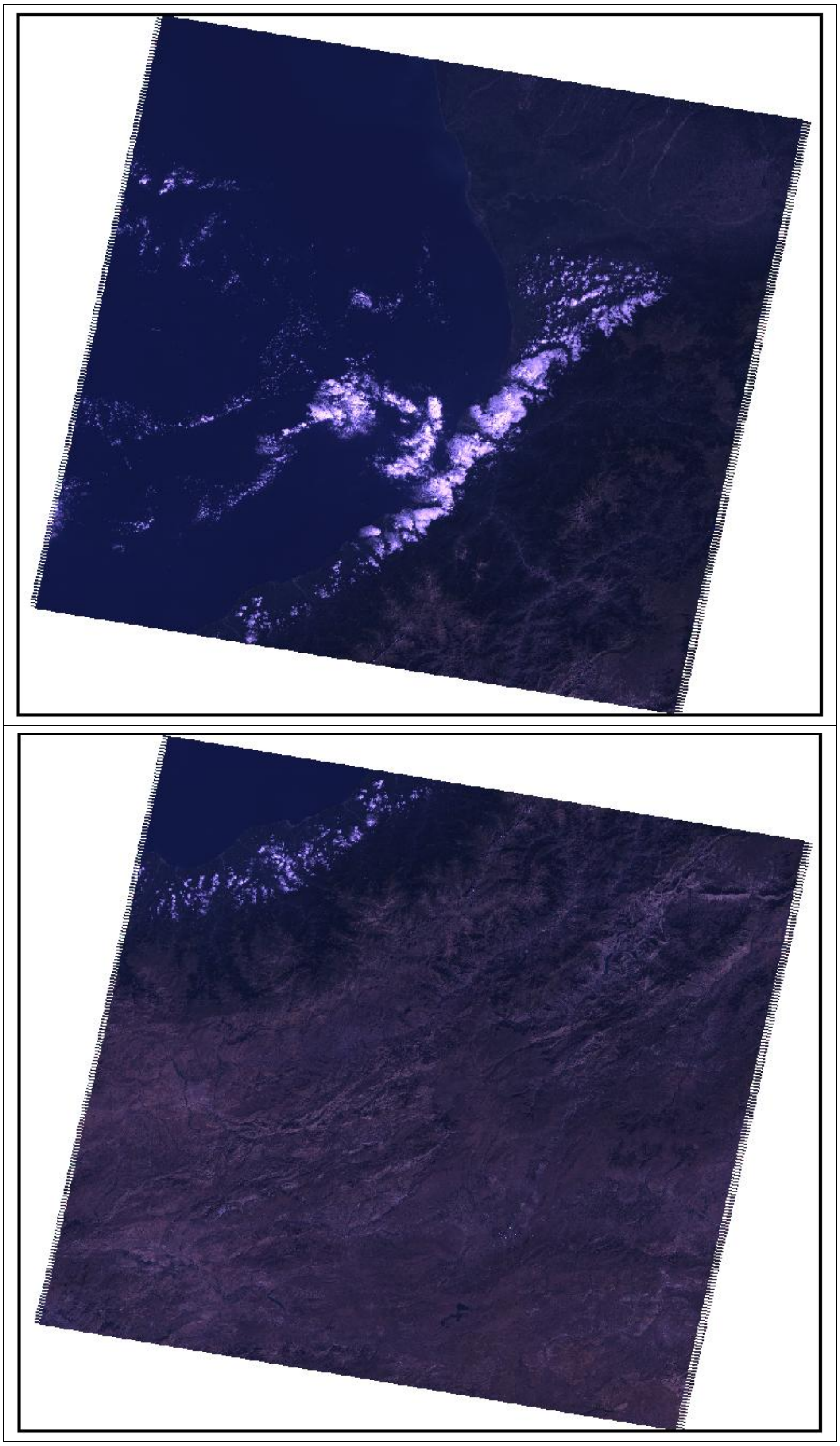

Figure 7.1: Two raw frames of Landsat 7 ETM images used in this study (3, 2, 1: RGB). Index numbers: 172-031 (upper), 172-032 (lower). Date: 08.09.2007.

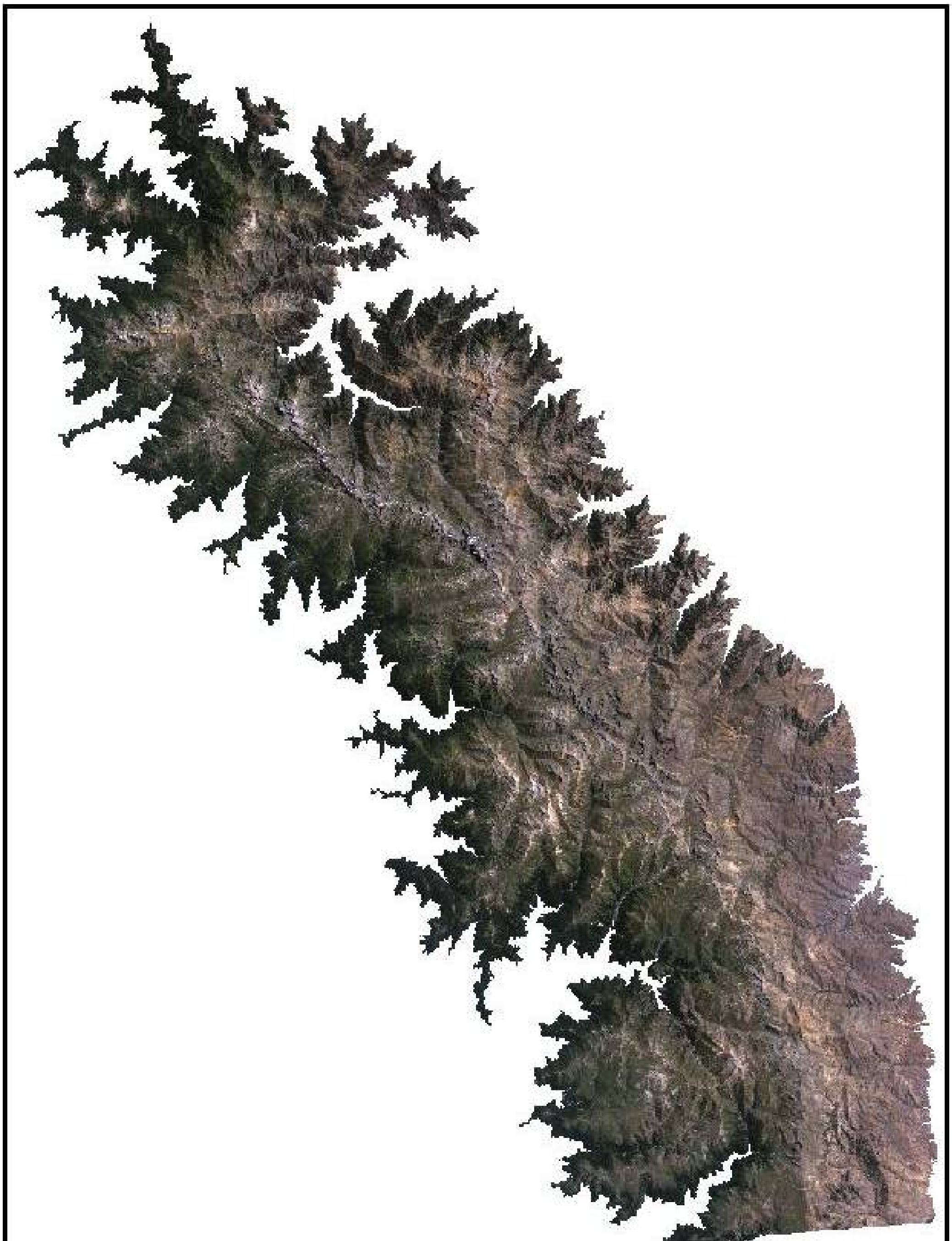

Figure 7.2: Final satellite images prepared for determining glaciers.

7.2. Determination of Active Glaciers

Two common methods mentioned in the literature to determine the active glaciers applied to Landsat images are Normalized Difference Snow Index (NDSI), and the Band Rationing. These two methods are applied here to identify the glaciers in the study area.

7.2.1. Normalized Difference Snow Index (NDSI)

Although NDSI is a snow index, it is also sensitive, and can be used for determining glaciers. The equation is NDSI=(TM band2 – TM band5) / (TM band2 + TM band5). By applying this index a new image is generated having values between -1 and +1. Certain threshold values are assigned to this scale to determine the glacier. Based on the trial and error as well as the threshold values known in the literature a threshold value of 0.5-1.0 is accepted. Accordingly, the pixels which have a value between 0.5 and 1.0 are representing the active glaciers. Consequently, through study area active glaciers are determined as small patches distributed at different places (Figure 7.3).

7.2.2. Band Rationing

Band rationing method is also commonly used for determining active glaciers. In this method Red Band of image is divided by Shortwave Infrared Band (SWIR). In the shorter wavelengths the red band is sensitive in glaciers. At this portion on electromagnetic spectrum, the glaciers reflect high energy, so the values saved via this band are greater. Inversely the SWIR band works with longer wavelength. The glaciers reflect lower energy at this portion, so the data detected by this band is lower then the Red Band. Consequently dividing Red band by SWIR band produces higher values for glaciers. Using the threshold values in the literature and the trial and error on these images the value of 4 is accepted as threshold. Therefore, the pixels that have value greater then 4 are assigned as glaciers in the final map. The last step is converting this raster map into vector format. The resultant map is shown in Figure 7.4.

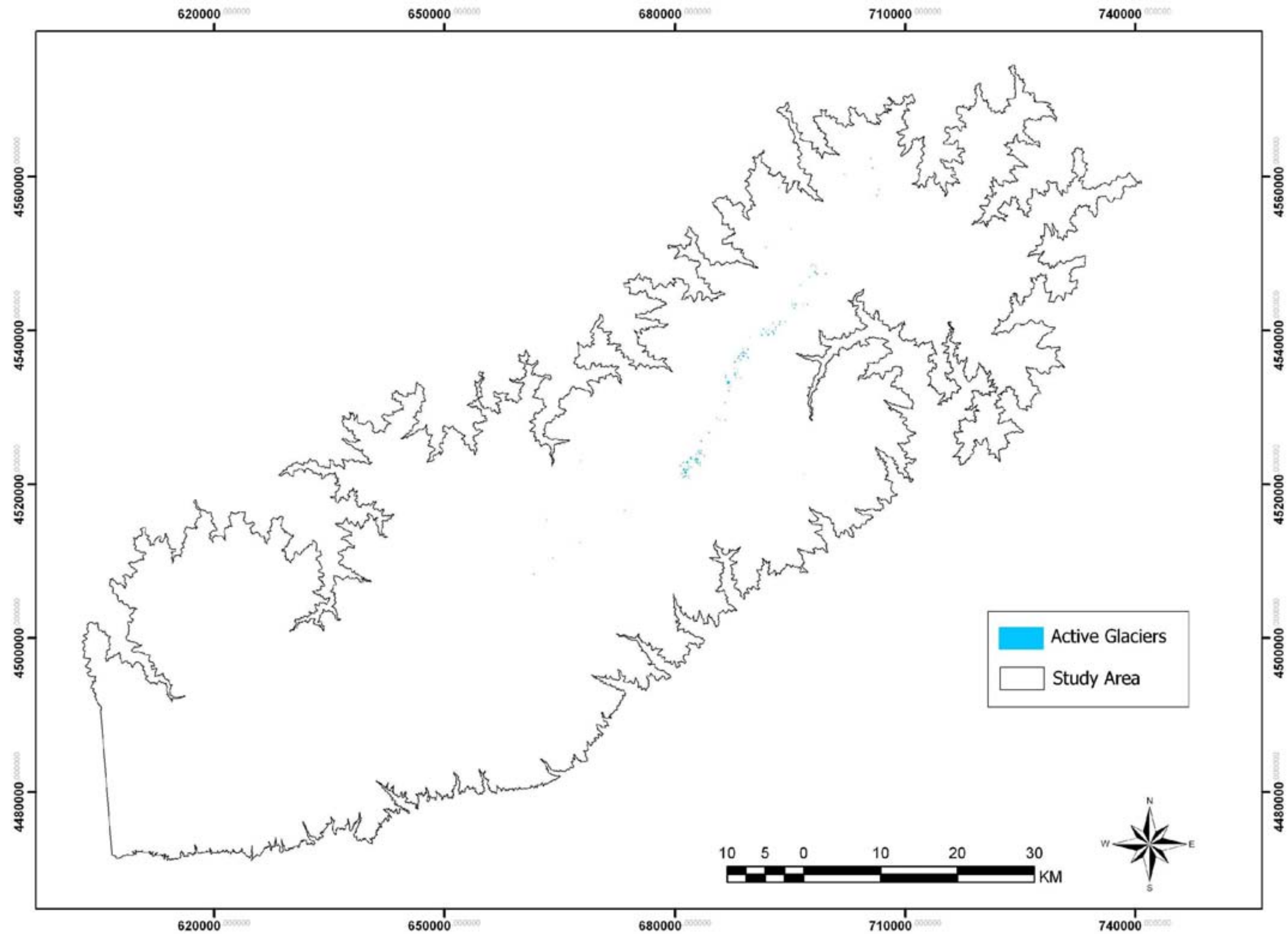

Figure 7.3: The map of active glaciers determined by NDSI.

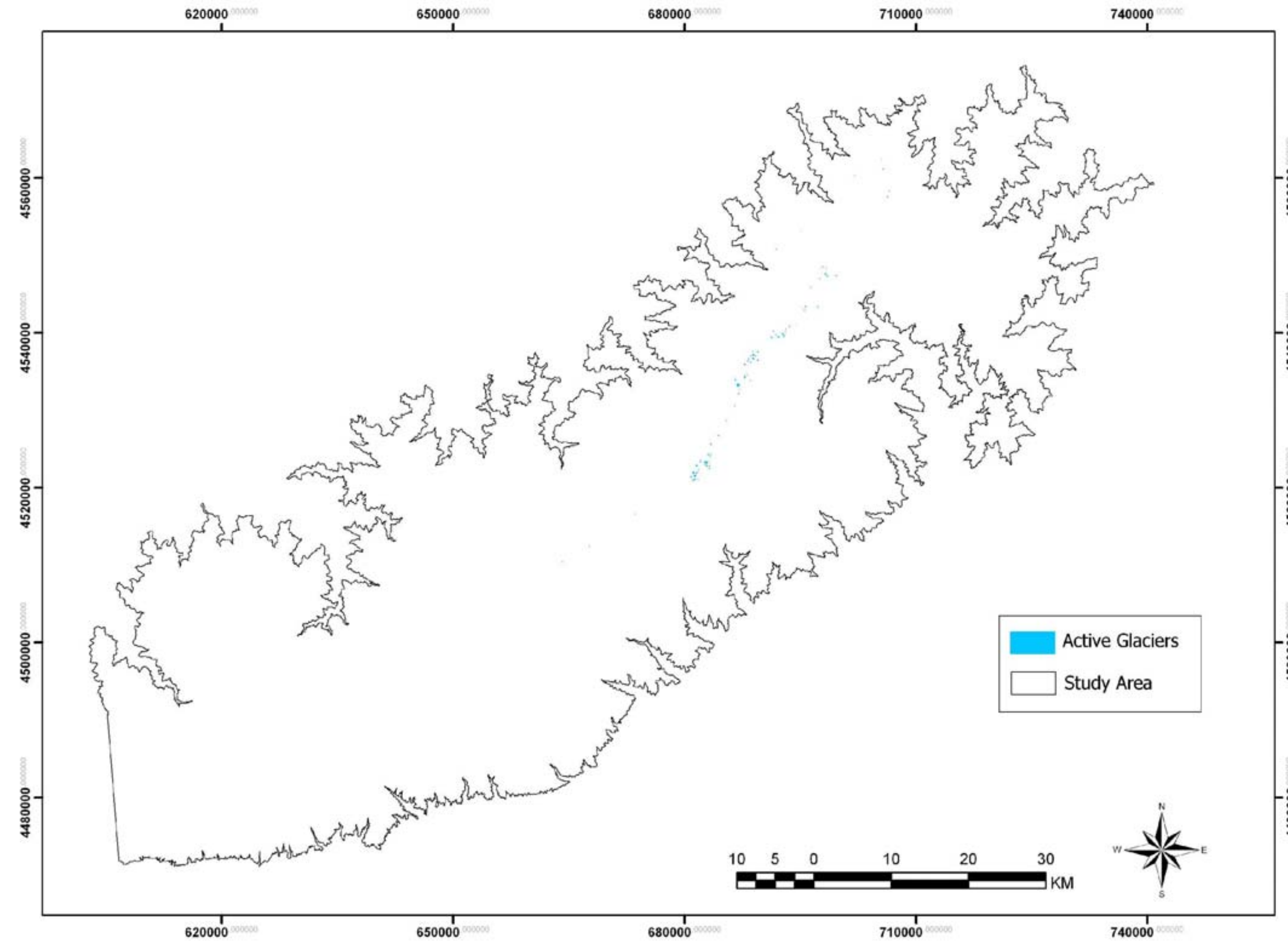

Figure 7.4: The map of active glaciers determined by Band Rationing (TM3/TM5).

7.3. Properties of Active Glaciers

The properties of glaciers identified by two methods are computed and given in Table 7.1. The NDSI methods identified 76 patches of active glaciers whereas the band rationing method detected 62 patches. In NDSI method, the lowest patch is located at 2819 m; band rationing identified the lowest block at 2830 m. The highest patches, on the other hand, are located at 3773 m and 3767 m by NDSI method and by Band Rationing method, respectively. The mean elevation value for NDSI method is 3196 m, and for Band Rationing is 3210 m. The smallest patch is the same for both methods having 967 meter square corresponding 1 pixel of Landsat ETM data. The greatest patch detected by NDSI method is 84388 meter square, whereas the one detected by Band Rationing method is 68692 meter square. A total area of 0.53 kilometer square was determined as active glaciers by NDSI method, while Band Rationing method detected 0.43 kilometer square area.

Table 7.1: Properties of active glaciers detected by two methods.

Method	Nubber of Patches	Minimum Elevation (m)	Maximum Elevation (m)	Mean Elevation (m)	Smallest Patch (m^2)	Largest Patch (m^2)	Total Area (m^2)
NDSI	76	2819	3773	3196	967	84388	525155
Band Rationing	62	2830	3767	3210	967	68692	431204

CHAPTER 8

RESULTS AND DISCUSSION

The results of different glacial features will be integrated and discussed in this chapter. The chapter is divided into four sections. In the first section the quality of data that affects the accuracy of the results will be dealt. This is followed by an evaluation of methodology applied in this study. The third section is the main part of the chapter discussing the results obtained in the study. In the last section, an assessment on the accuracy of results will be made.

8.1. Quality of Data

In this study digital topographic map at a scale of 1/25000, geological map at a scale of 1/500000, and Landsat 7 ETM images are used as raw data. DEM and its derivatives (aspect and slope) are generated from topographic map with the pixel size of 10 m. The vertical accuracy of DEM is 2.06 m. Spatial resolution of Landsat image is 30 m.

The resolution of DEM derived from topographic map is satisfactory for identifying the glacial valleys, cirques and glacial lakes. However, it is not sufficient for the investigation of moraine. For this reason moraine is not included in the scope of the study. Another reason, for the exclusion of moraine is the necessity of field studies which not a requirement for the glacial features included in the study. The resolution of the DEM provides adequate information to quantify the valleys, cirques and lakes as far as sinuosity, symmetry, elongation, roundness etc are considered. It has, however, deficiency to distinguish if the cirques are of nivation or glacial type.

Geological map has a very course resolution for a detailed relationship between the rock type and the glacial valleys. Another problem in geological maps is the absence of fault data. It is not known if there is any lake formed by the activity of faults or any valley truncated by faults. A reliable fault map could increase the quality of the results.

Landsat 7 ETM images take advantage of spectral resolution, because it has seven bands. But in respect to spatial resolution of 30 m, it is not satisfactory for determining the actual glaciers. The glacier patches with sizes smaller than 900 m^2 can not be detected by Landsat images.

8.2. Methodology

The methodology applied in this study is based on the use of GIS technology which enables to integrate various glacial features. Four main features included in the scope of the study are valleys, cirques, lakes and glaciers each represented by a different layer. A database is created for each layer which is actually an inventory of glacial features mapped in the area.

The first step in the methodology is the determination of the boundary of study area. This boundary is believed to correspond to the lowest elevation of glacial activity. Because the glaciers are developed more on the northern slopes of the mountain range, the boundary is determined in this flank which is found to be at an elevation of 1500 m. However, the lower boundary is not same for everywhere. On the southern side of the mountain chain the lowest elevation of glaciations is higher than northern.

The second step is to decide the glacial features to be investigated. Three main glacial landscapes are identified and investigated namely glacial valleys, cirques, and the lakes. Because of the resolution of the data several other glacial landscapes, such as moraines, arets are not considered in the study. For the selected three glacial features all possible spatial features are mapped and/or calculated.

The next step is the investigation of actual glaciers. The glaciers are determined using Landsat 7 ETM images using two common used methods namely NDSI, and Band Rationing.

8.3. Discussion of Results

This section is divided into two parts. In the first part the results obtained from previous chapters are discussed and evaluated individually. In the second part glacial shapes are integrated and the relationships between them are interpreted.

8.3.1. Glacial Features and Actual Glaciers

The glacial shapes determined in investigation area show different properties depending on their locations. Generally on northern side the landscapes are more widespread than the southern (Table 8.1). 19 of 30 main valleys, 49 of 63 tributary valleys, 820 of 1222 cirques and 431 of 685 glacial lakes are located on northern side of the mountain chain.

The lengths of valleys on northern side are longer. The starting elevations of valleys on both sides are close to each other but the ending elevations are different as on southern side the valleys terminate at about 350 m higher elevations. The average height difference of valleys on northern side is about 300 m more than the southern.

The cirques on northern side are distributed in a wide range of elevation. The density is located around 2950 m however several cirques are determined below the 2300 m. These lower ones might be nivation cirques. On southern side they are dense around at elevations of 3100 m. Similarly, glacial lakes are located at higher elevation on southern side than the northern side.

All these results indicate that the glaciation is more developed on northern side. This is because of illumination angle and humid conditions. In the study area the northern side gets sun illumination with lower angle, and because of sea effect of Black Sea this side has humid characteristics. Therefore the glaciation is more developed on northern side of Eastern Black Sea Mountain chain.

Table 8.1: The main properties of glacial landscapes on northern and southern sides of area.

	Northern Side	**Southern Side**
VALLEYS		
Number of Main Valleys	19	11
Number of Tributary Valleys	49	14
Mean Lengths of Valleys (km)	8.2	5.6
Mean Start Elevations (m)	2744.8	2788
Mean End Elevations (m)	1805.5	2154.8
Mean Heigth of Valleys (m)	939.3	633.3
Mean Slope of Valleys (%)	12.34	12.27
Mean Sinuosity of Valleys	1.11	1.16
Symmetric	9	4
Eastern Steep Slope	2	1
Western Steep Slope	8	6
CIRQUES		
Number of Cirques	820	402
Mean Elevation of Cirques (m)	2950	3100
Mean Slope of Cirques (degree)	28	29
Mean Area of Cirques (m^2)	472700	509681
LAKES		
Number of Lakes	431	254
Mean Elevation of Lakes (m)	2838	3001
Mean Area of Lakes (m^2)	9986	10314
Mean Elongation of Lakes	0.6	0.59
Mean Roundness of Lakes	0.9	0.89

Actual glaciers on study area are determined and investigated by applying two methods (NDSI and Band Rationing) and the results methods are reported (Table 7.1). Two methods produced similar results. The actual glaciers become dense around Kaçkar Mountain. Three glaciers are located on north face of Kaçkar Mountain and a glacier exists in a cirque located on south face of Kaçkar Mountain (Figure 8.1).

Erinç (1949) defined 6 glaciers, 3 of them as valley glaciers and named them as Kaçkar I, Kaçkar II, and Kaçkar III. Kaçkar I is the largest that reaches down to 2850 m, Kaçkar II and Kaçkar III descend down to 3000 and 2940 m, respectively.

Kurter (1991) investigated the glaciers in the same area using Landsat MSS images taken in 1975 and computed these three valleys glaciers (Kaçkar I, Kaçkar II and Kaçkar III) starting at 3650 m and descending down to elevations of 2900 m, 2990 m, and 3130 m respectively. He has computed the length for Kaçkar I as 1,5 km, Kaçkar II as 1 km, and Kaçkar II as slightly shorter.

Doğu et al. (1993) carried out a detailed field survey in the area who identified the same glaciers terminating at elevations of 3000 m, 3080 m, and 3100 m respectively. It is, therefore, clear that the actual glaciers have been retreated in a great amount.

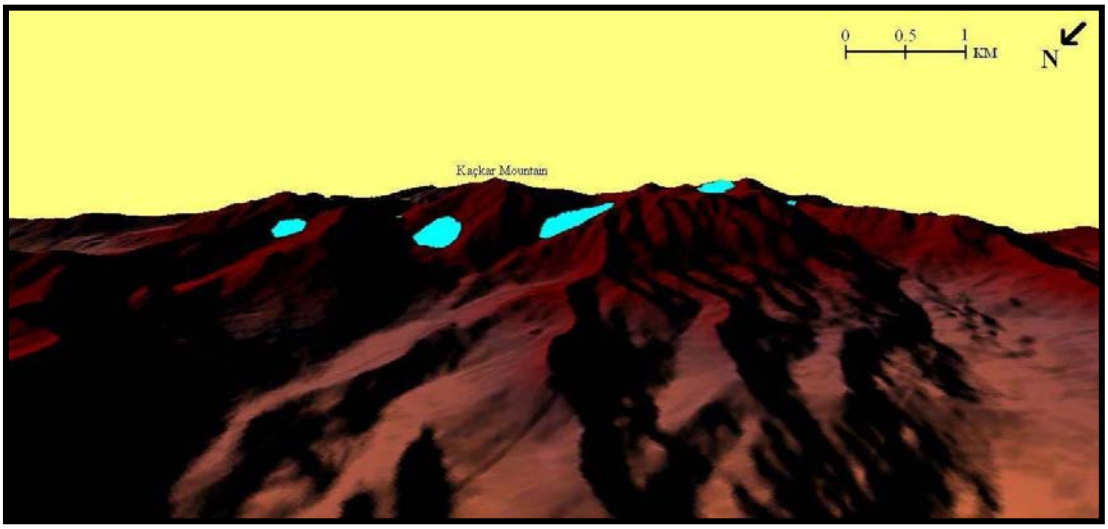

Figure 8.1: Three actual glaciers locate on north flank of Kaçkar

8.3.2. Relationships between Glacial Shapes

Glacial landscapes and actual glaciers through study area are investigated individually. Moreover these landscapes are related each other. In this part these relationships are handled and discussed.

8.3.2.1. Glacial Valleys versus Cirques

The glacial valleys mapped in the study are the most extensive features and contain other glacial features. For each glacial valley the basin which consists of accumulation area is digitized starting from the lowest end point of glacial valley traced up to the divide. The valleys are represented by polygons. The relationship between valleys and cirques are computed by overlaying these two layers. The properties of cirques within each valley are given in Table 8.2.

Table 8.2: Relationship between glacial valleys and cirques.

ID	Name	Basin Area (km^2)	% Basin Area	Number of Cirques	Mean Elevation of Cirques	Average Area of Cirques (m^2)	Total Area of Cirques (m^2)	% Area of Cirques
1	ALACAGOL	13.3	1.1	9	2558	457288	4115592	1.1
2	ABU	17.7	1.5	18	2653	412791	7430234	2.0
3	TUNCA	52.8	4.5	35	2671	585157	20480501	5.4
4	ERGUSU	21.4	1.8	22	2725	437184	9618053	2.5
5	TOPLUCA	14.0	1.2	9	2972	542927	4886344	1.3
6	KACKAR	21.9	1.9	11	2886	365259	4017848	1.1
7	AVUCUR	16.9	1.4	13	2817	508647	6612417	1.7
8	KAVRAN	80.0	6.8	65	2863	439224	28549559	7.5
9	PALOVIT	28.2	2.4	10	2916	448003	4480031	1.2
10	ELEVIT	78.4	6.7	37	2800	498271	18436010	4.9
11	TATOS	47.8	4.1	36	2857	486949	17530161	4.6
12	VERCENIK	80.8	6.9	58	2854	498106	28890126	7.6
13	INCESU	27.8	2.4	12	2758	434756	5217078	1.4
14	SALAR	124.1	10.5	54	2805	527490	28484450	7.5
15	SEYTAN	64.6	5.5	49	2901	433602	21246511	5.6
16	GOLPALA	38.4	3.3	23	2746	669605	15400915	4.1
17	ARZAVAN	62.5	5.3	32	2861	447846	14331074	3.8
18	ANZER	37.4	3.2	35	2952	479186	16771505	4.4
19	BADIR	29.2	2.5	37	2946	375424	13890696	3.7
20	BUYUKOVIT	62.7	5.3	32	2876	401570	12850232	3.4
21	GASURLUK	36.7	3.1	37	2854	495210	18322787	4.8
22	AKTAKAN	21.9	1.9	18	2943	454061	8173098	2.2
23	ANADAK	33.2	2.8	23	2869	533421	12268684	3.2
24	SOROH	21.6	1.8	14	2884	485032	6790447	1.8
25	DAVALT	27.7	2.4	19	2818	585128	11117428	2.9
26	HASTAF	52.2	4.4	33	2882	527781	17416772	4.6
27	BULUT	17.7	1.5	13	2957	477086	6202115	1.6
28	ONBOLAT	18.5	1.6	13	2877	460028	5980368	1.6
29	OZGUVEN	15.5	1.3	18	2723	392888	7071980	1.9
30	BICAKCILAR	13.7	1.2	7	2672	321321	2249247	0.6

The area of valley basins and total area of cirques within each basin show different values (Figure 8.2). In order to highlight this relationship the percentage of basin area is subtracted from percentage of total cirques area for each glacial valley (Figure 8.3). The valleys having positive values show more development of cirques, those with negative values show the inverse. Palovit, Elevit, Salar, Arzavan, and Buyukovit glacial valleys are distinct with their negative values that lack cirques comparing to others. These valleys have been well developed so that the valley glaciers have swept the cirques located over their slopes.

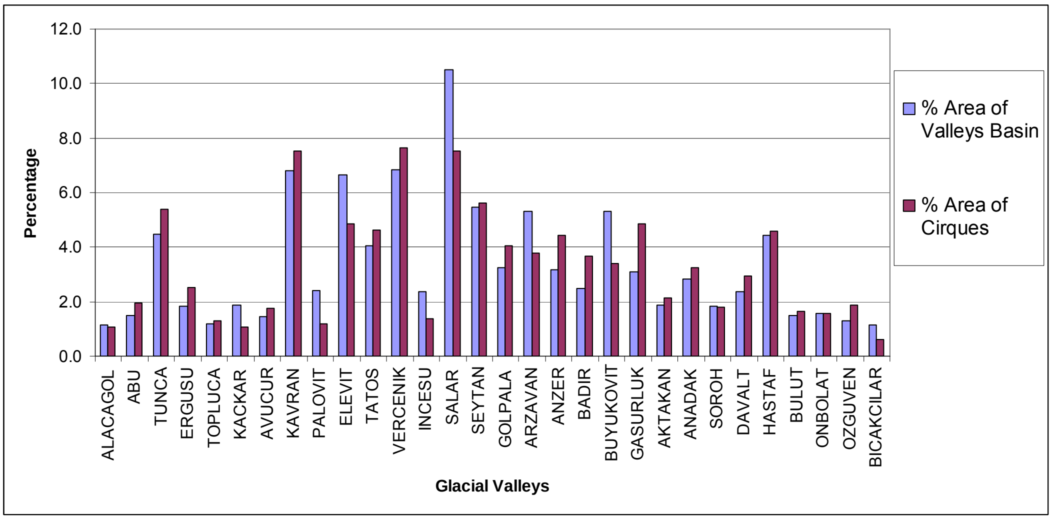

Figure 8.2: Distribution of area of basin and total area of cirques within basin of each glacial valley.

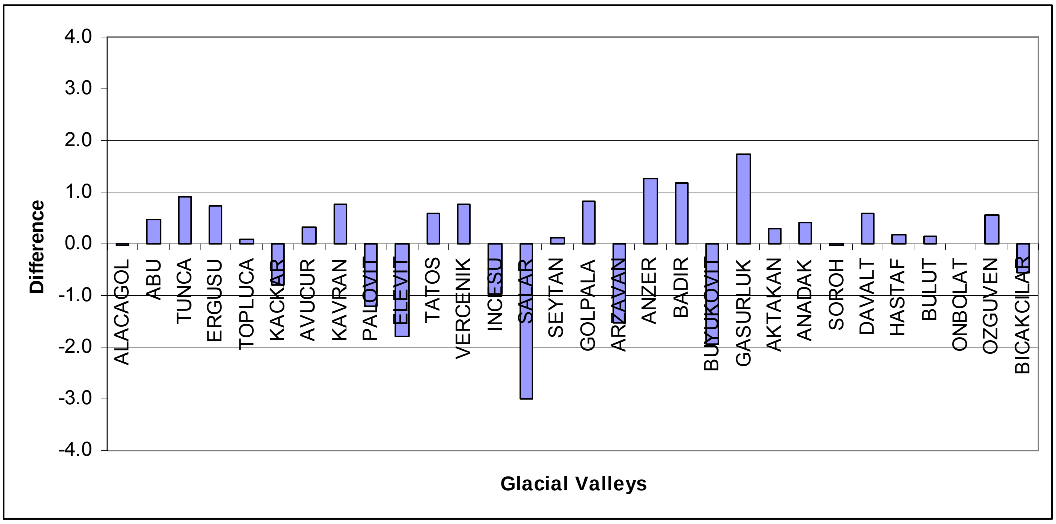

Figure 8.3: Differences of distribution between area of valley's basin and total area of cirques within each glacial valley.

8.3.2.2. Glacial Valleys versus Glacial Lakes

The relationship between glacial valleys and glacial lakes is determined by overlaying these two layers (Table 8.3). Accordingly, 529 of 685 glacial lakes are located within the main 30 glacial valley basins.

Table 8.3: Relationship between glacial valleys and glacial lakes.

ID	Name	Basin Area (km^2)	% Basin Area	Number of Lakes	Total Area of Lakes (m^2)	% Area of Lakes	Average Area of Lakes (m^2)	Average Elongation	Average Roundness
1	ALACAGOL	13.3	1.1	3	24333	0.4	8111	0.7	1.0
2	ABU	17.7	1.5	16	206357	3.8	12897	0.6	0.9
3	TUNCA	52.8	4.5	21	334646	6.2	15936	0.7	0.9
4	ERGUSU	21.4	1.8	14	191711	3.5	13694	0.6	0.9
5	TOPLUCA	14.0	1.2	6	99953	1.8	16659	0.7	0.9
6	KACKAR	21.9	1.9	5	12600	0.2	2520	0.6	0.9
7	AVUCUR	16.9	1.4	2	58170	1.1	29085	0.9	1.0
8	KAVRAN	80.0	6.8	30	256091	4.7	8536	0.6	0.9
9	PALOVIT	28.2	2.4	8	70888	1.3	8861	0.6	0.9
10	ELEVIT	78.4	6.7	23	240088	4.4	10439	0.6	0.9
11	TATOS	47.8	4.1	21	225956	4.2	10760	0.5	0.8
12	VERCENIK	80.8	6.9	51	633083	11.7	12413	0.6	0.9
13	INCESU	27.8	2.4	7	37313	0.7	5330	0.6	0.9
14	SALAR	124.1	10.5	45	415779	7.7	9240	0.6	0.9
15	SEYTAN	64.6	5.5	20	65122	1.2	3256	0.5	0.9
16	GOLPALA	38.4	3.3	4	9886	0.2	2472	0.5	0.9
17	ARZAVAN	62.5	5.3	17	121133	2.2	7125	0.7	0.9
18	ANZER	37.4	3.2	24	126042	2.3	5252	0.6	0.9
19	BADIR	29.2	2.5	25	265539	4.9	10622	0.6	0.9
20	BUYUKOVIT	62.7	5.3	17	176884	3.3	10405	0.6	0.9
21	GASURLUK	36.7	3.1	37	713228	13.2	19276	0.6	0.9
22	AKTAKAN	21.9	1.9	17	108489	2.0	6382	0.6	0.9
23	ANADAK	33.2	2.8	23	250582	4.6	10895	0.5	0.9
24	SOROH	21.6	1.8	20	102618	1.9	5131	0.6	0.9
25	DAVALT	27.7	2.4	14	211256	3.9	15090	0.6	0.9
26	HASTAF	52.2	4.4	26	190891	3.5	7342	0.6	0.9
27	BULUT	17.7	1.5	9	25328	0.5	2814	0.6	0.9
28	ONBOLAT	18.5	1.6	7	50960	0.9	7280	0.8	1.0
29	OZGUVEN	15.5	1.3	11	100567	1.9	9142	0.6	0.9
30	BICAKCILAR	13.7	1.2	6	84024	1.6	14004	0.6	0.9

Their percentages of glacial lakes within each glacial valley are shown in Figure 8.4. Comparing the percentage of basin's area and total area of glacial lakes within the valley, Gasurluk glacial valley has the highest concentration of lakes followed by Verçenik and Tunca valleys. Gölpala, Alacagöl, Kaçkar, and Bulut valleys, on the other hand, have minimum number of lakes compared to their areas.

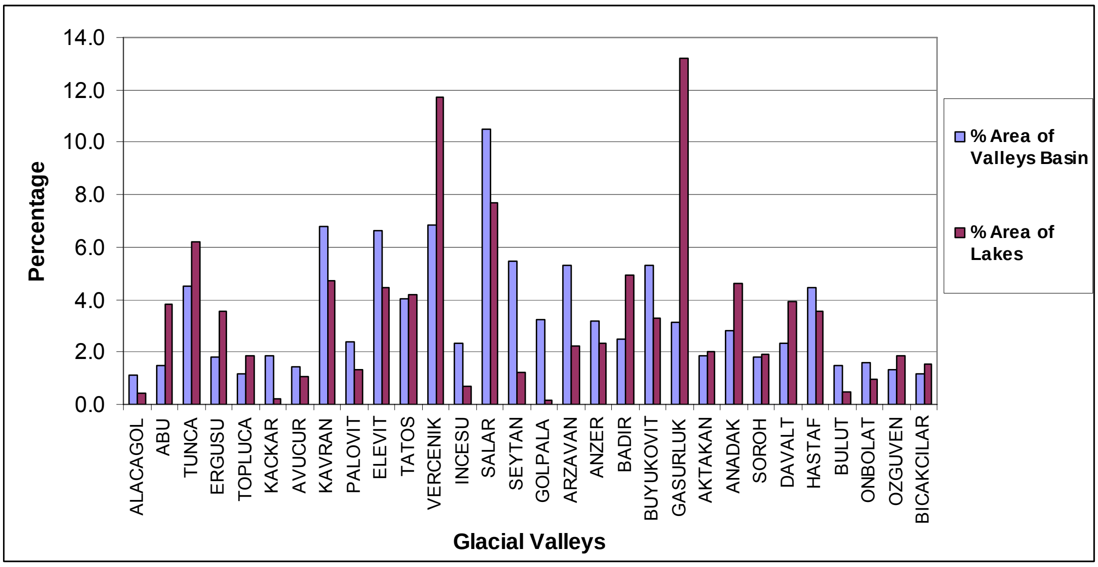

Figure 8.4: Distribution of glacial lakes area within basin of each glacial valley.

The size of glacial lakes within each valley show differences as determined by using average size value of glacial lakes located within each valley (Figure 8.5). The result shows that Avucur valley contains the largest lakes followed by Gasurluk valley. The lakes located within Kaçkar, Şeytan, Gölpala, and Bulut valleys,on the other hand, have smallest sizes.

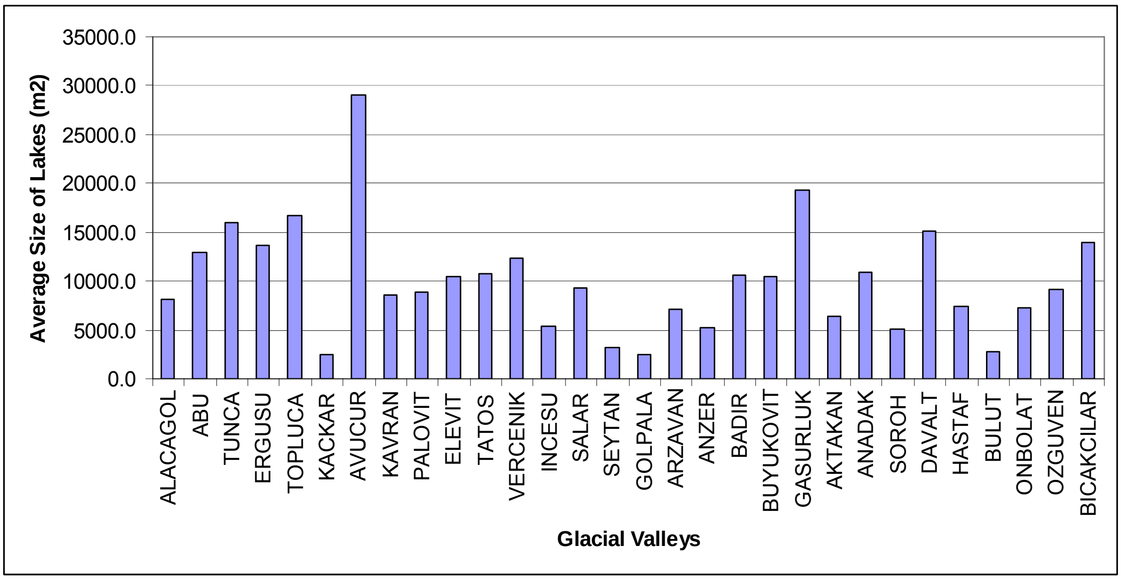

Figure 8.5: Average size of glacial lakes within basin of each glacial valley.

Elongation of lakes is another parameter measured in this study. The average value of lake elongation is computed for each valley (Figure 8.6). The result indicates that that there is not an obvious difference the glacial lakes. Avucur and Önbolat valleys contain more circular lakes whereas Tatos, Şeytan, and Gölpala valleys contain the lakes having elongated shapes.

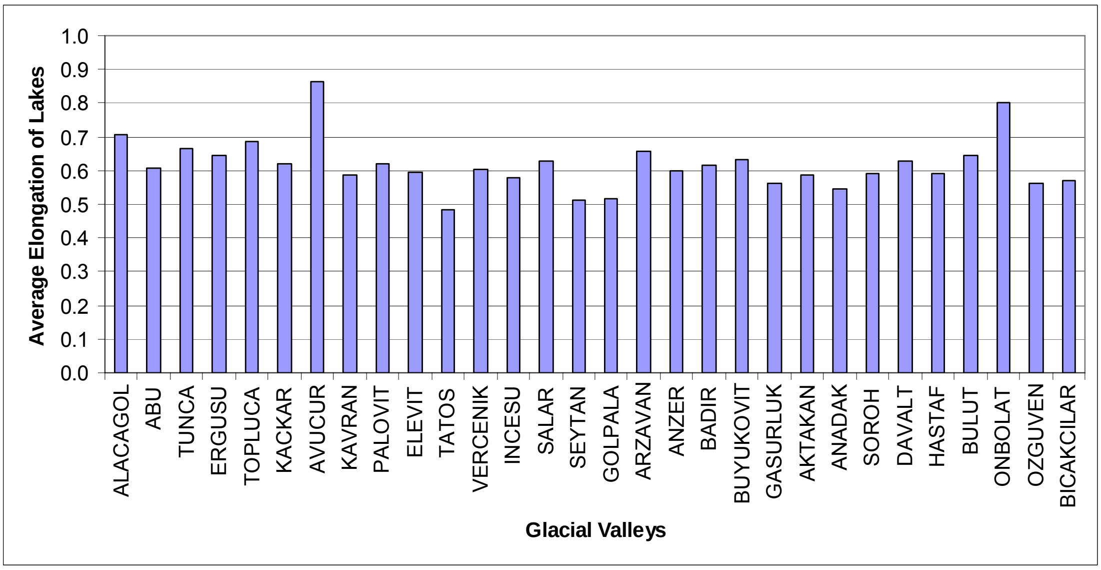

Figure 8.6: Average elongation of glacial lakes within basin of each glacial valley.

Finally the roundness property of lakes according to valley is investigated by using their average values (Figure 8.7). The lakes within Alacagöl, Avucur, and Önbolat valleys have smoother boundaries. On the contrary, the lakes located in Palovit, Tatos, and Bıçakçılar valleys show the opposite characteristics.

8.3.2.3. Glacial Valleys versus Actual Glaciers

The actual glaciers are located in eleven valley systems with different amount (Table 8.4). More then half of the actual glaciers are located in Kavran, and Hastaf valleys. Both valleys are located over the Kaçkar Mountain; Kavran valley on the north and Hastaf valley on the south. Bulut, Önbolat, and Bıçakçılar valleys are other regions containing most portions of remaining actual glaciers (Figure 8.8). These three systems are located at the eastern part of study area.

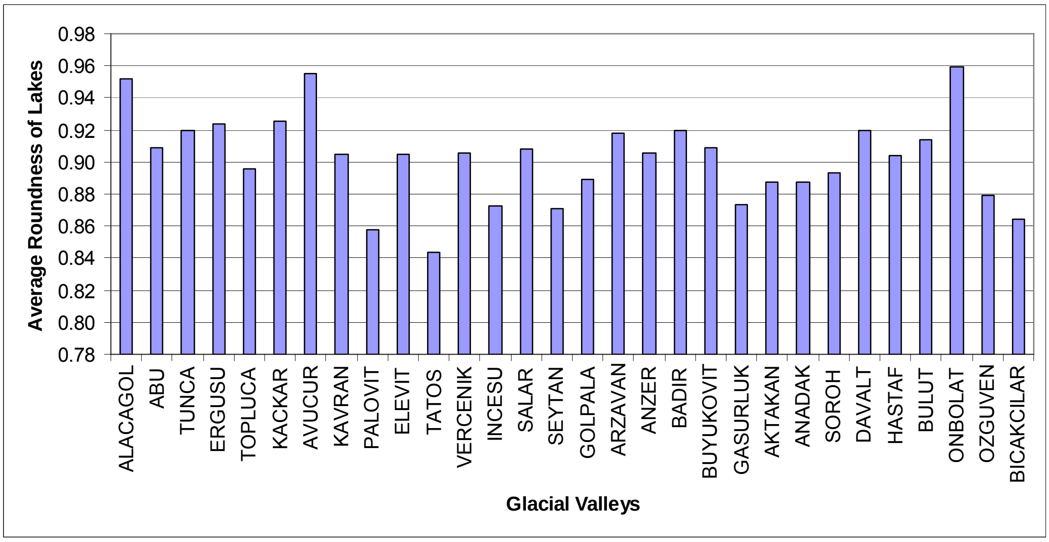

Figure 8.7: Average roundness of glacial lakes within basin of each glacial valley.

Table 8.4: Distribution of actual glaciers according to glacial valley systems.

ID	Valley Name	Area of Actual Glaciers (m2)
4	ERGUSU	1174
7	AVUCUR	6393
8	KAVRAN	173903
10	ELEVIT	967
22	AKTAKAN	967
25	DAVALT	9916
26	HASTAF	139010
27	BULUT	57701
28	ONBOLAT	67977
29	OZGUVEN	5878
30	BICAKCILAR	14578

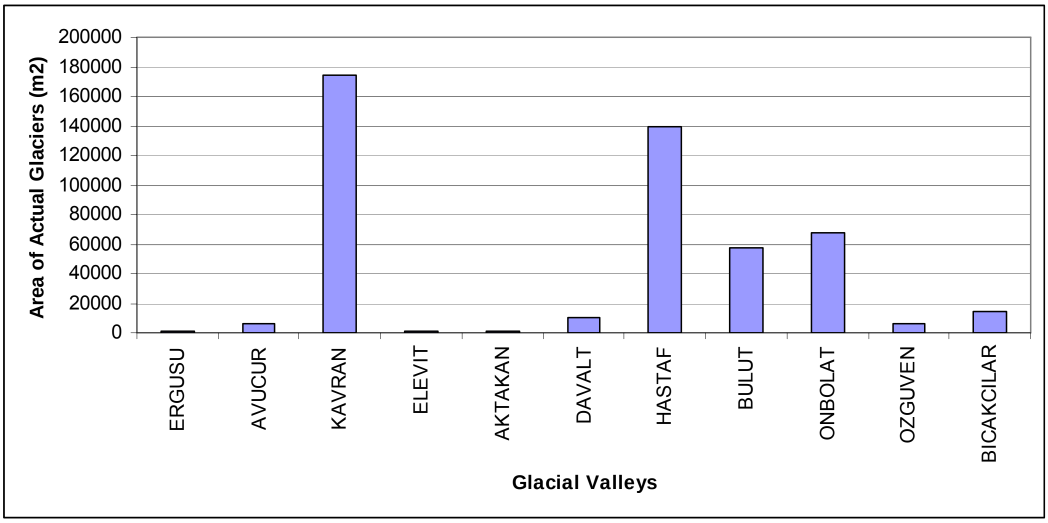

Figure 8.8: Distribution of actual glaciers according to glacial valley systems.

8.3.2.4. Glacial Cirques versus Glacial Lakes

Almost all the lakes (639 of 685) are located in cirques. This is because the cirques are suitable regions for development of glacial lakes. Generally the cirques have potential landscapes for glacial lakes particularly after glaciers melting.

8.3.2.5. Glacial Cirques versus Actual Glaciers

Almost all actual glaciers (486092 m2 of 525155 m^2) exist in cirques. The remaining little portion locates as small patches through steep hillsides that getting less sun illumination. When glaciers melt and retreat, they shrink into cirques and finish in this area. Considering the melting of glaciers in recent times, through study area they have been retreated, shrunk, and receded into cirques.

8.4. Accuracy Assessment

The accuracy of outputs produced in this study is tested by comparing them with maps prepared by previous studies. For this reason, four areas are selected to validate the results for valleys, cirques, lakes and actual glaciers. The comparison is made below in the same order.

The glacial valleys layer is overlaid on the geomorphology map created by Doğu et al. (1996) (Figure 8.9). In this part of area, they identified five glacial valleys whereas in this study nine glacial valleys are identified. Two valleys are classified as main glacial valleys (Verçenik and Tatos), and seven valleys assigned as tributary valleys. Doğu et al. (1996) have computed 10 km length and 10 % average slope for Verçenik valley, in this study the length and average slope for this valley are 11.2 km and 9.3 %, respectively. This valley starts from a cirque located at 2900 m and terminated down to 1860 m elevations. In their study the Tatos valley starts from 2850 m and change into fluvial valley at 2000 m elevations. The length and average slope for this valley are computed as 7.5 km and 10 % by them. In this study Tatos valley is identified starting from cirques located at 2929 m and changes into fluvial character at 2011 m elevation. This valley has 7.6 km length and 12 % average slope. Therefore, the results, in general, are very similar to each other.

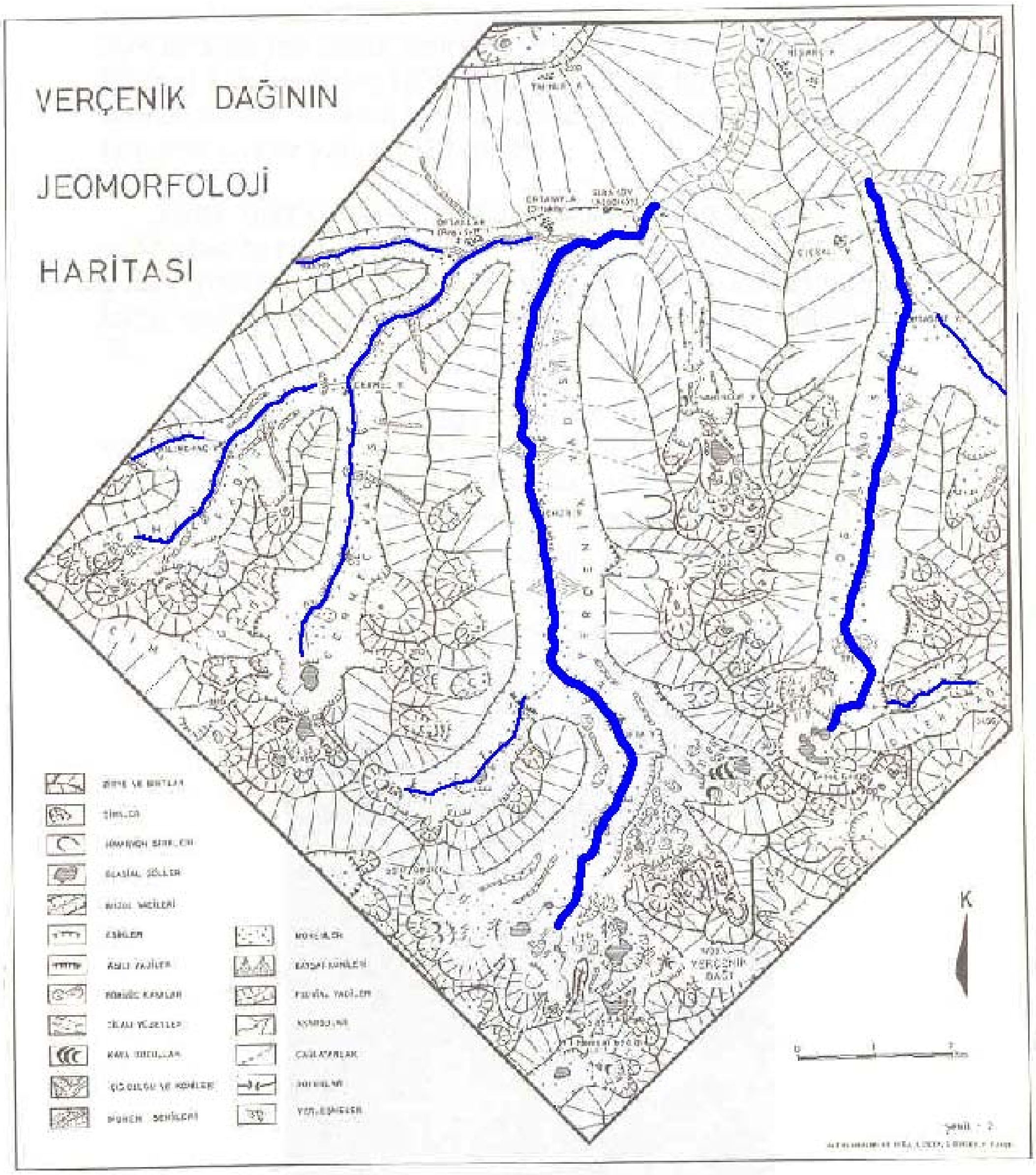

Figure 8.9: Comparison of the glacial valleys determined in this study with geomorphology map generated by Doğu et al. (1996). The main valleys are indicated by thick blue and tributary valleys by thin.

The cirques identified in this study are verified by overlaying the map created by Doğu et al. (1994) (Figure 8.10). The most distinguishing difference is that in their map the cirques are represented by symbols; however, in this study, the cirques are digitized as polygons. In their map area a total of 83 cirques are determined in this study. Although in general there is a consistency in the location and and size of the cirques there are four minor differences between the two maps. The first difference is shown in area (A) in the figure where two cirques are identified in this study which are absent in their map.

Contrary to this there are some areas labeled as cirque in their map which is not determined in this study. Two cirques shown around (B) are examples of this case. The third difference is indicated in area (C) where multiple cirques in their map is combined into one single cirque in this study. The last difference is the cirque identified in this study and missed in their map. It is believed that the differences between the two maps are not due to the methodological approach but rather due to the expertise and skills of the users.

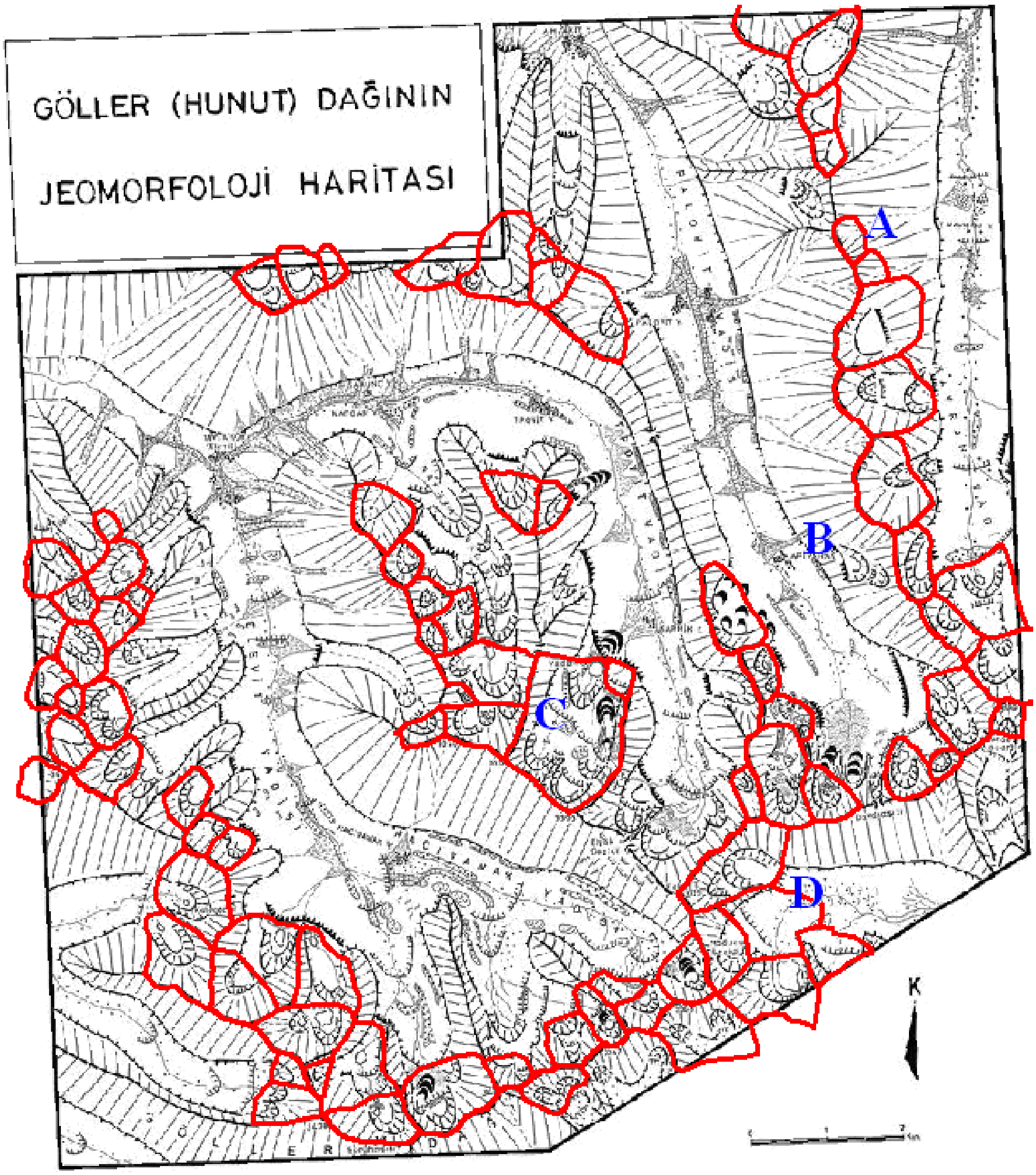

Figure 8.10: Comparison of the cirques determined in this study (shown as red line) with geomorphology map generated by Doğu et al. (1994).

The glacial lakes determined in this study are compared with geomorphology map generated by Doğu et al. (1996) (Figure 8.11). A total of 61 lakes are identified in this study. 45 lakes are coincident in both studies (blue ones in the figure). On the other hand, 15 lakes are missed in their map (red ones in the figure). Therefore, the number of lakes in this study is more than their works. This is most probably, due the fact that in this study all hollows are identified as lakes, however, they have determined the lakes with water.

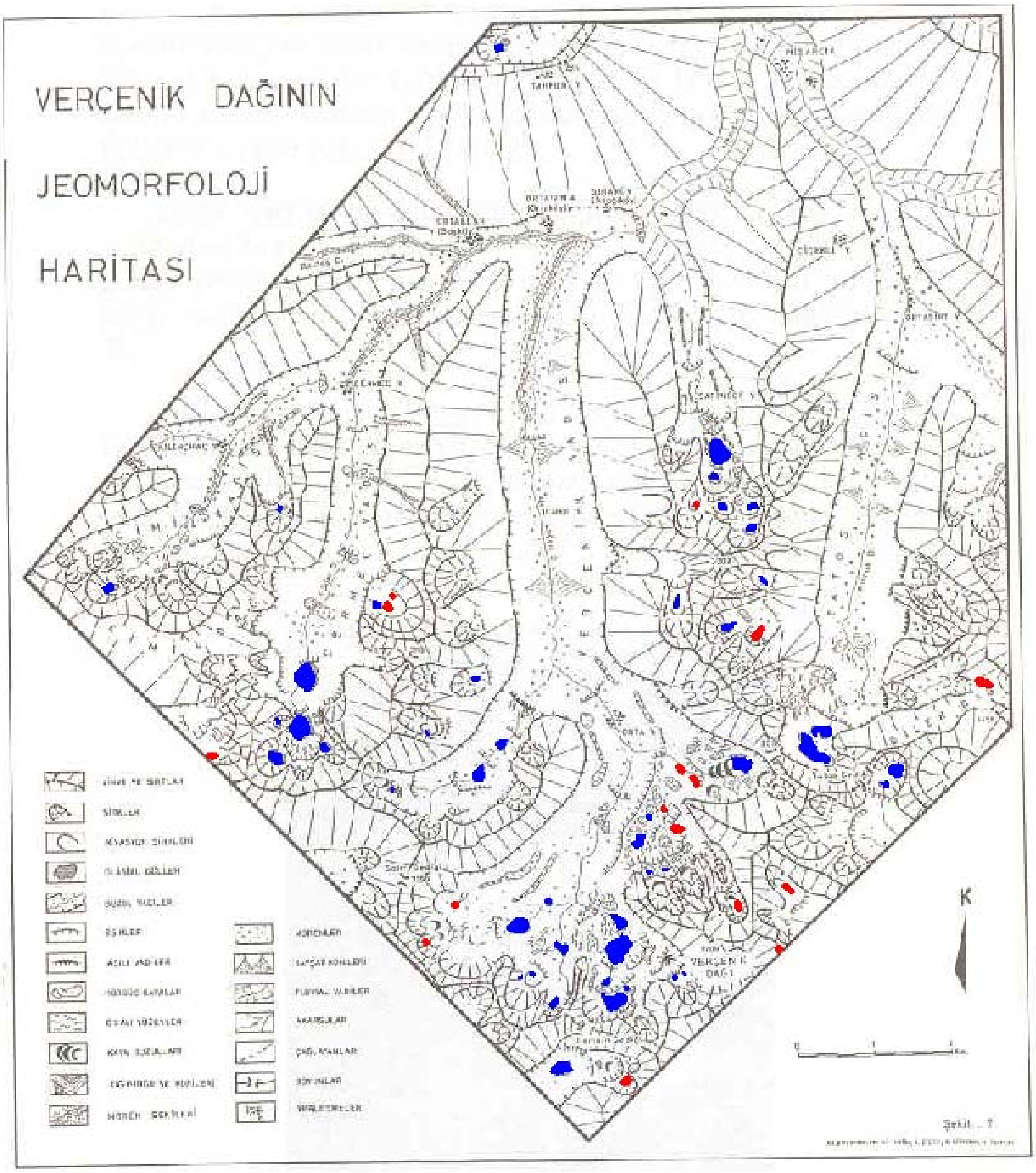

Figure 8.11: Comparison of the glacial lakes determined in this study with geomorphology map generated by Doğu et al. (1996). Blue color indicates the lakes determined in both studies. The red ones are identified only in this study.

Actual glaciers determined in this study by remote sensing techniques are compared with the map generated by Doğu et al. (1993) (Figure 8.12). They have identified five glaciers on this area as indicated by arrows. Four of these glaciers are identified in this study all having smaller sizes (blue glaciers in the figure). This decrease in the size can be attributed to global warming. The fifth one could be melt out and disappear. However, there are several other small patches of glaciers detected in this study which do not exist in their map.

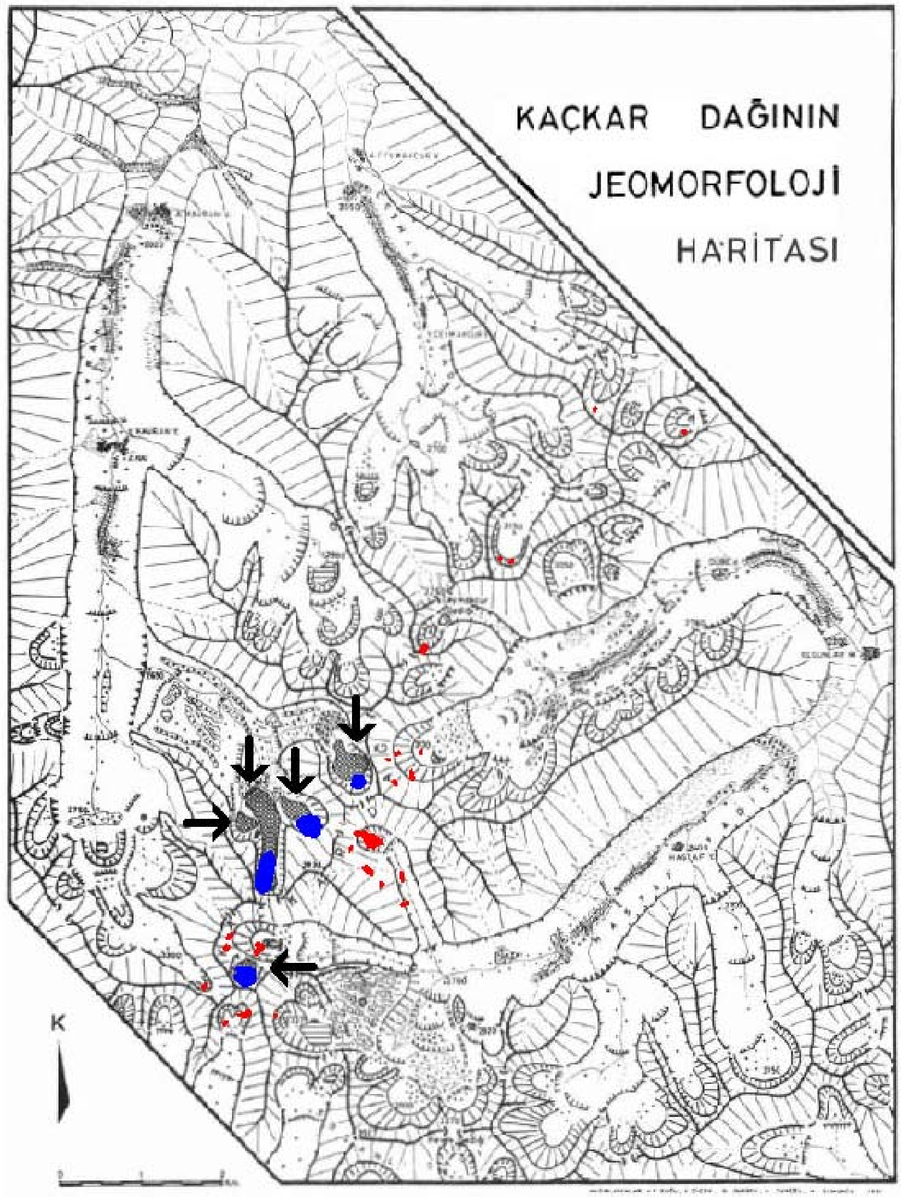

Figure 8.12: Comparison of actual glaciers detected in this study with the map prepared by Doğu et al. (1993). Blue ones are coincident in both maps. Red ones are identified only in this study.

CHAPTER 9

CONCLUSIONS

The main conclusions reached in this study are as follows:

- The investigation area is a glaciated area containing actual glaciers and many glacial landscapes. The boundary for region affected by glaciers is determined the 1500 m elevation line.
- There are 93 glacial valleys in the area. Thirty of these are classified as main valleys which start from a cirque and change into the fluvial valleys at the end point of glaciation. Sixty three of valleys are tributary that start from a cirque and connect to the main glacial valleys. Nineteen of main glacial valleys and forty nine of tributary valleys are located on northern part of area which are longer then the southern ones. Thirteen main valleys are symmetric, fourteen asymmetric with eastern steep slope, and three asymmetric with western steep slopes. The dominant orientation of valleys is SE-NW perpendicular to the elongation of Eastern Black Sea mountain chain.
- A total of 1222 cirques are identified in the study area. Two-third of them (820) are located on northern part. The majority of cirques on north side distribute between 2700 and 3200 m, on south side between 2900 and 3300 m elevations. The size of cirques changes in accordance to elevation; as the elevation increases the size decreases. Almost all cirques (98.8 %) are developed within volcano-sedimentary rocks and intrusive rocks.
- There are 685 glacial lakes in the area and cover an area of 6.9 km^2. 431 lakes are located on northern part, whereas 254 lakes on the southern. Most of the lakes on north side are distributed between 2700 and 3100 m while on south side between 2900 and 3300 m. The size of lakes range between 114 and 115509 m^2. The size has a negative relationship with elevation; as the elevation increases, the size of lakes decreases. In general the lakes have

circular shape and have smooth boundaries. 96.3 % of lakes are developed within volcano-sedimentary rocks and intrusive rocks. The density of lakes is high at crest zone of area.

- Several patches of actual glaciers are located in the area. In cumulative 0.53 km^2 area of active glaciers is detected. Three cirque glaciers are located on the northern flank and a cirque glacier is located on the southern flank of Kaçkar Mountain.

REFERENCES

Akçar, N., Yavuz, V., Ivy-Ochs, S., Kubik, P.W., Vardar, M., Schlüchter, C., 2007 a, "Paleoglacial records from Kavron Valley, NE Turkey: Field and cosmogenic exposure dating evidence", Quaternary International 164–165 p. 170–183.

Akçar, N., Yavuz, V., Ivy-Ochs, S., Kubik, P.W., Vardar, M., Schlüchter, C., 2007 b, "A case for a downwasting mountain glacier during Termination I, Verçenik valley, northeastern Turkey", J. Quaternary Sci., ISSN 0267-8179.

Akkan, E., Tuncel, M., 1993, "Esence (Keşiş) Dağları'nda Buzul Şekilleri", Ank. Ünv. Türkiye Coğrafyası Araştırma ve Uygulama Merkezi, Türkiye Coğrafyası Dergisi, s. 225-239, Ankara.

Altın, B.N., 1998, "Aladağlar ve Bolkar Dağları Üzerinde Karstlaşma ve Glasio-Karstik Şekiller", Fırat Üniversitesi Jeoloji Müh. 20. Yıl Sempozyumu Bildiriler, s. 531-550, Elazığ.

Altın, Türkan., 2006, "Aladağlar ve Bolkar Dağları üzerinde görülen periglasyal Jeomorfolojik şekiller", Türk Coğ. Derg. Sayı 46 Syf: 105-123.

Amerson, B. E., Montgomery, D. R., Meyer, G., 2008, "Relative Size of Fluvial and Glaciated Valleys in Central Idaho", Geomorphology 93, p. 537–547.

Andrews, J.T., 1972, "Glacier Power, Mass Balances, Velocities and Erosion Potential", Geomorph. N.F.13, p. 1-17.

Ardos, M., Pekcan, N., 1994, Jeomorfoloji Sözlüğü, İ.Ü Coğ.Enst Yay. No.3397, s. 80, İstanbul.

Arpat, E., Özgül, N., 1973, "Orta Toroslar'da, Geyik Dağı Yöresinde Kaya Buzulları", MTA Dergisi No. 80, s. 30-35, Ankara.

Atalay, İ., 1984, "Mescit Dağı'nın Glasyal Morfolojisi", Ege Coğ. Dergisi: 2, s. 129-138, İzmir.

Atalay, İ., 1987, Türkiye Jeomorfolojisine Giriş (2. Baskı), Ege Üniv. Ed.Fak.Yay., No. 9, İzmir.

Bakırcı, M., 2002, "Bir Dağlık Bölge Planlaması Olarak Doğu Karadeniz Projesi (DOKAP)", İ.Ü. Ed. Fak. Coğ.derg. sayı 10, syf: 99.

Benedict, J.B., 1973, “Origin of Rock Glaciers”, J. Glacio l.12, p. 520-522.

Benedict, J.B., 1991, “Experiments on Lichen Growth II. Effects of a Seasonal Snow Cover”, Arctic and Alpine Research, Vol. 23, p. 189-199.

Bilgin, T., 1969, “Gavur Dağı Kütlesinde Glasiyal ve Periglasiyal Topografya Şekilleri”, İ.Ü Coğ. Enstitüsü. Yay. No. 58, İstanbul.

Bilgin, T., 1972, “Munzur Dağları Doğu Kısmının Glasiyal ve Periglasiyal Morfolojisi”, İ.Ü Coğ. Enstitüsü. Yay. No. 69, İstanbul.

Birman, J.H., 1968, “Glacial Reconnaissance in Turkey”, Geological Society of America Bulletin, Vol. 79, p. 1009-1026.

Bolch, T., Menounos, B., Wheate, R., 2010, “Landsat-Based Inventory of Glaciers in Western Canada, 1985–2005”, Remote Sensing of Environment 114, p. 127–137.

Chen, X., Cui, P., Li, Y., Yang, Z., Qi, Y., 2007, “Changes in glacial lakes and glaciers of post-1986 in the Poiqu River basin, Nyalam, Xizang (Tibet)”, Geomorphology 88, p. 298–311.

Çiner, A., 2003, “Türkiye’nin Güncel Buzulları ve Geç Kuvaterner Buzul Çökelleri”, Türkiye Jeoloji Bülteni, Cilt: 46, Sayı:1.

Denton, G.H., Karlen, W., 1973, “Holocene Climatic Variations-Their Pattern and Possible Cause”, Quat. Res.3, p. 155-205.

Doğu, A.F., 1993, “Sandıras Dağı’nda Buzul Şekilleri”, A.Ü Türkiye Coğ. Arşt ve Uyg. Mrk. Derg. Sayı. 2, s. 263-274, Ankara.

Doğu, A.F., Çiçek, İ., Gürgen, G., Tunçel, H., 2000, “Akdağ’ın Buzul ve Karst Jeomorfolojisi (Fethiye-Muğla)”, Cumhuriyetin 75. Yıldönümü, Yerbilimleri ve Madencilik Kong. Bildiriler Kitabı I, s. 371-384, Ankara.

Doğu, A.F., Çiçek, İ., Gürgen, G., Tunçel, H.,Somuncu, M., 1994, “Göller (Hunut) Dağı’nda Buzul Şekilleri, Yaylalar ve Turizm”, A.Ü Türkiye Coğ. Arşt ve Uyg. Mrk. Dergisi. Sayı. 3, s. 193-218, Ankara.

Doğu, A.F., Çiçek,İ., Gürcan, G., Tunçel, H., 1997, “Bulut-Altıparmak Dağlar’ında Buzul Şekilleri (Doğu Karadeniz Bölümü)”, A.Ü Türkiye Coğ. Arşt ve Uyg. Mrk. Dergisi, Sayı. 6, s. 63-91, Ankara.

Doğu, A.F., Çiçek,İ., Gürgen, G., 2000, “Demirkapı Dağı ve Uzungöl Çevresinin Jeomorfolojisi”, Cumhuriyetin 75. Yıldönümü, Yerbilimleri ve Madencilik Kong. Bildiriler Kitabı I, s. 387-399, Ankara.

Doğu, A.F., Çiçek,İ., Gürgen,G.,Tunçel,H.,1996, “Üçdoruk (Verçenik) Dağı’nda Buzul Şekilleri, Yaylalar ve Turizm”, A.Ü Türkiye Coğ. Arşt ve Uyg. Mrk. Derg. Sayı.5, s. 29-52, Ankara.

Doğu, A.F., Somuncu, M., Çiçek, İ., Tunçel, H., Gürgen, G., 1993, “Kaçkar Dağlar’ında Buzul Şekilleri, Yaylalar ve Turizm”, A.Ü Türkiye Coğ. Arşt ve Uyg. Mrk. Derg. Sayı. 2, s.157-184, Ankara.

Dönmez, Y., 1984, Genel Klimatoloji ve İklim Çalışmaları, İ.Ü Edb Fak. Yay. No: 102, İstanbul.

Emre, Ö., Güner, Y., 1983, “Erciyes Dağı’nda Pleistosen Buzullaşması ve Volkanizma ile ilişkisi”, 37. Türkiye Jeoloji Bilimsel ve Teknik Kurultayı Bildiri Özleri, s. 151-153, Ankara.

Erinç, S., 1945, “Doğu Karadeniz Dağlar’ında Buzul Morfolojisi Araştırmaları”, İ.Ü Ed. Fak. Yay. Coğ. Enstitüsü, Doktora Tez. Seri.1, İstanbul.

Erinç, S., 1949, “Kaçkar Dağı Grubunda Diluvial ve Bugünkü Glasyasyon”, İ.Ü Fen Fak. Mecmuası B:14, No..3, s. 243-245, İstanbul.

Erinç, S., 1951, “Glasyal ve Postglasyal Safhada Erciyes Glasiyeri”, İ.Ü Coğ. Enst. Derg.1, s. 82-90, İstanbul.

Erinç, S., 1952 a, “The Present Glaciation of Turkey”, Proc. Eighth Gen. Assembly and Seventeenth Internat. Congress of internat. Geographical Union: Nat’l Acad. Sci.-Nat. Research Council, Washington, D.C.

Erinç, S., 1952 b, “Glacial Evidence of Climatic Variations in Turkey”, Geog. Ann., Stockholm, Arg. 34, h.1-2, p. 89-98.

Erinç, S., 2000., Jeomorfoloji I (3.Baskı). DER Yayınları, İstanbul.

Erinç, S., 2001, Jeomorfoloji II (3.Baskı). D.E.R Yayınları, İstanbul.

Erol, O., 1978, “The Quaternary History of the Lake Basins of Central and Southern Anatolia”, Ed.by W.C. Brice . The Environmental History of the Near and Middle East Since the Last ıce Age (pp.111-139). London: Academic Press.

Erol, O., 1999, Genel Klimatoloji (5. Baskı), Çantay Kitapevi, İstanbul.

Evans, I. S., 2006, “Allometric Development of Glacial Cirque Form: Geological, Relief and Regional Effects on the Cirques of Wales”, Geomorphology 80 p. 245–266.

Frankl, A., Nyssen, J., Calvet, M., Heyse, I., 2010, “Use of Digital Elevation Models to understand and map glacial landforms — The case of the Canigou Massif (Eastern Pyrenees, France)”, Geomorphology 115, p. 78–89.

Hendriks, J. P. M., Pellikka, P., 2007, “Semi-automatic glacier delineation from Landsat imagery over Hintereisferner in the Austrian Alps”, Zeitschriftfür Gletscherkunde Undglazialgeologie, Band 41, p. 55-75, Helsinki.

İzbırak, R., 1986., Coğrafi Terimler Sözlüğü, Milli Eğitim Basımevi, İstanbul.

Johnson, M.H., Menzies, J., 1996, “Pleistocene Supraglacial and Ice-Marginal Deposits and Landforms”. Ed. by J.Menzies, Past Glacial Environments. Sediments, Forms and Techniques. Glacial Environments Series. Vol. 2, p. 137-160, London.

Kaufmann, V., Ploesch, R., 2000, “Mapping and Visualization of The Retreat of Two Cirque Glaciers in the Austrian Hohe Tauern National Park”, International Archives of Photogrammetry and Remote Sensing, Vol. XXXIII, Part B4, Amsterdam.

Kemmis, T.J., 1996, “Lithofacies Associations for Terresrial Glacigenic Successions”. Ed. by J.Menzies Past Glacial Environments. Sediments, Forms and Techniques. Glacial Environments Series. Vol. 2, p. 285-300, London.

Ketin, İ., 1959, ‘Türkiye’nin Orojenik Gelişmesi’. MTA Dergisi., No.53, Ankara.

Ketin, İ., 1960, ‘Anadolu’nun Tektonik Birlikleri’. MTA Dergisi., No. 66, s. 20-34.

Komori, J., 2007, “Recent Expansions of Glacial Lakes in the Bhutan Himalayas”, Quaternary International.

Kurter, A., 1979., Türkiye’nin Morfojenetik Bölgeleri. İ.Ü Coğ. Enst. Yay. No. 106, İstanbul.

Kurter, A., 1991., “Middle East and Africa, Satellite Image Atlas of Glaciers of the World”, United States’ Geological Survey Professional Paper 1386-G, p.8-22, United States Government Printing Office, Washıngton.

Kurter, A., Sungur, K., 1978., Present Glaciation in Turkey, in World Glacier Inventory, Proceedings of the Workshop at Riederalp, Switzerland, 17-22 September, 1978: International Association of Hydrological Sciences, Publication 126, p. 155-160.

Manley, G., 1971, “Interpreting the Meteorology of the Late and Post-Glacial Paleogeogr”, Palaeoclimatol. Palaeoecol.10, p. 163-175.

Mann, D.H., Sletten, R.S., Reanier, R.E., 1996, “Quaternary Glaciations of the Rongbuk Valley, Tibet”, Journal of the Quaternary Science, Vol. 11, p. 267-280.

Napieralski, J., Harbor, J., Li, Y., 2007, “Glacial Geomorphology and Geographic Information Systems”, Earth-Science Reviews 85, p. 1–22.

Paul, F., Kaab, A., Haeberli, W., 2007, “Recent Glacier Changes in the Alps Observed by the Satellite: Consequences for future monitoring strategies”, Global and Planetary Change, Vol.: 56, pg: 111-122.

Planhol, X., Bilgin, T., 1961, “Karagöl Kütlesi Üzerinde Pleistosen ve Aktüel Glasyasyon ile Periglasyal Topografya Şekilleri”, İ.Ü Coğ. Enst. Dergisi, Sayı. 12, s. 127-146, İstanbul.

Porte, S.C., 1964, “Late Pleistocene Glacial Chronology of North Central Brooks Range”, Am.J.Sci. 262, p. 446-460, Alaska.

Schneider, C., Schnirch, M., Acuna, C., Casassa, G., Kilian, R., 2007, “Glacier inventory of the Gran Campo Nevado Ice Cap in the Southern Andes and glacier changes observed during recent decades”, Global and Planetary Change 59, p. 87–100.

Silverio W., Jaquet, J., 2005., “Glacial cover mapping (1987–1996) of the Cordillera Blanca (Peru) using satellite imagery”, Remote Sensing of Environment 95, p. 342-350.

Sugden, E.D., Jhon, B.S., 1996., Glaciers and Landscape (Thirteenth Edition), St. Edmundsbury Press Limited, 376 pp, London.

Tonbul, S., 1997., “Bingöl Dağlar’ında Buzul Şekilleri”, A.Ü Türkiye Coğrafyası, Araştırma ve Uygulama Merkezi Dergisi. Sayı. 6, s. 347-374, Ankara.

Tonbul, S., Ege, İ., 2002, “Tahtalı Dağları Üzerinde Buzul Şekilleri” Doğu Coğ. Derg. Sayı: 7 syf: 165-187.

Tüfekçi, K., 1991, “Gölhisar Doğusunda Balıkdağ ile Rahat Dağı Dolayının Jeomorfolojisi”, İ.Ü Deniz Bil. ve Coğ. Enstitüsü. Doktora Tezi (Yayınlanmamış), İstanbul.

Walsh, S. J., Butler, D.R., Malanson, G.P., 1998, “An overview of scale, pattern, process relationships in geomorphology: a remote sensing and GIS perspective”, Geomorphology 21, p. 183-205.

Wright, W.B., 1937, The Quaternary Ice Age (Second Edition), McMillian and Co. Limited, 478 pp, London.

Yalçınlar, İ., 1951, “Soğanlı-Kaçkar ve Mescit Dağı Silsilesinin Glasyasyon Şekilleri”, İ.Ü Coğ. Enstitüsü Dergisi, S. 2, s. 20-55, İstanbul.

VITA

PERSONAL INFORMATION

Reşat Geçen
Date and Place of Birth: 1.6.1977, Elazığ
Nationality: Turkish (TC)
Marital Status: Married
Phone: +90 5416908886
email: rgecen@metu.edu.tr, rgecen@gmail.com

EDUCATION

Ph.D.	Geodetic and Geographic Information Technologies, The Graduate School of Natural and Applied Sciences, Middle East Technical University (M.E.T.U.), Ankara, Turkey	2003 – 2011
B.Sc.	Department of Geography, Faculty of Arts and Sciences, Fırat University University, Elazığ, Turkey	1998 – 2002

WORK E XPERIENCE

METU - Middle East Technical University Research Assistant 2002-2011

FOREIGN LANGUAGES

Advanced English, Basic German

PUBLICATIONS

Gecen R., Sarp G., Toprak V., Düzgün Ş., 2011, "Morphotectonic Properties of Yenicaga Basin Area in Turkey", 34th International Symposium on Remote Sensing of Environment, Sydney, AUSTRALIA

Gecen R., 2009, "Remote Sensing Applications in Archeology", Workshop on The Formation and Transformation of Space and Knowledge in Ancient Civilizations-Berlin, GERMANY

Gecen R.., G.Sarp 2008. "Automated Road Detection From High and Low Resolution Satellite Images" XXI ISPRS Congress 3-11 Jul. Beijing, CHINA

Ege I., **Gecen R**., 2008, "Evaluating Tourism Potential at Crests Zone of Bolkar Mountains Using GIS" 5th International Conferences on Geographic Information Systems, 2-5 July, Istanbul, TURKEY

Altın B. N., **Gecen R.,** 2008, "Mersin–Silifke Arasında Kıyı Çizgisi Değişimlerine Coğrafi Bilgi Sistemleri Teknolojileri ve Uygulamalı Jeomorfoloji Açısından Yaklaşımlar", Mersin Sempozyumu, 19-22 Kasım, Mersin.

Altın B. N., **Gecen R.,** Toprak V., 2008 "Damsa Ve Devret Çayı Havzalarında 'Akarsu Yoğunluğu Ve Morfolojik Evrim' İlişkisinin Cbs Ortamında Değerlendirilmesi" Ulusal Jeomorfoloji Sempozyumu, 20-23 Ekim. Çanakkale.

Gecen R., Toprak V., 2008 "Doğu Karadeniz Dağları'nda Yer Alan Buzul Göllerinin Envanteri", Ulusal Jeomorfoloji Sempozyumu, 20-23 Ekim. Çanakkale.

Altın T., **Gecen R**., 2008, "Bolkar Dağları Akarsu Havzalarının Hipsografik Eğrisi Ve Tektonizma Arasındaki İlişki", Ulusal Jeomorfoloji Sempozyumu, 20-23 Ekim. Çanakkale.

Gecen, R., Sarp, G., 2008 "Akarsu Drenajı ile Litolojik Birimler Arasındaki İlişki" 1.Ulusal Jeolojik Uzaktan Algılama Sempozyumu 22-23 Mayıs, Sivas.

Karadoğan S., **Gecen R.,** 2008, "Kuvaterner dolgularının oluşum süreci ve fasiyes olarak belirlenmesinde ve ayrımlanmasında uzaktan algılama teknolojisinin kullanılabilirliği" 1.Ulusal Jeolojik Uzaktan Algılama Sempozyumu 22-23 Mayıs. Sivas.

Gecen, R., Sarp, G., 2007. "Yüksek ve Düşük Çözünürlüklü Uydu Görüntülerinden Yolların Tayini". Coğrafi Bilgi Sistemleri Kongresi. 30 Ekim-2 Kasım. Trabzon.